Preparation and Characterization of New Nanostructured Organic/Inorganic Composite Coatings for Anti-Fog Applications

Doctoral Thesis

(Dissertation)

To be awarded the degree of Doctor rerum naturalium

(Dr. rer. nat.)

Submitted by

Mohamed Shafick Taha Zoromba

(From El Manzala, Egypt)

Approved by the Faculty of Natural and Material Sciences,

Clausthal University of Technology

Date of oral examination

03.11.2009

Chairperson of the Board of Examiners: Prof. Dr. Dieter Kaufmann

Chief Reviewer: Prof. Dr. Diethelm Johannsmann

Reviewer: PD Dr. Jörg Adams

Curriculum vitae

Name	Mohamed Shafick Taha Zoromba
Birth Date	12/02/1975
Nationality	Egypt
Sex	Male
Social Status	Married
Address	Port Said Faculty of Science, Chemistry, Department, Egypt
Email Address	mohamedzoromba@yahoo.com
Mobile Number	0049/017629999657
Language	English
Language	Arabic

Scientific Qualifications

General Grade	Very Good
01.08.2004-27.8.2007	Chemistry (1997)
28.07.2007 up to now	Chemistry (2003)

Professional Experience

28.02.1999 – 30.07.2004	Instructor in Faculty of Science, Aswan, Egypt
01.08.2004-27.8.2007	Assistant Lecturer in Faculty of Education, Port Said, Egypt
28.07.2007 up to now	TU Clausthal University, Physical Chemistry Institute, (Prof. D. Johannsmann group)

List of Publications:

No	Titles	Authors
1	A Study on Complexation Equilibria and Spectrophotometric Determination of CrIII, MnII and FeIII with Thiourea Monophosphazene Derivative	A.E. Arifien, G.M. Taha, A.A.M. Gad and *M. Sh. Zoromba* *Acadimic Open Internet Journal* WWW.acadjournal.com volume 11 (2004)
2	The effect of surface modified kaolinite filler on the physico-mechanical properties of NR and SBR vulcanizates.	*M. Sh. Zoromba*, A. A. M. Belal, A. E. M. Ali, A. S. Badran and A. A. Abd El-Hakim *Egyptian Journal of Applied science,* V21, N6,(2006)
3	Preparation and characterization of some PVC composites containing surface modified kaolinite incorporated with surface modified natural or precipitated $CaCO_3$	*M. Sh. Zoromba*, AA. M.Belal, A.E.M. Ali, A.A. Abd El-Hakim and A.S. Badran, *International Journal of Pure and Applied Chemistry* 1(4), pp539-548 (2006)
4	Physicochemical Studies on Some Metal Chelates of Cyclodiphosphazane and Thiourea Monophosphazene Derivatives	Gad, A. A. M.; Taha, G. M. H.; Arifien, A. E.; *Zoromba, M. Sh. Phosphorus, Sulfur, and Silicon and the Related Elements*, Volume 182, Number 10, , pp. 2425-2438(14) ,(2007)
5	Preparation and characterization of some NR and SBR formulations containing different modified kaolinite	*M. Sh. Zoromba*, A. A. M. Belal, A. E. M. Ali, F. M. helaly, A. S. Badran and A.A. Abd El-Hakim, Polymer-*Plastic technology and Engineering*,46,1-7, (2007)

Conferences:

1 International Symposium Microstrctural Control in free radical polymerization October, 5-8, (2008), Clausthal, Germany (Oral Presentation)

2 8^{TH} European Coating Symposium, September 7-9, (2009), Karlsruhe, Germany

Dedicated to

My Parents and My Wife

Acknowledgements

I wish to express my sincere gratitude and respect to *Prof Dr. Diethelm Johannsmann*, for his constant support, allowing and helping me to think and work independently, seed innovations to my work and constantly encouraging during the course of my work. I am will be remaining ever grateful to him for his teaching, guidance, friendship and wonderful personality.

I am particularly thankful to Associated *PD. Dr. Jörg Adams* for reviewing my thesis, numerous interesting helpful discussions, and for the support in all stages.

I am grateful to Prof. *Ahamed S. Badran*, Research National Center, Cairo. Egypt. (Blessing and merciful of Allah be upon him)

I am grateful to Prof. *Dr.Abo-Elfetouh* A. Abd El-Hakim, Research National Center, Cairo for his encourage me and his continuously discussion in Egypt.

I wish to express my sincere gratitude and Special thanks got to Associated *Prof. Dr. Arafa A. M. Belal*, Faculty of Science, Port Said, Egypt, Suez Canal University for his encourages and supports me.

I am very much thankful to *Dr. Esha E. Ali*, Faculty of Science, Ismailia, Suez Canal University, Egypt for her cooperation

Of course I am also deeply grateful to Prof. Dr. Wihelm Oppermann for helpful discussion.

I am also very thankful to all people who contributed to this work (in no particular order)

- I am very much thankful to Sylvia Hanke for her help with the translation of my abstract.
- Alexander M. König always supported me with his effort, especially in the filed of texture analyzer system and companion in the different meeting and conferences in Mainz and Clausthal and Karlsruhe
- Dr. Paloma Sivelliano (Genthe X Coating Company) supported me with photo-initiators and many helpful discussions
- Dr. Arne Langoff helped me in the measurements with confocal microscope and also helpful discussion.
- Astrid Peschel helped me in the measurement of Differential Scanning Calorimetry.
- Michael Tölle was never hesitating to support me when practical help, materials, or reactants were needed.
- Uwe Cronjäger for cutting polycarbonate sheets and many helpful technical components.

I must thank my lab mates and friends, Svenja, Annika, Markus, Julia, Anne, Najah, Saadet and Volkan.

Special thanks go to Ms. Goertz and Ms. Kornhardt

Of course I am also deeply grateful to all other people in our institute for numerous discussions, for practical help whenever it was needed and for the perfect working atmosphere. In addition, I want thank all the people from the priority program (PWT) for pleasant meetings and many stimulating discussions.

I take this opportunity to express my sincere gratitude to my sisters, my brothers

The financial support to this work was provided by Egyptian mission which is gratefully acknowledgment, special thankful to both Education faculty and Science faculty, Port Said, Suez Canal University and all my colleagues there.

Abstract

We report on the development of an anti-fog transparent coating based on poly-urethane-PEG-Acrylate copolymers. Both thermal and UV curing was pursued. In order to render the polymer hydrophilic, a poly(ethylene glycol) (PEG) chain is used as the poly-ol portion of the polyurethane. The molecular weight of the PEG chain was either 1000 or 400 g/mol (PEG_{1000} and PEG_{400}). An aliphatic diisocyanate, namely isophorone di-isocyanate (IPDI) was used in order to prevent yellowing. A PEG-IPDI polymer was produced in a first step. Because IPDI was used in excess, the polymer has isocyanate ends groups. These were reacted with 2-hydoxyethyl acrylate (HEA) in a second step. Dibutyl tin dilaureate (DBTL) was employed as the catalyst for formation of the urethane bond. Crosslinking occurred via free radical polymerization of the acrylate group. We employed either azo-bis-isobutyro-nitrile (AIBN) as a thermal initiator or a commercial photoinitiator for UV curing. Films with wet thicknesses of 30, 60, 90, and 120µm were produced on glass and polycarbonate surfaces. The performance parameters such as fog resistance in hot humid atmosphere, tackiness, scratch resistance, adhesion were determined as a function of preparation parameters such as time of thermal curing, IPDI/PEG ratio, irradiation time, and content of wetting agent. A variety of techniques, such as microscopy, confocal laser scanning microscopy, atomic force microscopy, differential scanning calorimetry, hardness testing and dynamic light scattering were employed for characterization.

While anti-fog activity was obtained with a wide variety of recipes, optimization of other properties – hardness and scratch resistance, in particular – turned out to be in conflict with the anti-fog activity. Anti-fog activity requires carefully timed uptake of water. Hard films, on the other hand, have limited swellability.

In order to avoid – or at least diminish – this problem, anti-fog coatings containing nano-sized inorganic fillers were developed. Various types of fillers were tested. Dry silica powder such as Aerosil R972 is economical widely used in the industry. However, proved to be impossible to disperse the aggregates to the extent that they would not scatter light. The resulting films were hazy. An aqueous dispersion of silica (Köstrosol 2040) proved impractical because the PU was dissolved in acetone and phase transfer from water to acetone could not be achieved. Clay particles (laponite RD) aggregates inside the film and also resulted in slightly turbid films.

These problems could be solved with self-prepared silica particles. It turned out, that the Stöber synthesis typically carried out water can also be done in mixtures of water and acetone. The water/acetone ratio could be chosen such the polymer would not precipitate when adding the dispersion of silica particles to the polymer. Silane coupling agents improved the optical properties of the resultant coating.

This technique provides for a novel route to create scratch resistant anti-fog coatings. The anti-fog activity will be optimized in further work by suitable additivation. With regard to the hardness, the use of an organic/inorganic nanocomposite proved to be a decisive advantage.

Zusammenfassung

Die Dissertation behandelt die Synthese einer transparenten „Anti-Fog"-Beschichtung (beschlagsvermeidende Beschichtung), basierend auf einem Polyurethan-PEG-Acrylat Copolymer. Dessen Aushärtung erfolgte sowohl thermisch als auch durch UV-Strahlung. Die Hydrophilie des Polymers konnte durch Verwendung einer Poly(ethylenglycol) (PEG)-Kette als Poly-ol-Komponente des Polyurethans gewährleistet werden. Das Molekulargewicht der PEG-Kette variierte zwischen 400 und 1000 g/mol (PEG_{400} bzw. PEG_{1000}). Zur Vermeidung von Gelbfärbung wurde ein aliphatisches Diisocyanat, Isophoron-di-isocyanat (IPDI), eingesetzt. In einem ersten Schritt wurde ein PEG-IPDI Polymer synthetisiert. IPDI wurde im Überschuss eingesetzt, wodurch das Polymer Isocyanat-Endgruppen aufwies. In einem zweiten Schritt reagierten diese mit 2-Hydroxyethylacrylat (HEA). Die Bildung der Urethan-Bindung erfolgte mit Dibutyl-Zinn-dilaureat (DBTL) als Katalysator. Durch freie radikalische Polymerisation der Acrylat-Gruppe wurde das Polymer vernetzt. Dabei diente entweder Azo-bis-(isobutyronitril) (AIBN) als thermischer Initiator oder aber ein kommerziell erhältlicher Photoinitiator zur Aushärtung. Es wurden Filme mit einer Nassdicke von 30, 60, 90 und 120 μm auf Glas- und Polycarbonat-Oberflächen aufgebracht. Leistungsparameter wie „Anti-Fog"-Eigenschaften, Klebkraft, Kratzfestigkeit und Haftung wurden als Funktion der Herstellungsparameter untersucht. Dazu zählen beispielsweise die Aushärtzeit, die Monomere, die Bestrahlungszeit und der Gehalt an Benetzungsmittel. Eine Vielzahl von Untersuchungsmethoden wie etwa das Konfokale Laser Scanning Mikroskop, das Rasterkraftmikroskop, die Differentialkalorimetrie, Härtetests und die dynamische Lichtstreuung wurden für die Charakterisierung der Polymerfilme herangezogen.

Während „Anti-Fog"-Eigenschaften bei vielen Rezepturen erhalten werden konnte, gingen sie bei zusätzlicher Optimierung anderer Leistungsparameter, insbesondere der Härte und der Kratzfestigkeit, oft verloren. Gute „Anti-Fog"-Eigenschaften erfordern auf der einen Seite eine genau kalkulierte Aufnahmezeit von Wasser. Auf der anderen Seite begrenzen harte Polymerfilme die Wasseraufnahmefähigkeit.

Um dieses Problem zu mindern oder zu vermeiden wurden „Anti-Fog"-Polymere entwickelt, welche anorganische Nano-Füllstoffe enthalten. Unterschiedliche Füllstoffe wurden untersucht. Trockene Silica Pulver wie beispielsweise Aerosil R972 sind in der Industrie weit verbreitet. Es stellte sich jedoch heraus, dass diese nicht soweit dispergiert werden können, dass sie Licht nicht mehr streuen. Die daraus resultierenden Filme waren trüb. Eine wässrige Dispersion von Silica (Köstrosol 2040) wurde untersucht und verworfen, da PU in Aceton gelöst war und ein Phasentransfer von Wasser zu Aceton nicht ermöglicht werden konnte. Tonpartikel (Laponite RD) bildeten innerhalb des Polymerfilms Aggregate, wodurch dieser ebenfalls leicht eintrübte.

Diese Problematik konnte mit selbst hergestellten Silica-Partikeln umgangen werden. Es stellte sich heraus, dass die Stöber-Synthese – welche typischerweise in Wasser durchgeführt wird – auch in einer Mischung aus Wasser und Aceton funktioniert. Das Wasser / Aceton Verhältnis wurde so gewählt, dass die Zugabe der Dispersion das Polymer nicht kollabiete. Silankupplungsreagentien verbesserten die optischen Eigenschaften der resultierenden Filme.

Diese Technik bietet einen neuen Weg zur Herstellung kratzfester, „Anti-Fog"-Beschichtungen. Die „Anti-Fog"-Eigenschaften werden in weiteren Arbeiten durch Zugabe geeigneter Additive optimiert werden. Im Hinblick auf die Härte ist der Einsatz von organisch/anorganischen Nanokompositen der entscheidende Faktor um zeitgleich auch die Beschlagsvermeidung zu erhalten.

Table of Contents

1 Introduction

Economic competitiveness and environmental interests have driven the coating technologist to research newer chemistry and approaches to improve the efficiency of organic coatings at a minimum content of volatile organic component (VOC). Organic coatings or paints on a substrate give aesthetic appearance as well as protection from corrosion. Coatings can provide materials with the desired aesthetical properties such as color and gloss, but they are of vital importance in the protection against environmental influences, including moisture, radiation, biological deterioration or damage from mechanical or chemical origin. This applies to both interior and exterior applications. The effectiveness of protection of a substrate against natural deterioration depends on factors such as the quality of the coating, the substrate characteristics, the properties of the coating/ substrate interface, and the corrosiveness of the environment. The challenge within the industry is the improving properties at reasonable cost, while at the same time meeting the need for environmentally friendly coatings. Several new types of coatings, such as radiation curable and waterborne coatings have obtained an increased market share since they address some of these issues. On the other hand, solvent-borne coatings have had particular importance in the area of industrial coatings, where performance is essential. Therefore, some researchers have focused on methods to improve the solid content of the binder by utilizing relatively low molecular weight polymer that build in properties during cure through the formation of crosslink networks. The presence of crosslinks provides thermoset coatings with enhanced tensile strength, good abrasion, acid, alkali and solvent resistance, which are lacking in thermoplastic coatings. During the development of new systems, numerous aspects must be considered: the production of the coating formulation, storage of the coating, application and film formation must work with the techniques intended.

This thesis consists of is considered with polyurethane as a base material for anti-fog coatings.

1.1.1 Polyurethane (PU)

Otto Bayer and coworkers at I.G. Farben, Germany in 1937 were the first to discover polyurethanes in response to the competitive challenge.[1] and this text adopted from D.K. Chattopadhyay et. Al. Further research on this subject demonstrated that the reaction of an aliphatic isocyanate with a glycol produces new materials with interesting properties. Dupont and ICI soon recognized the desirable elastic properties of polyurethanes. The industrial scale production of polyurethane started in 1940, but market growth of polyurethane was seriously impacted by World War II. A noticeable improvement in the elastomeric properties of polyurethane waited until 1952, when polyisocyanate, especially toluene diisocyanate (TDI), become commercially available. In 1952–1954, Bayer developed different polyester–polyisocyanate systems. In 1958, Schollenberger introduced a new crosslinked thermoplastic polyurethane elastomer. In 1959, Dupont introduced a "Spandex" fibre, which is a polyurethane based on polytetramethylene glycol (PTMG), 4,4`-diphenylmethylene diisocyanate (MDI) and ethylene diamine. In 1960s, BF Goodrich produced Estane, Mobay marketed Texin, and Upjohn marketed Pallethane in the USA. Bayer and Elastogran marketed Desmopan and Elastollan, respectively in Europe.[2] With the development of low-cost polyether polyols, polyurethane coatings opened the door to automotive applications. Formulations and processing techniques continuously developed as one- and two-pack systems were developed. The polyuretahne coating industry has entered a stage of stable progress and advanced technological utilization. Today, polyurethane coatings can be found on many different materials, to improve their appearance and lifespan. On automobiles, polyurethane coatings give the demanded exterior high gloss, improved color preservation, improved scratch and corrosion resistance. Different types of polyurethane coatings are used in construction, where building floors, steel trusses and concrete supports are spray coated to make them more durable against environmental deterioration and less costly to maintain. The wide applicability of polyurethane coatings is due to versatility in selection of monomeric materials from a huge list of macrodiols, diisocyanates and chain extenders (CE). The chemistry involved in the synthesis of polyurethane is centered on the isocyanate reactions. The three important components of polyurethanes are macrodiol, diisocyanate and chain extender. The synthesis of polyurethane involves on addition reaction between a di- or polyisocyanate with a di- and/or polyol.

1.1.2 Isocyanates

Polyfunctional isocyanate used to prepare polyurethane coatings can be aromatic, aliphatic, cycloaliphatic or polycyclic in structure. The commonly used isocyanates in the manufacturing of polyurethanes are toluene diisocyanate (TDI), methyl diphenyl diisocyanate (MDI), 4,4`-dicyclohexylmethane diisocyanate ($H_{12}$MDI), xylene diisocyanate (XDI), tetramethylxylylene diisocyanate (TMXDI), hydrogenated xylene diisocyanate (HXDI), naphthalene 1,5-diisocyanate (NDI), p-phenylene diisocyanate (PPDI), 3,3`-dimethyldiphenyl-4,4`-diisocyanate (DDDI), hexamethylene diisocyanate (HDI), 2,2,4-trimethylhexamethylene diisocyanate (TMDI), isophorone diisocyanate (IPDI), norbornane diisocyanate (NDI), 4,4`-dibenzyl diisocyanate (DBDI), etc. Aromatic isocyanates have high reactivity than aliphatic or cycloaliphatic diisocyanates. Different diisocyanates contribute to the polyurethane properties in different ways. For example, aromatic diisocyanates give more rigid polyurethanes than aliphatic diisocyanates, but their oxidative and ultraviolet stabilities are lower than the ones of aliphatic diisocyanates.[3]

1.1.3 Isocyanate Reactivity

Isocyanates are extremely reactive chemicals and create several chemically different products when combined with –OH and –NH functional substances. Desired products and side products are formed in different amounts. The basic reactions of isocyanate with different reagents are shown in Scheme (1.1). The high reactivity of isocyanate groups toward nucleophilic reagents is mainly due to the positive character of the carbon atom in the double bond sequence consisting of nitrogen, carbon and oxygen, especially in aromatic systems. The electronegativity of the oxygen and nitrogen imparts a large electrophilic character to the carbon in the isocyanate group. The common reactions of isocyanates can be classified into two main classes: (1) the reaction of isocyanates with compounds containing reactive hydrogen to give addition products, and (2) the polymerization of isocyanates, i.e., self-addition reaction. Isocyanates react with hydroxyl compounds to give urethanes (a) and with amines to give ureas (b). For primary and secondary alcohols, the uncatalysed reaction proceeds readily at 50–100 °C, tertiary alcohols and phenols react more slowly. Typical primary and secondary aliphatic amines and primary aromatic amines react rapidly with isocyanate at 0–25 °C to form urea functional substances. Similarly, water reacts with a diisocyanate and primarily

forms of an unstable carbamic acid, which decomposes to an amine (c) and carbon dioxide. Amine is a nucleophilic reagent and further reacts with an isocyanate function to produces an urea linkage (d). The availability of a lone pair of electrons on the nitrogen atom of urea group makes them nucleophilic centers, which upon reaction with one molecule of isocyanate produces biuret (e). Similarly, isocyanates react with urethanes and produce allophanates (f). The reactions leading to the formation of allophanates and biurets are influenced by reaction conditions such as temperature, humidity level, and the type of isocyanate used. The self-condensation of the isocyanate produces in uretidione rings (dimer-, g), isocyanurate (trimer-, h) or carbodiimide (j).

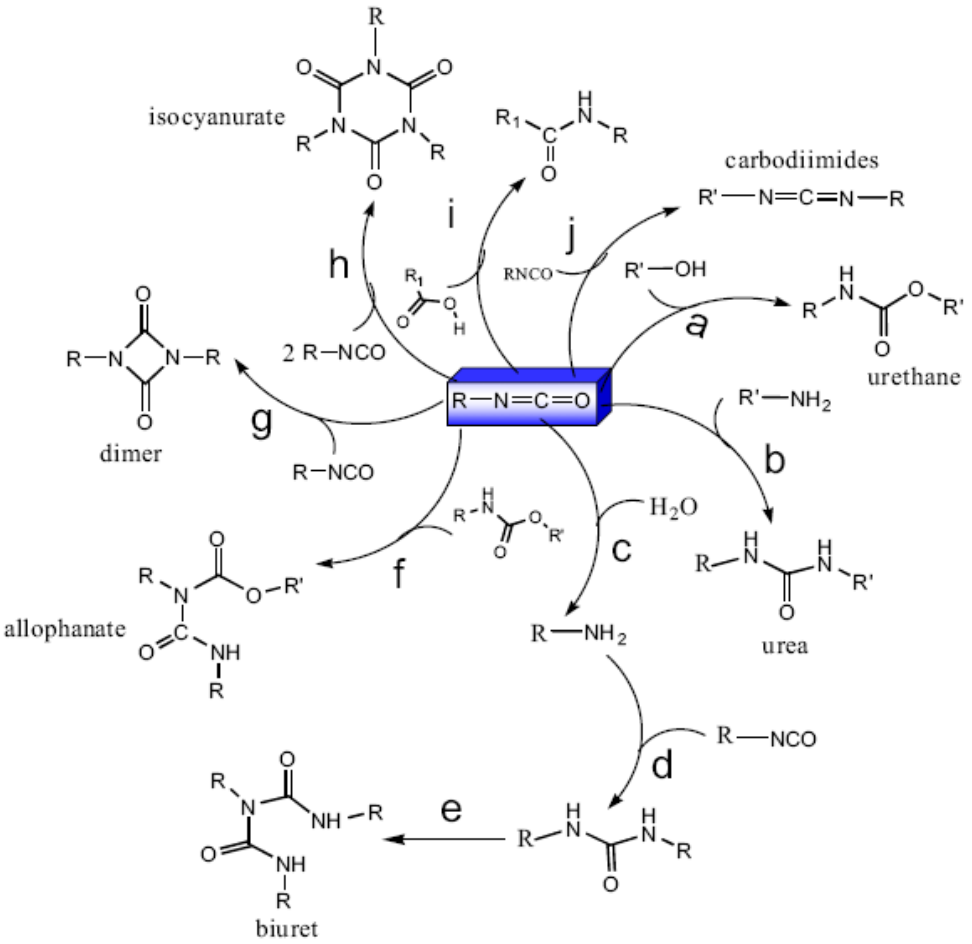

Scheme (1:1): Basic reactions of isocyanate with different reactants.[4]

The formation of carbodiimides is not usually considered a polymerization reaction, but it could be classified as a condensation polymerization between isocyanate molecules with elimination of CO_2. This is due to degradation of isocyanates which takes place at high temperatures.[5] When isocyanate reacts with carboxylic acids, the mixed anhydrides

break down and form amide groups (i). The trimer isocyanurate rings, unlike uretidione rings, are very stable. The high reactivity of isocyanates may cause detrimental secondary reactions and uncontrolled condensations leading to the formation of unfeasible crosslinked materials that are difficult to process. Therefore, blocking of isocyanate capped material or monomer may sometimes helps for improving the stability.[6] The blocked isocyanate can be converted to the active isocyanate form when required. More recently, commercial availability of blocked isocyanates has increased greatly. In particular, these reagents are suitable for light-stable two-component and single-package blocked adduct urethane coatings in which high temperatures (>100 °C) are used to regenerate the isocyanate and the blocking agent. The regenerated isocyanates react with hydroxyl or amine functionalized co-reactants to form thermally stable urethane or urea bonds, respectively.[7],[8],[9]

1.1.4 Type, position and structure of isocyanate groups

The type, position and structure of isocyanate group affect the reactivity with nucleophiles and the material properties of the derived polyurethane coatings.[10] The reactivity of primary and secondary isocyanate groups of IPDI are different due to stereo-electronic configuration and their reactivity depends on the reaction environment such as type and nature of catalyst, solvent, etc. Similarly, 2,4 and 2,6 TDI isomers differ noticeably with respect to their structure as well as reactivity.[11] The 2, 6 isomer is symmetric (scheme 1.2b) as compared with the 2, 4 isomer (scheme 1. 2a) and is therefore expected to form hard segments with better packing characteristics. Again, the reactivity of the ortho position in the 2, 4 isomer is approximately 12% of the reactivity of the isocyanate group in the para position because of the steric hindrance caused by the methyl group. However, when the reaction temperature approaches 100 °C, the steric hindrance effects are overcome, and both positions react at nearly the same rate. In comparison, the isocyanate groups on the 2,6 isomer have equal reactivities when both groups are unreacted. However, after one of the isocyanate groups reacts, the reactivity of the second group drops by a factor of about three.[12],[13] Sung and Schneider[14] reported that the strength of hydrogen bonds in polyurethanes prepared from 2,6 TDI exceed those in 2,4 TDI-based polyurethanes. Nierzwicki and Walczynski investigated[15] PTMG/BDO-based polyurethane elastomers synthesized from different amount of 2,4 and 2,6 TDI isomers and showed that increasing content of the 2,6 TDI isomer resulted in a systematic increase in tensile strength, modulus and microphase

separation. It was suggested that the symmetric nature of the 2,6 TDI isomer enhanced the stiffness of the hard domains.

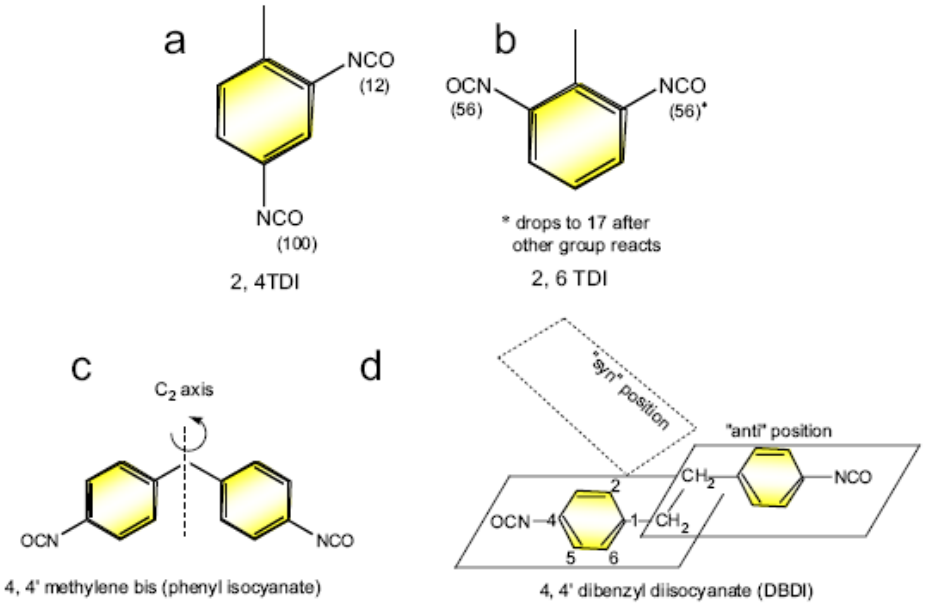

Scheme (1.2): Schematic of (a) 2, 4 TDI, (b) 2, 6 TDI (The numbers indicate relative rates of reaction of the isocyanate groups at the different positions.) (c) MDI and (d) DBDI.[12]

Barbeau et al.[16] observed strong hard–hard inter urethane associations in 2,6-TDI based prepolymers; these led to microphase segregation between polyether chains and urethane groups. Different studies[17],[18] showed that the MDI-based polyurethane in contrast to TDI-based materials possess a more perfect domain organization due to long-range order and show a higher extent of segregation between soft and hard segments. Generally symmetric isocyanates form crystallizing hard segments with good packing ability, producing higher strength materials. However, from a kinetic point of view, phase separation becomes more complete with aliphatic hard segments because of increased mobility. Rogulska et al.[19] reported that the polyurethanes prepared from HDI had higher ability to crystallize than the MDI-based polyurethane. The structure of MDI and DBDI (scheme 1.2 c & d) differ only in the number of the methylene (CH_2) groups located between the two aromatic rings bearing the isocyanate (NCO) groups in the para position. Polyurethanes prepared from DBDI (i.e., even number of CH_2 groups located between the aromatic rings) are considerably higher melting than MDI-based

polyurethanes (i.e., odd-number of CH_2 groups situated between the aromatic rings). The MDI molecule introduces the rigid –Ph–CH_2–Ph– moiety in the elastomeric polyurethane hard segments. In contrary, when using DBDI, the specific –Ph–CH_2–CH_2–Ph– moiety introduces a variable geometry into the hard segments due to the possibility of internal rotation of this isocyanate around the –CH_2–CH_2– ethylene bridge. This leads to the appearance of both syn and anti rotational conformations, of which the anti conformation is most stable. Therefore, polyurethanes prepared from DBDI can adopt compact packing due to the anti conformation of DBDI, which significantly enhance ordering and hard segment–hard segment hydrogen bonding.[20]

1.1.5 Aliphatic Diisocyanate and transparency

Aliphatic isocyanates H_{12}MDI and IPDI are now well established as being preferred for the production of transparent polyurethane elastomers. Transparency arises because of the presence of geometric isomer in these isocyanates. Typically IPDI is a mixture of 28% trans and 72% cis isomer whilst H_{12}MDI commonly contains 65%cis-trans, 30%trans-trans, 5% cis-cis isomers scheme (1.3).

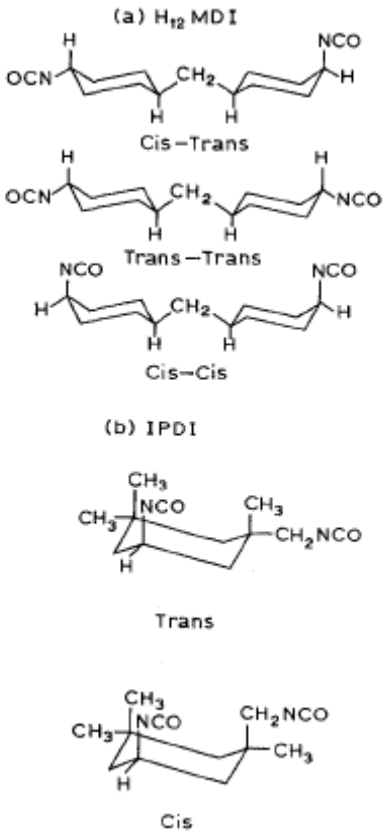

Scheme (1.3)

The effect of H_{12}MDI isomers on transparency of some polyurethane are shown in table (1.1). Increasing in trans-trans content of polyurethane hard segment leads to an increased rigidity, but at the same time to loss in the transparence.[21]

Table (1.1): the optical properties of some polyurethane elastomer prepared from the geometric isomers of H_{12}MDI

Sample	Hard segment isomer content			Appearance
	Trans-Trans	Cis-Trans	Cis-Cis	
12	20	75	5	Optically clear, flexible
2	30	65	5	Optically clear, flexible
3	70	25	5	Opaque, stiff

1.1.6 Diols/polyols

The polyol component of the polyurethanes can be a polyfunctional polyether (e.g., polyethylene glycol, polypropylene glycol, poly(tetramethylene glycol) (PTMG) or polycaprolactone diol), polyester polyol (PEPO), acrylic polyol (ACPO), polycarbonate polyol, castor oil or a mixture of these. A wide variety of branched or crosslinked polymers can be formed since the functionality of the hydroxyl-containing reactant or isocyanate can be adjusted. The simplest polyols are glycols, such as ethylene glycol, 1,4-butane diol (BDO) and 1,6-hexane diol. The low molecular weight reactants result in hard and stiff polymers because of a high concentration of urethane groups. On the other hand, the use of high molecular weight polyols as the main reactants produces polymer chains with fewer urethane groups and more flexible alkyl chains. Long-chain polyols with low functionality (1.8–3.0) give soft, elastomeric polyurethanes while short chain polyols of high functionality (greater than 3) give more rigid, crosslinked products. Polyether polyols are produced by the addition of either ethylene oxide or propylene oxide to a polyhydroxy starter molecule in the presence of a catalyst (scheme 1.4a). Typical starter molecules include glycerol, ethylene glycol, propylene glycol and trimethylolpropane. PEPOs are produced by the condensation reaction of polyfunctional carboxylic acids or anhydrides with polyfunctional alcohols (scheme 1.4b). ACPOs are produced by free radical polymerization of hydroxyethyl acrylate (HEA)/methacrylate with other acrylic precursors [22] (scheme 1.4c). Depending on the type of application, PEPO, ACPO or polyether polyols have been chosen. In commercial applications, it is common to find polyesters prepared from a mixture of two or more di-acids reacted with two or more glycols, which gives plenty of scope for a range of very complex products. [23], [24] Polyurethanes which are based on PEPO and ACPO are susceptible to the gradual hydrolysis of the ester group but they are sufficiently stable against natural weathering. Additionally, the in situ formation of carboxylic acid catalyze further ester hydrolysis, thus accounting for an autocatalytic effect [25] and a significant reduction of average molar mass. Consequently, a deterioration of mechanical properties occurs on prolonged exposure to humid atmosphere. To slow down the hydrolysis of polyester groups, polycarboimides can be added to poly(ester urethanes).These act as acid scavengers and suppress the autocatalytic effect.[25], [26]

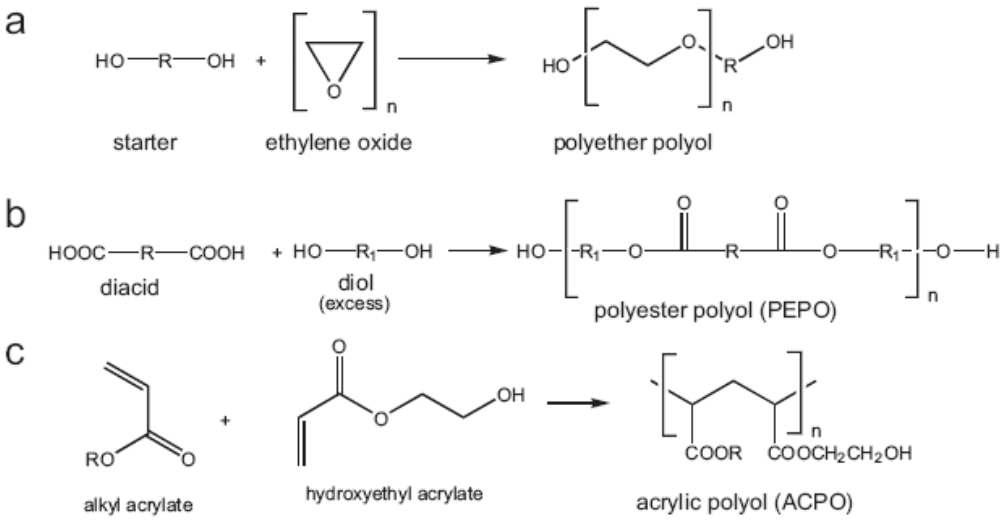

Scheme (1.4): preparation method of polyether polyol, PEPO and ACPO.

1.1.7 Catalysts

Catalysts are usually added to allow the reaction to take place at a rapid rate and at lower temperatures. For the reaction of an isocyanate with an alcohol, many effective urethane catalysts are available. Most often used catalysts are tertiary amines[27], especially 1,4 diazabicyclo [2.2.2] octane (DABCO), triethyl amine (TEA), and organo-tin compounds[28], especially dibutyltin dilaurate (DBTDL) and stannous octate. Tetravalent tin compounds of the type $R_nS_nX_{(4-n)}$ with R being a hydrocarbon group (alkyl, aryl, cycloalkyl, etc.) and X being a halogen atom or a carboxylate group (acetate, laurate, etc.) have also shown a catalytic effect in the urethane reaction.[29] The catalytic effect of organometallic compounds is due to their complex forming ability with both isocyanate and hydroxyl groups.[30],[31] The mechanism proposed by Britain and Gemeinhardt[32] is shown in (scheme 1.5). The interaction of the metal cation with the isocyanate and the alcohol molecule results an intermediate complex (scheme 1.5a), which may then readily rearrange to yield the urethane product (scheme 1.5b). Lenz [33] suggested that the catalytic mechanism of tertiary amines (NR_3) for urethane reaction involves the complexation of the amine and isocyanate groups (scheme 1.5c) followed by reaction of the complex with alcohol to form urethane product (scheme 1.5d).[34]
The mercury catalyst “thorcat”, however, is less efficient than either catalyst, perhaps due to a higher stability constant for the latter compound. Furthermore, mercury salt catalysts

are thought to possess delayed action properties,[35]which may also account for their reduced performance compared with other metal compounds.[36] In the absence of a strong catalyst, allophanate and biurets formation do not take place for aliphatic isocyanates.

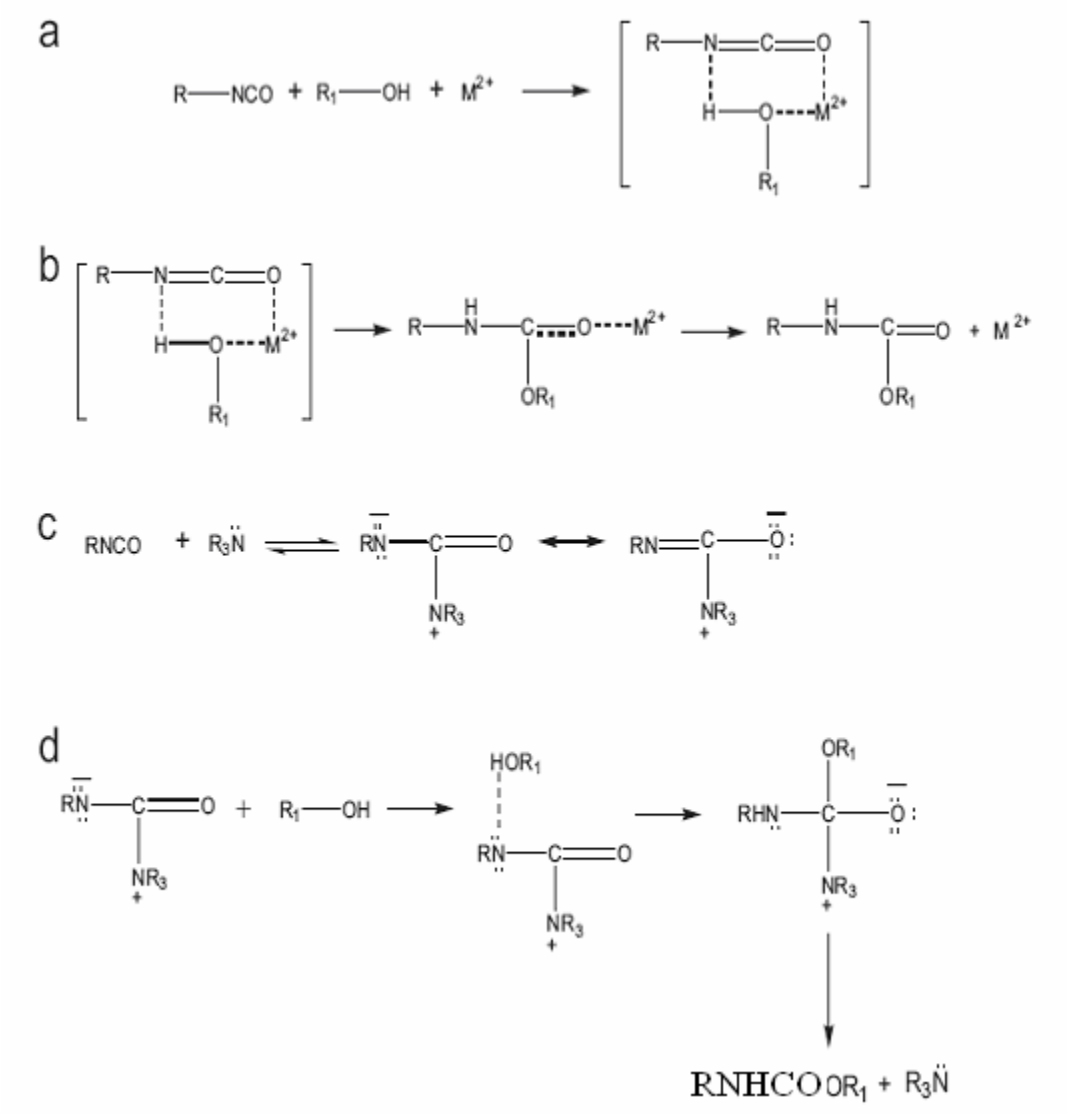

(Scheme 1.5): Reaction mechanism of the NCO/OH in presence of: (a) and (b): organometallic catalysis.[31] (c) and (d): tertiary amine catalysis[31], [35]

1.1.8 Polyurethane coating classification

American Society for Testing and Materials (ASTM) has grouped six different polyurethane coating types in the ASTM D16 Standard.[37] Table (1.2) summarizes the characteristics of six ASTM polyurethane coating types. Most high solids and solventless polyurethane coatings for high performance application and corrosion protection are designed using the plural component format of the ASTM D16-type V.

Table (1.2): Different type of coatings according to ASTM classification

ASTM	Type I	Type II	Type III	Type IV	Type V	Type VI
description	onepackage (prereacted)	onepackage (moisture cured)	onepackage (heat cured)	twopackage (catalyst)	twopackage (polyol)	onepackage (nonreactive lacquer)
Polymer	Alcoholyic products of drying oils reacted with isocyanate	Higher molecular weight diols and triols	Prepolymer forms an adduct with blocking agents	Prepolymer similar to type II, but catalyst could contain polyol/amine	Relatively lower molecular weight	Thermoplastic polymer with relatively high molecular weight
Characteristics	Unsaturated drying oil modified; no free isocyanate	Contains free isocyanate	Blocked isocyanate	Isocyanate prepolymer and catalyst	Part A: isocyanate rich, Part B: polyols or amines	Fully polymerized PUs dissolved in solvents
Curing mechanism	Oxidation of drying oil; solvent evaporation	Reaction with atmospheric moisture	Thermal release of blocking agent and then reaction	Reaction of isocyanate with moisture and or/ components in catalysts	Reaction between Parts A and B; instant curing is possible	Solvent evaporation

1.1.8.1 Thermoplastic polyurethane coatings

Thermoplastic polyurethane may be described as the linear structural block copolymer of soft segment and hard segment type. Due to the wide variety of properties between soft segment and hard segment, phase separation may be observed in the final material. Phase separation occurs due to the intrinsic incompatibility or thermodynamic immiscibility between the hard and soft segments. The hard segments, composed of polar materials, can form carbonyl to amino hydrogen bonds and thus tend to cluster or aggregate into ordered hard domains,[38] whereas soft segments form amorphous domains. The hard segment acts as filler particle as well as crosslinker to hold back the motion of soft segment chains. Such a structure was first proposed by Cooper and Tobolsky in 1966[39] The early work of Schollenberger[40] and of Cooper and Tobolsky[39] established that segmented polyurethanes consist of high glass transition temperature (Tg) or high melting temperature (Tm) hard segment microphase separated from relatively low Tg soft segment. The degree, to which the hard and soft segments phase separate, plays a very important role in determining the solid-state properties of these multi-block coatings. The properties of thermoplastic polyurethane coatings depend upon several factors such as the composition of soft and hard segments, the lengths of soft and hard segments and the length distribution, the chemical nature of the units composing the polymer, anomalous linkages (branching, crosslinking), molecular weight and the morphology in the solid state. At room temperature, soft macroglycol segments are above their glass transition temperature and easily therefore segmental rotations, which therefore impart the material its rubber-like behavior and elastomeric properties. On the other hand, hard domains are below their glass or melt transition temperature and are thought to govern the hysteresis, permanent deformation, high modulus, tensile strength, and dimensional stability.[41] Compositional variables and processing conditions such as structure of soft and hard segments,[42] symmetry of diisocyanate, type of chain extender (diol or diamine), [43],[44] number of carbons in linear low molecular weight chain extender,[44] the type (polyester or polyether) and chain lengths of soft segments [44],[45],[46],[47] crystallizability of either segment,[48] thermal history of the polyurethanes[46],[49],[50] and the method of synthesis [42]are known to affect the degree of phase segregation, phase mixing, hard segment domain organization, and subsequent polyurethane coating properties.

1.1.8.2 Effects of the soft segment

The chemical composition and molecular weight distribution (MWD) of the incorporated soft block influence the macroscopic properties of the resulting coatings. For example, Yoo et al.[51] claimed that the deformation and thermal properties of the polyurethanes were strongly affected by the molecular weight of soft segment. Additionally, varying the chemical structure of soft segment changes its solubility parameter and hence the compatibility between soft and hard segments in polyurethane coatings. Investigations by Van Bogart et al.[52] and Hartmann et al.[53] revealed that increasing the soft segment molar mass at a fixed hard segment length gave rise to an increased tendency for the hard segment domains to be isolated in the soft segment matrix. A similar conclusion was reached in polyurethane based on MDI and polycaprolactone using various instrumental techniques.[54] This phenomenon resulted in a higher degree of phase separation between hard and soft blocks, which produced a lower glass transition temperature value. In addition, increasing soft segment prepolymer molar mass at constant functionality (i.e., increasing the molar mass per functional group or equivalent weight) results[55],[56],[57],[58] in a higher degree of phase separation, again owing to increased thermodynamic incompatibility between the two copolymer segments, resulting from the higher Flory–Huggins interaction parameter (χ) [59] and/or the higher crystallizability[47] Stanford et al.[60] showed that increasing soft segment functionality significantly increases the strength of polyurethane and reduces the overall degree of phase separation developed in these materials due to increased domain boundary mixing.

1.1.8.3 Effects of the hard segment

Hard segment structure, length and distribution are very important parameters and strongly affect morphology, thermal behavior as well as performance of segmented polyurethane coatings.[61],[62],[63] Wang and Cooper[47]observed that the mechanical properties of polyether polyurethanes depend primarily on the hard segment content. The presence of three-dimensional hydrogen bonding within hard domains leads to usually strong hard domain cohesion. On increasing the hard segment content, a morphological change occurs from isolated interconnecting to hard domains. The effect of hard segment content on the phase separation in polyurethane based on MDI was studied by measuring the glass transition temperature of the soft segment. [64] The soft segment glass transition

temperature was influenced by the restricted movement imposed at the hard segment junctions and at phase boundaries, where the hard domain acts as a filler particle.[65]

1.1.8.4 Effect of the chain extender

The effect of different chain extenders on the morphology and properties of polyurethanes were reported by various authors.[66], [67], [68] The chain length, the molecular volume and the functionality of the chain extender as well as its conformation can influence hard segment packing and crystallinity in the hard domains.[69],[70],[71] Blackwell and Nagarajan[72] and Blackwell et al.[66],[73] suggested that for chain extended polyurethanes, chain extenders containing an even number of carbons produced polymers with a more phase separated structure than those containing an odd numbers of carbons. Auten and Petrovic[74] reported the effect of unsaturation in the chain extender on the structure and properties of derived polyurethanes. They utilized chain extenders of the 1,4-butane diol (BDO) series with increasing bond order at the 2,3 carbons such as BDO, cis-2-butene- 1,4-diol (BED) and 2-butyne-1,4-diol (BYD) and showed that increasing bond order progressively limit backbone chain flexibility. Consequently, hard segment size may increase, but hydrogen bondings groups may be forced into positions that do not allow effective inter chain bonding, resulting in poor physicochemical properties. In addition, the relative acidity of the terminal alcoholic protons is expected to increase with increasing chain extender bond order because electron density at the oxygen atoms would be progressively shifted toward the π-bonds. As the acidity of the chain extender O–H group increases, the reaction rates during polymer synthesis, polymer molecular weight, and thermal stability of the urethane groups formed could all be adversely affected. It has also been shown that the physicochemical properties of thermoplastic elastomers are improved using diols with higher molecular weight as chain extenders.[75] While working with hydroxyl-terminated polybutadiene (HTPB)-based polyurethanes, Zawadski and Akcelrud [76] observed that the mechanical properties improved with decreasing number of carbon atoms in the chain extender. Their findings disagree with previous results, which showed a zigzag pattern,[77] or an improvement in property with diol chain length.[78] Yen et al.[79] observed a higher tensile strength for diamine chain extended polyurethanes in comparison to BDO chain extended polyurethanes. They also observed that ethylenediamine chain extended polyurethane showed better tensile strength than diethyltriamine chain-extended polyurethane.[79] Earlier studies[43],[44],[68],[80] compared urea with urethane with regard to their influence on polymer properties and found that an

increase in the urea group content would enhance the extent of hydrogen bonding between hard segments.

1.1.9 Thermoset polyurethane coatings

The major problems of thermoplastic polyurethane coatings are their poor resistance towards mechanical strains and high temperatures deformation and/or degradation. Generally, their acceptable mechanical properties disappear above 80 °C and thermal degradation takes place above 200 °C.[81] The presence of crosslinks provides thermoset coatings with enhanced tensile strength, abrasion, acid, alkali, and solvent resistance, which is lacking in thermoplastic polyurethane coatings. These performance criteria are essential for most industrial coatings. Therefore, with the aim to further increase final performances and working temperature range, the introduction of chemical crosslinker in the polyurethane structure was also evaluated. Normal crosslinking in the urethane elastomer is reported to occur by reaction of terminal isocyanate groups with urethane groups to form allophanate linkage. Chemical crosslinking was also obtained and controlled by substitution of a trifunctional hydroxyl compound in place of the normal glycol chain extender. Increasing the functionality of the polyether or polyester soft segment also increase the crosslinking concentration. Coatings may contain triols or higher functional polyols[82],[83],[84],[85],[86],[87] isocyanates with functionalities greater than two [88],[89] NCO/OH ratios greater than one [85],[86],[87],[90] or combinations thereof.[85],[86],[87] Peroxides and tri-functional chain extenders have also been utilized to chemically modify the hard domain cohesiveness using chemical crosslinks.[82] The introduction of crosslinker into the hard segment, soft segment or chain extender would reduce the mobility of hard segments and cause a steric hindrance that reduces the ability of hard segments to form hydrogen bonding.[83],[91] Crosslinked polyurethanes have shown great potential in the coatings area due to their high Tg's, ability to form high quality films, good solvent resistance and ease of synthesis and processing. In general, higher crosslinking promotes phase mixing.[92],[93],[94],[95] For example, Thomas et al.[92] altered the level of crosslinking by changing the functionality of the polyol (2.56–2.76) via adjusting the mix of the mono-functional polyether with multifunctional components. These articles suggested that increasing the polyol functionality increased the phase mixing. Therefore, in order to modify the properties of segmented polyurethane for high performance coatings applications, a well-adjusted amount of crosslinker is needed. The presence of crosslinks by deliberate addition of a

crosslinker or in situ generation due to the side product formation seriously prevents the phase separation and produces a polymer which shows both the phase-mixed and phase-separated behavior, depending on the concentration of crosslinker.

1.1.9.1 UV-curable polyurethane coatings

UV-curable polyurethane coatings represent a class of polyurethanes with no or little VOCs. This technique is based on the polymerization of an unsaturated resin system, induced by radiation, to obtain a three-dimensional network. During the cure reaction, the liquid polymer transforms within few seconds into a solid having rubbery or glassy properties at room temperatures. UV-crosslinking has been widely applied in many industrial fields for manufacturing, decoration, and protection of different materials. In fact, there are many advantages to produce coatings by UV-curing, such as: (i) low energy requirement; (ii) very fast and efficient polymerization; (iii) cure selectively limited to the irradiated area; and (iv) no environmental pollution by VOC. The disadvantages are the oxygen inhibition and the need for a UV source. Molecular oxygen at the coating surface is effective at terminating polymerization, which results in low molecular weight and tacky films. A number of methods such as the use of an oxygen scavenger (e.g., tannin, carbohydrazide, etc.), high radiation intensity or initiator concentration, have been used in the recent past to overcome the oxygen inhibition effect.[96] Sometimes, the addition of free amines such as methyl diethanol amine (MDEA) has a beneficial effect on the UV cure process, as they are able to donate a proton to hydrogen abstracting photoinitiators, such as benzophenone. The resultant amine free radicals initiate polymerization in the UV cure process. The main components of UV curable formulations are an oligomer (e.g., acrylated polyurethane as shown in (scheme 1.6), a reactive diluent, and a photoinitiator.[97] The reactive diluent is used not only to control the formulation viscosity, but also to control the cure speed and extent of polymerization, as well as the properties of the cured film. Multifunctional acrylates are the preferred reactive diluents in radiation-cured systems because of their rapid curing rates and low price. The nature of the resultant cured films depends not only on the properties of the components, but also on the photopolymerization kinetics, i.e., the photopolymerization rate and final conversion. The irradiation flux, temperature, sample thickness, photoinitiator concentration, and reactive diluent content for a given resin affect the photopolymerization kinetics to a large extent. Therefore, coatings produced

by UV-curing have lower shrinkage, better flexibility, lower VOC and less sensitivity to oxygen [98] than the coatings obtained with free radical photopolymerization.

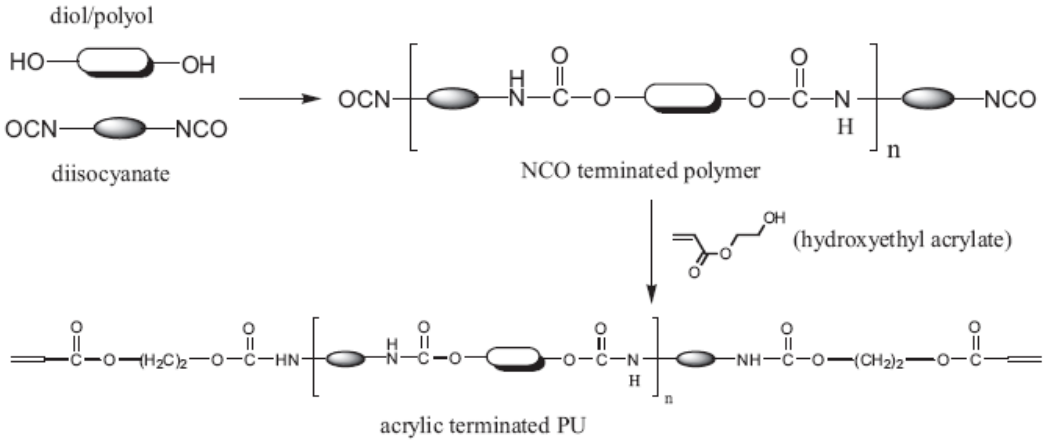

Scheme (1.6): Preparation of acrylic-terminated polyurethane prepolymer for UV cure coatings.

A series of newly developed UV-curable polyurethane coatings were prepared by blending multifunctional thiol- and ene-terminated polyurethane aqueous dispersions. The composition, structure, solution stability and mechanical properties of these coatings were characterized in detail by FT-IR, photo-DSC and DMA measurements. It was found that the resulting polyurethane coatings showed good solution stability and high photopolymerization activity even after a long time (i.e. 1 month). The incorporation of a water soluble polyurethane chain into both the multifunctional thiols and the ene monomers promoted their solution stability and avoided any reaction between thiols and ene groups as a result of their high reacting activity in non-aqueous systems. UV-cured films prepared by this method were found to exhibit excellent physical properties with improvements over what can be attained directly with current UV-curable urethane–acrylate based systems. This method allows for the preparation of high performance UV-curable polyurethane aqueous coatings based on thiol-ene chemistry systems.[99] The polyurethane acrylate resin was synthesised using polyester and polyol (ethylene glycol, adipic acid and 1,6 hexane diol), isophorone diisocynate (IPDI) and 2-hydroxy ethyl methacrylate (HEMA). The different formulations were developed using various reactive diluents viz. monofunctional, difunctional, trifunctional and tetra-functional (ethoxylated phenol monoacrylate, 1, 6 hexane diol di acrylate, dipropylene glycol di acrylate, trimethylol propane triacrylate, propoxylated trimethylol propane triacrylate, pentaerythrol triacrylate – PETA). These samples were cured under UV radiation. For

effective curing, various compositions of oligomers, photoinitiator and reactive diluents were used. The mechanical, optical, rheological, chemical, and stain resistance properties were evaluated. The designed polyurethane acrylate gave good performance properties when used with reactive diluents having different functionality in different ratios for application over metal surfaces as protective coatings for various industrial applications. While using reactive diluents, the coating compositions showed significant improvement of mechanical, physical and chemical resistance properties. Owing to different functionality of reactive diluents used, highly cross-linked structures are formed, which lead to excellent mechanical and chemical properties. The optimum results were obtained with PETA as reactive diluent.[100]

1.1.9.2 Waterborne coatings

The increase interest in waterborne coatings is due to its low VOC content. Waterborne coating technologies require new types of resins for binder dispersions and additives to fulfill high quality requirements.[101][102] An aqueous polyurethane dispersion (PUD) is a binary colloidal system in which the particles of polyurethane are dispersed in a continuous water phase. The particle size tends to be about 20–200 nm, and the particles have a high surface energy. This results in a strong driving force for film formation after water evaporation. Usually, polyurethane polymers are not soluble in water and the degree of hydrophilicity is one of the key factors determining the particle size distributions in the polyurethane dispersion. The shelf life and the colloidal stability of polyurethane dispersions are influenced by their particle size distribution. Therefore, a special treatment or structural modification is necessary for the polymer to be dispersible in water. Generally, aqueous polyurethane dispersions can be prepared by incorporating hydrophilic groups into the polymer backbone or by adding a surfactant. The former material is known as a polyurethane ionomer in which the ionic groups act as internal emulsifiers. Therefore, waterborne polyurethane ionomers consist of polyurethane backbones with a minority of pendant acid or tertiary nitrogen groups, which are completely or partially neutralized or quaternized, respectively, to form salts. Various processes have been developed for the preparation of aqueous polyurethane dispersions. In all of these processes, a medium molecular weight polymer (the prepolymer) is formed by the reaction of suitable diols or polyols (usually macrodiols such as polyethers or polyesters) with a molar excess of diisocyanates or polyisocyanates in the presence of an internal emulsifier as first step. The emulsifier is a diol with an ionic group (carboxylate, sulfonate, or quaternary ammonium salt) or a non-ionic group [poly (ethylene oxide)] is

usually added to allow the dispersion of the polymer in water. The critical step in which the various synthetic pathways differ is the dispersion of the prepolymer in water and the molecular weight buildup. The most important processes are the acetone process, prepolymer mixing process, melts dispersion process and ketimine process.[103],[104],[105],[106],[107],[108] Aqueous polyurethane dispersions are of three types; non-ionic, cationic and anionic depending upon the type of hydrophilic segments present in the polyurethane backbone. Depending on the type of ionic species, a minimum ionic content is required for the formation of a stable polyurethane ionomer. The interaction between ions and their counter ions is responsible for the formation of stable dispersion. The ion-dipole interaction between the ionomer and dispersing media (e.g., water) results in the formation of a solvation sheath , where the ionomer properties depends on the degree of neutralization and content of ionic component.

1.1.9.3 UV-curing technique

A key requirement for UV curing is a UV source that produces high intensity UV irradiation at low cost without generating extreme infrared radiation. The major sources in commercial use are medium pressure mercury vapor lamps. The irradiation has continuous wavelength distribution with major peaks at 254, 313, 366, and 405 nm, among others visible radiation and a minor, but insignificant, amount of infrared radiation that causes some heating. Radiation is emitted in all directions around tubular lamps, and its intensity drops off with the square of the distance from the source. To increase the efficiency, lamps are equipped with an elliptical reflector with a focal length that the radiation is focused at the coating. Thermal energy is also produced. UV irradiation is hazardous and can lead to severe burns. It is essential to avoid exposure of eyes to the radiation. Some amount of ozone is usually generated depending on the radiation source. Since ozone is toxic,the UV unit must be ventilated.[109] For initiation via UV radiation, there must be absorption of radiation by photoinitiator. The fraction of radiation absorbed (I_A/I_o) is related to molar absorptivity (ε), the concentration of photoinitiator (c) and the optical path length of radiation in the film (x). The fraction of absorbed radiation can be expressed by the following equation:

$$IA/Io = 1 - 10^{-\varepsilon cx}$$

Molar absorptivity varies with wavelength. Therefore the fraction of radiation absorbed also varies with wavelength; also the radiation intensity from the source varies as fraction

of wavelength. The total number of absorbed photons per unit time depends on the combination of these factors. When a photoinitiator absorbs a photon, it is raised to an excited state. Some reactions of this excited state lead to generation of an initiating species, but there are also other reactions pathways. For example, molecule may emit energy of a longer wavelength that is it may fluoresce or phosphoresce. It may be quenched by some component of the coating such as oxygen. It can undergo other reactions beside those that lead to initiator generation. The rate of polymerization reactions is related to the concentration of initiating radicals or ions. Higher initiator concentration leads to fast curing. If the concentration is too high, most of the radiation is absorbed in the upper few micrometers of the film and little radiation reaches the lower layers. Since the half-life of a free radical is short, they must be generated within a few nanometers of the depth in the film where they are to initiate polymerization. Optimum photoinitiator concentration is dependent on the film thickness: the greater the film thickness, the lower the optimum concentration. The problem is further a worse when surface cure is oxygen inhibited, as the case in free radical polymerization. The problem of achieving both surface and through cure can be improved by carefully selecting the photoinitaitor or a mixture of photoinitiators that have has two absorption maximums with different molar absorptivities near different emission bands of the UV source. The emission band that is highly absorbed by the photointiator(s) is absorbed molar strongly near the surface and less UV is available for absorption in the lower layers. This band is most important for countering oxygen inhibition. Another factor that affects absorption of UV by the photoinitiator is the presence of competitive absorbers or materials that scatter UV irradiation. The film thickness is not the only variable that affects the path length if the coating is applied on a highly reflective substrate; the rate of cure on a metal substrate is closed to twice as high as over a black substrate.[110]

1.1.9.4 General kinetics of UV-curing

The curing starts when UV light activates the photoinitiator: the photoinitiator splits up into two radicals which may react with the (meth)acrylate groups and subsequently initiate the free radical polymerization. The polymer chain continues to grow until it meets another free radical with which it forms a stable chemical bond or until it abstracts a hydrogen-atom from another molecule that subsequently forms a new radical. The polymerization may be strongly retarded or completely inhibited if the radicals are consumed in competing reactions with other compounds, which are referred to as inhibitors. When present in small quantities, an inhibitor will be completely

consumed in the first moments of the curing, once consumed it plays no further role. However, atmospheric oxygen also acts as an inhibitor and may be replenished from the air; to prevent this oxygen inhibition, radical polymerizations are commonly performed under a nitrogen atmosphere. For a system with ideal behavior, the relationship between the curing rate Rp and the intensity of the UV-light as well as the concentration and reactivity of the photoinitiator and (meth)acrylate is given by: [1*]

$$R_p = k_p \cdot [M] \cdot \sqrt{1000 \cdot \Phi \cdot I_0 \cdot \left(1 - 10^{-\varepsilon \cdot [PI] \cdot d}\right) / \left(d \cdot k_t\right)} \qquad [1^*]$$

where kp is the propagation rate constant in s^{-1}, [*M*] is the concentration of (meth)acrylate in mol/L, Φ is number of initiated polymer chains per absorbed photon, I_0 is the intensity of the incident light in Einstein cm^{-2} s^{-1}, ε is the extinction coefficient in L mol^{-1} cm^{-1}, [*PI*] is the photoinitiator concentration in mol/L, *d* is the thickness of the sample in cm, and *k*t is the termination rate constant in s^{-1}. Rp expressed in mol L^{-1} s^{-1}. Important factors like absorption of the light by components other than the photoinitiator, the effects of the light gradient over the coating, differences in reactivities in monomer mixtures, and changes of the mobility of reactive groups during curing are not taken into account here. Hence, the given equation is useful for getting a feeling for the importance of some process parameters, but the model is too crude for allowing the equation to be used for fitting of experimental data.

1.1.9.5 Derivation of the curing rate equation

The curing rate is mostly determined by the propagation rate Rp for the polymerisation of the (meth)acrylate groups. This propagation rate is determined by the probability that the radical and a (meth)acrylate group meet and the probability that this encounter results in a reaction:

$$R_p = k_p \cdot [M] \cdot [R^*] \qquad [2]$$

Here kp is the propagation rate constant in mol^{-1} L s^{-1}, [*M*] is the concentration of (meth)acrylate in mol/L, and [*R**] is the radical concentration in mol/L. The number of free radicals in the system is determined by the rate at which they are generated and the rate at which they are consumed. The radicals are generated by illumination of the photoinitiator. The rate of this process depends on the number of photons that are absorbed by the photoinitiator and the efficiency with which the absorption of a photon results in the formation of initiating radicals:

$$R_i = 1000 \cdot \Phi \cdot I_a \qquad [3]$$

Ri is the rate of radical generation in mol radicals L^{-1} s^{-1}, Φ is the efficiency of the photoinitiator in radicals $photon^{-1}$, and I_a is the amount of absorbed light in a certain volume in Einstein cm^{-3} s^{-1}. For a system, where the light is only absorbed by the photoinitiator, the amount of absorbed light can be calculated by:

$$I_a = I_0 \cdot \left(1 - 10^{-\varepsilon[PI] \cdot d}\right) \cdot \frac{A}{V}$$

I_0 is the flux of incident light through a certain area in Einstein cm^{-2} s^{-1} (note that the dimensions of Ia and I_0 are not equal), ε is the extinction coefficient of the photoinitiator in L mol^{-1} cm^{-1}, [*PI*] is the photoinitiator concentration in mol/L, A is the exposed area of the sample in cm^2, V is the volume of the sample in cm^3, and *d* is the thickness of the sample in cm. The main process for radical consumption is the reaction between two radicals; the two radicals may form a new covalent bond or one hydrogen atom may be transferred from one radical to the other. The rates of both reactions scale with the probability that two radicals meet and the probability that such an encounter results in either reaction. In a simplified form the radical consumption is expressed by:

$$R_t = k_t [R^*]^2 \qquad [5]$$

Rt is the rate of radical consumption in mol L^{-1} s^{-1} and kt is the termination rate constant in mol^{-1} L s^{-1}. During curing the radical concentration rapidly changes until the rate of radical consumption is in equilibrium with the rate of radical generation (steady state approximation):

$$R_t = R_i \text{, therefore: } \quad k_t [R^*]^2 = 1000 \cdot \Phi \cdot I_a \qquad [6]$$

Leading to:

$$[R^*] = \sqrt{1000 \cdot \Phi \cdot I_a / k_t} = \sqrt{1000 \cdot \Phi \cdot I_0 \cdot \left(1 - 10^{-\varepsilon \cdot [PI] \cdot d}\right) \cdot A/(k_t \cdot V)} \quad [7]$$

It should be noted that due to the light intensity in the coating there is also a gradient in the radical concentration and the calculated [R*] is an average value. This averaged value should only be used if the light absorbance is small, as this implies that also the gradient of the light intensity and hence the gradient of the radical concentration will be small. Combining of equation [7] with equation [2] and V/A = d, the expression for the curing rate becomes:

$$R_p = k_p \cdot [M] \cdot \sqrt{1000 \cdot \Phi \cdot I_0 \cdot \left(1 - 10^{-\varepsilon [PI] \cdot d}\right)/(k_t \cdot d)} \quad [1^*]$$

This equation predicts that thicker coatings give faster curing, which is opposite to general experimental observations.[111]

(But this equation agrees with our experimental observation).

1.1.9.6 Oxygen inhibition

Oxygen inhibits free radical polymerization. In coating application, this inhibition is particularly severe, since the coating films have a high surface area, and oxygen exposure concomitances high. Oxygen reacts with the terminal free radical on propagating molecules to form a peroxy free radical. The peroxy free radical does not readily add to another monomer molecules; thus the growth of the chain is terminated. Furthermore, the excited states of certain photoinitiators are quenched by oxygen, thereby reducing the efficiency of generation of free radicals. Oxygen inhibition can also be reduced by using unimolecular photoinitiators and adding small amount of amines. This produce is useful when low intensity lamps or short exposure times are employed.[112]

1.1.9.7 Overcoming oxygen inhibition in UV curing of acrylate coatings

The free radicals formed by the photolysis of the initiator are rapidly scavenged by oxygen molecules to yield peroxyl radicals.[112] These species are not reactive towards the acrylate double bonds and can therefore not initiate or participate in any polymerization reaction. They usually abstract hydrogen atoms from the polymer backbone to generate hydroperoxides. Moreover, this premature chain termination modifies the mechanical properties of the film. An additional amount of photoinitiator (and UV energy) is therefore needed to consume the oxygen dissolved in the resin as well as the atmospheric oxygen diffusing into the sample during UV-exposure, in order to obtain tack-free coatings showing the required mechanical properties. Overcoming these undesirable reactions has turned into a major challenge. Different methods have been proposed:

1) The addition of amines, which readily undergo a chain peroxiadtion reaction and thus consume the dissolved oxygen.[113] However, the presence of amines in the coating has harmful effects, such as yellowing of the film, odor, and softening of the coating resulting from chain transfer reactions.
2) A conversion of the dissolved oxygen into its excited singlet state by means of red light irradiation in the presence of dye sensitizer. The resulting singlet oxygen will be rapidly scavenged by 1,3-diphenylisobenzofuran to generate the 1,2 dibenzoylbenzene which can work as photoinitiator.[114],[115] However, this method cannot be used for a wide range of applications.
3) An increase of the formulation reactivity to shorten the UV exposure time during which atmospheric oxygen can diffuse into the film. This can be achieved by increasing the photoinitiator concentration and by operating at high light intensities.[116] Oxygen inhibition can be further reduced by using high intensity flashes which generate large concentrations of initiator radicals reacting with oxygen, but again, hydroperoxides are being formed.
4) Wax barrier coats[117] or performing the UV exposure under water[118] to slow down the diffusion of atmospheric oxygen into coatings. This will affect in the surface properties of the UV-cured polymer.
5) Performing the radical photopolymerization under inert conditions[119],[120],[121] which is noticeably the most efficient way to overcome oxygen inhibition. Nitrogen is continuously flushed over the sample during UV-exposure. On industrial UV-curing lines , which cannot be made completely air light, nitrogen

losses can yet be important, thus making the process expensive, and even more so if argon is used to achieve an oxygen free environment. It has been shown that nitrogen can be advantageously replaced by carbon dioxide to achieve a fast UV-curing under oxygen.[122] This technique has the following advantages.

- Carbon dioxide is well available and it is not more expensive than nitrogen. Carbon dioxide is heavier than air and can therefore be easily maintained in a container without much loss. By excluding oxygen, this technique will ensure a faster and more completely curing, thus providing UV-cured coatings shown improved surface properties, in particular a higher gloss, and better scratch resistance than cured in the presence of air.[116] By using a pool-type photoreactor, 3D objects can be readily UV cured by this process even under dim light.[123]

1.1.9.7 Vehicles for free radical initiated UV-cure

Most current coatings use acrylated reactants. Acrylate, rather than methacrylate, esters are used, since acrylates cure more rapidly at room temperature; they are also less oxygen inhibited. Furthermore, polymerization of acrylates tends to terminate by combination, whereas methacylate polymerization terminates largely by disproportionation. The extent of the crosslinking, as well as high molecular weights is favored when termination of growing radicals occurs by combination. In general, the vehicle consists of two types of acrylate esters: multifunctional acrylate-terminated oligomers and acrylate monomers. The monomers range from mono- to hexafunctional. Most common are mixtures of mono-,di- and trifunctional acrylates. The monomers are called reactive diluents. Multifunctional oligomers increase the rate of crosslinking, owing to their polyfunctionality. They control the properties of the final such as abrasion resistance, flexibility, and adhesion.[124] A range of monofunctional acrylates have been used. Those with lowest molecular weight tend to reduce the viscosity most effectively, but may be too volatility. Hydroxyl acrylate has low volatility. Exthoxethyl acrylate, isobornyl acrylate, 2-hydroxyethyl acrylate (HEA) and others are also used. Small amounts of acrylic acid are common monomers promote adhesion. 2-hydroxyethyl acrylate has low volatility, high reactivity, and imparts low viscosities, but the toxic hazard is too large in many applications. N-vinylpyrrollidone (NVP) is an example for a nanoacrylate monomer that copolymerizes with acrylates at speeds comparable to acrylate polymaerzation. NVP is particularly useful because the amide structure

promotes adhesion to metal and reduces oxygen inhibition. However it introduces a possible toxic hazard.[125]

1.1.10 Thermal-initiated crosslinking

The energy required for the dissociation of the initiators can also be supplied thermally. The generation of the free radicals depends on the minimum energy to required break the covalent bond, then bond dissociation energy a (D). Thermal initiation can be used, should the bond dissociation energy be about 120-170 kJ/mol. Initiator molecules having dissociation energies values outside this range dissociate either too slowly or too rapidly. Compounds involving oxygen-oxygen, suphur-oxygen or oxygen-nitrogen single covalent bonds have been found to be in the desired range.[126] Azo compounds containing a nitrogen atom connected to carbon and nitrogen atom through a single and double bond respectively, can also be used as thermal initiators. However the driving force for the azo type initiators is not only the dissociation energy, but the stable nitrogen formed in the dissociation reaction.[127] The most widely used thermal initiators are peroxides due to availability, stability, efficiency and rate of dissociation. The decomposition of the peroxides and the radical formation mechanisms has been reviewed earlier.[128],[129]

1.1.11 Dual curing of urethane acrylate coatings using UV and thermal curing

A number of investigations on thermal and photochemical curing of isocyanate and acrylate functionalized oligomers have been already addressed by developing "dual cure" systems which contain two types of reactive functions,[130],[131],[132],[133],[134],[135],[136] a UV-curable functional group and a thermally curable system. After heating and exposure to UV-light, such resins will generate a crosslinked polyurethane polyacrylate network exhibiting good mechanical properties, even in the non-irradiant areas. One can combine either hydroxyl functionalized acrylate oiligomers with isocyanate crosslikers or isocyanate functionalized acrylate oligomers with polyols by using a low viscosity isocyanate allophonate polyurethane acrylate developed by BASF.[137] Dual-cure formulations have been developed in applications of UV-irradiation curing and achieve a sufficient cure of the non-illuminated areas of protective coatings, like the shadow areas of three dimensional substrates or deep-lying layers of thick pigment coatings.[138] Most UV-curable resin are applied to a flat substrate (metal, glass, wood, plastic, paper).

Nowadays there is a growing demand to apply UV-technology to coat three dimensional objects. Achieving a uniform illumination of large three dimensional objects has already been successfully addressed,[139],[140],[141] but there is still an important issue, which on greater from the presence of some shadow areas which can hardly be reached by UV-irradiation and will therefore remain uncured. Dual-cure systems combining UV-irradiation and thermal treatment have been developed.[142],[143],[144],[145],[146]

1.1.11 Selection and modification of polyurethane coatings

In modifying the backbone structure of polyurethane coatings, it is necessary to consider the end use for the coating and the cost of modification. The following factors must be considered while selecting a material in a specified environment: (1), the properties of the modified polyurethane coating such as hardness, strength, stiffness, thermal stability and expansion coefficient. (2) The resistance of the coating towards mechanical, thermal and chemical stress during service. (3) The compatibility of the coating and the substrate over the temperature range of expected application. This includes minimizing thermal stresses (by matching thermal coefficients) and providing good coating–substrate adhesion. (4) Ultimately, whether or not a particular coating will be used depends on the trade-off between the benefits to be gained and the additional cost to be incurred. When the application is critical and the consequences of failure are disastrous, higher costs are justified, particularly when there is no other alternative. Additionally, for a better protection of the substrate, knowledge of the following parameters is of paramount importance: coating application method, composition, thickness, hardness, coating–substrate adhesion, friction coefficient, wear resistance, Young's modulus, thermal expansion coefficient, heat conductivity, density, specific heat of both coating and substrate and information on residual stresses to assess the overall stress level exhibited by the coated body.[147]

1.2 Nanoparticles

1.2.1 Clay

Talc, mica montmorillonite, hectorite, laponite and saponite belong to the general family of 2:1 layered or phyllosilicates and are characterized by a moderate negative surface charge (qualified by cation exchange capacity (CEC) and expressed in meq/100 g). Montmorillonite is an expandable dioctahedral smectite with a mean layer charge density of 0.25–0.50 equiv/mol and consist of disc-like shaped layers of 100 nm in diameter and 1 nm thickness. The layers are made up of two silicate tetrahedrons fused to an edge-shared octahedral sheet of either aluminum or magnesium hydroxide. Isomorphic substitution within the layers generates negative charges, which are compensated by alkaline earth or hydrated alkali-metal cations (Na^+, Ca^{2+}, Mg^{2+} or K^+) residing in the gallery space.[148] The layers swell in water and the 1-nm-thick layers can be easily exfoliated by shearing, giving platelets with high aspect ratio. The ion exchange reactions of montmorillonite with various organic cations such as alkyl ammonium cations or cationic surfactants produce hydrophobic and organically modified montmorillonite. The organic cations lower the surface energy of the silicate layers and increase the basal-plane spacing (d spacing). This improves wetting, swelling, miscibility between the silicate layers and the polymer and exfoliation of the aluminosilicate in the polymer matrix. Additionally, the organic cations may contain various functional groups that react with the polymer to improve adhesion between the inorganic phase and the matrix.[149],[150],[151],[152]

1.2.1.1 Laponite clay –nanofiller

Laponite is synthetic hectorite clay with a thickness of 1 nm and diameter about 30 nm. Laponite has the advantages over natural clays of being chemically pure and free from crystalline silica impurities. The shape of the laponite crystals combined with its anionic nature enables laponite to produce films which can be used in the manufacture of low cost, electrically conductive, antistatic, protective coatings and in optical waveguide applications.[153] Laponite RDS is a sol forming grade of synthetic layered crystalline silicate incorporating an inorganic polyphosphate peptiser. Its composition is 54.5% SiO_2, 26.0% MgO, 0.8% Li_2O, 5.6% Na_2O and 4.4% P_2O_5. When added to water, Laponite RDS hydrates and swells to give colorless, transparent, low viscosity colloidal

dispersions. The nanoscale Laponite crystals can be understood as two-dimensional discs with negatively charged surfaces and positively charged edges. The Laponite crystals interact with the silica network in two ways: firstly the crystals stack and are held in a gel-like structure through electrostatic bonds; secondly, hydroxyl groups on the edges of the crystals bond with newly formed silica aggregates. In this mixing way and porous stacking structure of Laponite and silica is achieved. The structures have up till now to be investigated by high resolution transmission electron microscopy (TEM) which should help reveal the true nanostructure. As the concentration of the Laponite dispersion is increased, the crystals are forced into closer contact and more particle-particle interactions between positively charged edges and negatively charged faces occur. This reduces the mobility of the particles within the dispersion, resulting in an increase in viscosity. With the higher concentration samples, the crystal interactions begin before silica sol formation and a Laponite gel-like structure results early in the sol-gel process. Laponite improves the performance and properties of a wide range of material. There are two key areas of functional use for Laponite:

1) As a rheology modifier-Laponite may be added to the formulation of many waterborne products such as surface coatings, household cleaners and personal care products. It will impart thixotropic, shear sensitive viscosity and improve stability.
2) As a film former - Laponite is a film forming agent and is used to produce electrically conductive, antistatic and barrier coatings.[154]

1.2.2 Silica nanoparticles

1.2.2.1 Aerosil-nanofiller

Aerosil is a fine white, light and amorphous powder consisting of primary particles in the nanometer range (10-40nm) and very large specific surface area (50-400m^2/g). The primary particles are not isolated but are fused together in relatively stable chain-like aggregates, which in turn from larger agglomerates in the micrometer range. The physical and chemical properties of aerosil can be varied within wide limits depending on the process parameters**.** The silanol groups of the aerosil, i.e freshly formed hydrophilic aerosil, can react with organosilicon compounds to form hydrophobic aerosil. Freshly prepared hydrophilic aerosil is treated directly after the deacidification step.[155]

1.2.2.2 Köstrosol

Köstrosol is a colloid solution of dispersed SiO_2 particles in water (colloidal silica). The particles are not visible by naked eye, but are clearly identifiable under an electron microscope. They have average a diameter of around 20 nm. The colloidal silica is generally odorless (apart from AS types), non flammable, miscible with water at any ratio and it is opaque to milky white in appearance. In the paints and coatings industry, colloidal silica is used for production of zinc-based primer compounds for anti-corrosion coatings. Furthermore, if it is applied with silanes, a protective coating can be produced, for example for the coil coating and sector, with significantly increased scratch resistance.[156]

1.2.3 Silane coupling agent

Silane coupling agents have the ability to form a durable bond between organic and inorganic materials. Encounters between dissimilar material often involves at least one member that is siliceous or has surface chemistry with siliceous properties; silicates, aluminates borate, etc. Interfaces involving such materials have become a dynamic area of chemistry in which surfaces have been modified in order to generate desired heterogeneous environment or to incorporate the bulk properties of different phases into a uniform composites structure.

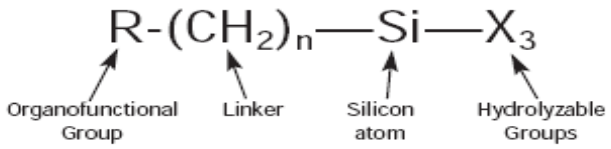

Scheme (1.7): Silane coupling agent

The general formula for a silane coupling agent as shown in (scheme 1.7). Typically, there are two classes of functionality. X is a hydrolyzable group typically alkoxy, acyloxy, or halogen. Following hydrolysis, a reactive silanol group is formed, which can condense with other silanol groups, for example, those on the surface of siliceous fillers, to form siloxane linkages. Stable condensation products are also formed with other oxides such as those of aluminum, zirconium, tin, titanium, and nickel. Less stable bonds are formed with oxides of boron, iron, and carbon. Alkali metal oxides and carbonates do

not form stable bonds with Si-O-. The R group is a nonhydrolyzable organic radical that may posses a functionality that imparts desired characteristics.

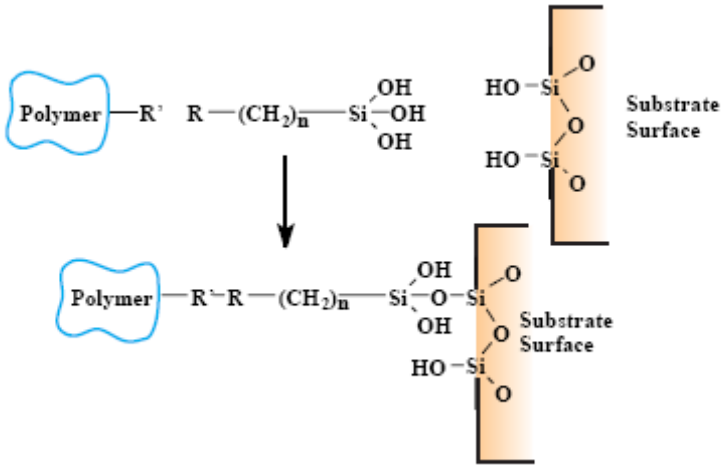

Scheme (1.8): Coupling agent mechanism

As shown in scheme (1.8), the resulting product is an organosilane. Its influence on the substrate properties ranges from altering the wetting or adhesion characteristics of the substrate, the catalyzing chemical transformations at the heterogeneous interface, ordering the interfacial region, and modifying its partition characteristics. Significantly, this type of modifications includes a covalent bond between organic and inorganic materials. Most organosilanes have one organic substituent and three hydrolyzable substituents. In the vast majority of surface treatments, the alkoxy groups of the trialkoxysilanes are hydrolyzed to form silanol-containing species.[157]

1.2.4 Sol–gel reactions

The reaction is generally divided into two steps: hydrolysis of metal alkoxides to produce hydroxyl groups in the presence of stoichiometric water (usually in the presence of acid or base catalyst), followed by polycondensation of the resulting hydroxyl groups and residual alkoxyl groups to form a three-dimensional network as shown in scheme (1.9). Different metal alkoxides based on silicon, aluminum, transition metal alkoxides such as titanium and zirconium also have been used as sol–gel precursors in combination with a variety of organic components. For non-silicate metal alkoxides, no catalyst is needed for hydrolysis and condensation because these are very reactive themselves. The sequence of reactivity is expressed as follows:

$Zr(OR)_4$, $Al(OR)_3$> $Ti(OR)_4$> $Sn(OR)_4$> $Si(OR)_4$

However, owing to the loss of volatile by-products formed in the hydrolysis–condensation reactions, it is difficult to control sample shrinkage during three dimensional network formation.[158],[159],[160],[161],[162] Factors such as the nature of the alkyl group, solvent, temperature, water to alkoxide molar ratio, presence of acid or base catalysts, etc., are known to effect the hydrolysis reaction.[163] For example, in the presence of base catalyst, the rate of condensation is fast compared to hydrolysis and results in the formation of dense, colloidal particles. On the other hand, the rate of condensation is slow relative to the rate of hydrolysis under acid catalysis and the resultant silica has a highly ramified, low fractal dimensional structure with many silanol groups on the silica surface.[164]

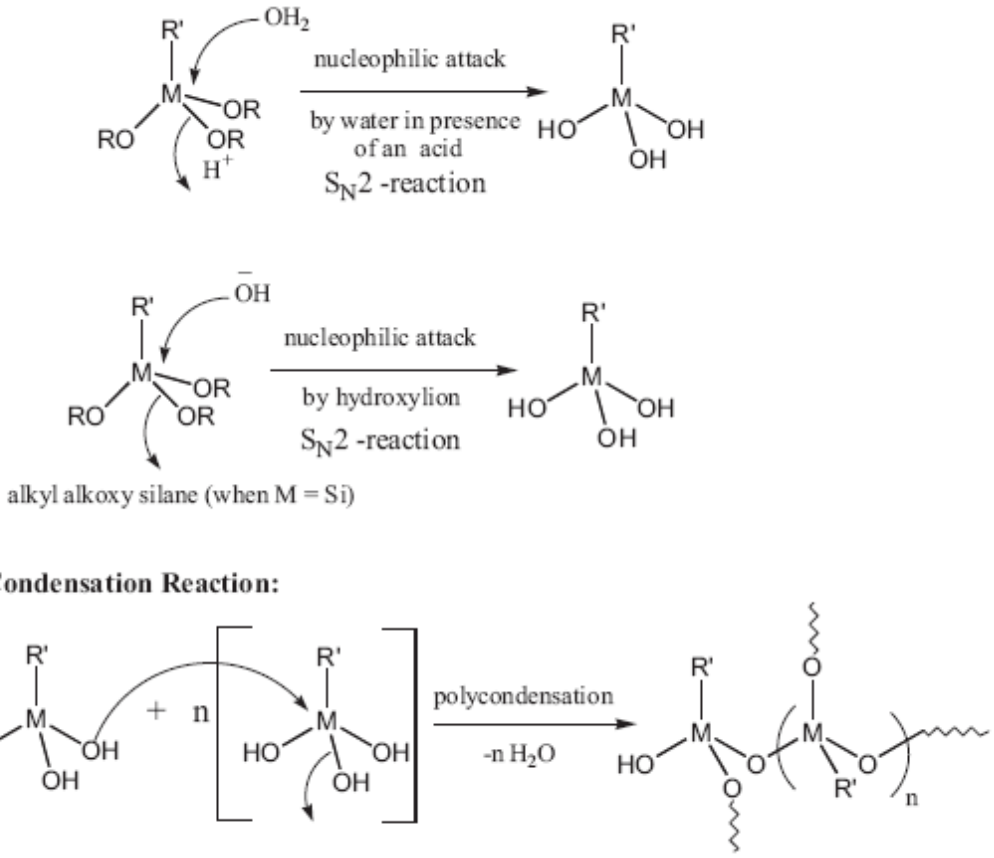

Scheme (1.9): Sol-gel hydrolysis and condensation polymerization reaction.[158]

The precursors of which compounds are organo-substituted silicic acid esters of general formula $R`_nSi(OR)_{4-n}$ and bridged precursors of silsesquioxanes $X_3Si–R`–SiX_3$ (X = Cl, Br, OR); where R` can be any organo functional group and is usually 1 or 2. If R` bears any reactive group that can, for example, polymerize or copolymerize (e.g., methacryloyl, epoxy, amino, isocyanate, vinyl or styryl groups) or undergo hydrolysis-condensation (trialkoxysilyl groups), it will act as a network former. Therefore, siloxane hybrids can be easily synthesized as the $Si_2C_{sp}^3$ bonds are covalent and stable towards nucleophilic attack by water, alcohols, hydroxylated ligands, etc. They can be used, for example, as building blocks for the formation of highly ordered polyhedral oligomeric silsesquioxane (POSS) clusters[165],[166] and as organosilane coupling agents for ceramic particle coatings [167],[168] Some sol-gel precursors is shown in scheme (1.10).[169]

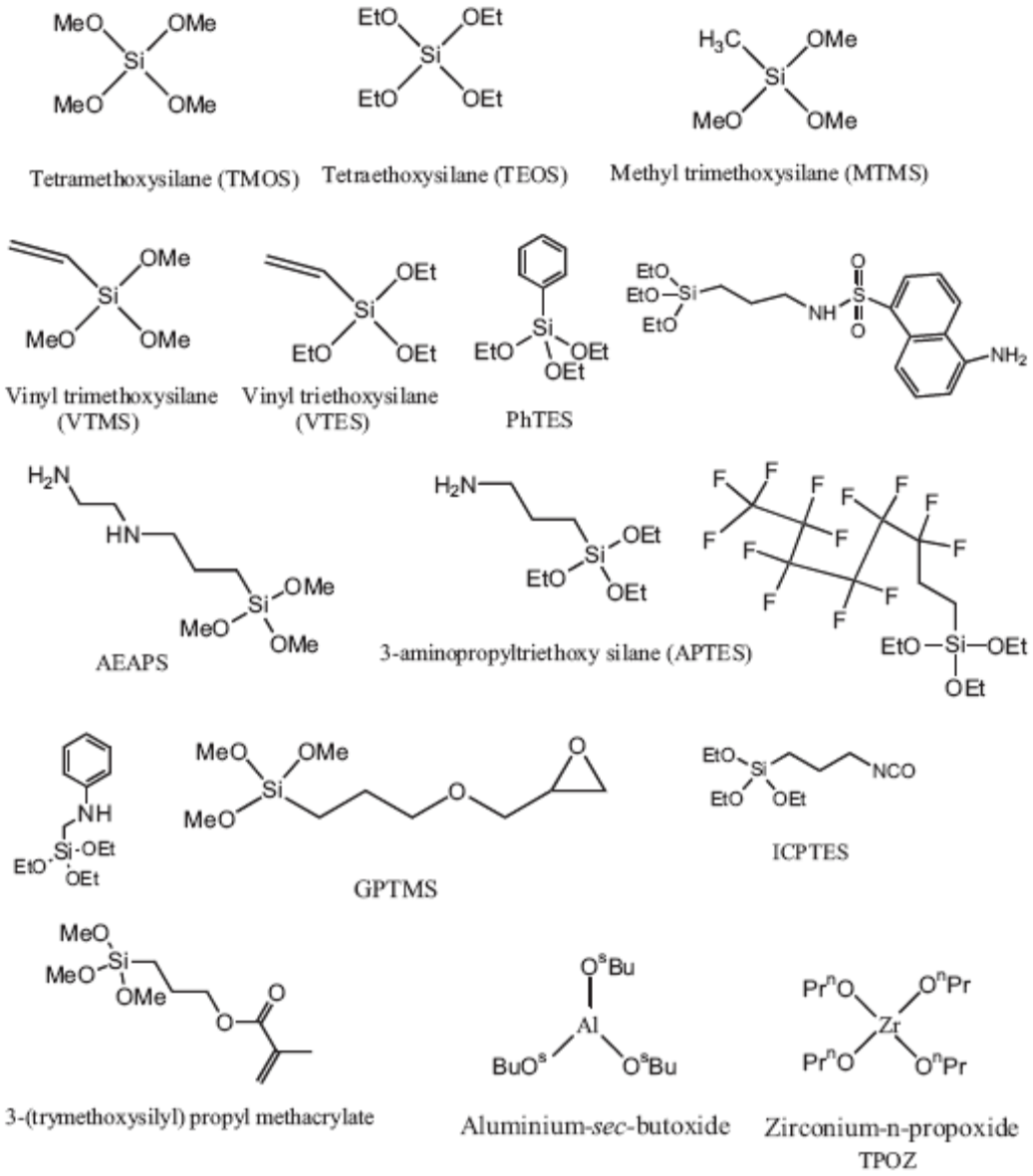

Scheme (1.10): Different sol-gel precursors which used in coating applications.[170]

1.2.4.1 Application of sol–gel process in coatings

Atanacio et al.[169] studied the mechanical properties of various hybrid sol–gel films on copper substrates using nanoindentation and tensile testing and observed the dramatic change in indentation response and interfacial adhesion with the change in organic alkyl substituents (R`) to the inorganic sol–gel network. Goda and Frank [164] observed that even though a silica component may destroy the ordered hydrogen bonded structure of hard segment in the polyurethane, at appropriate concentrations of silica the

derived material showed improved mechanical and thermal properties. Zhang et al.[171] synthesized self-crosslinkable polyurethane-urea formulations extended with different contents of aminoethyl aminopropyltrim-ethoxysilane (AEAPS). Two routes for the synthesis of sol–gel polyurethane coatings from the reaction of NCO-capped polyurethane prepolymer with triethoxy silane precursor (aminophenyl) triethoxysilane (APTES) and AEAPS are shown in scheme (1.11).

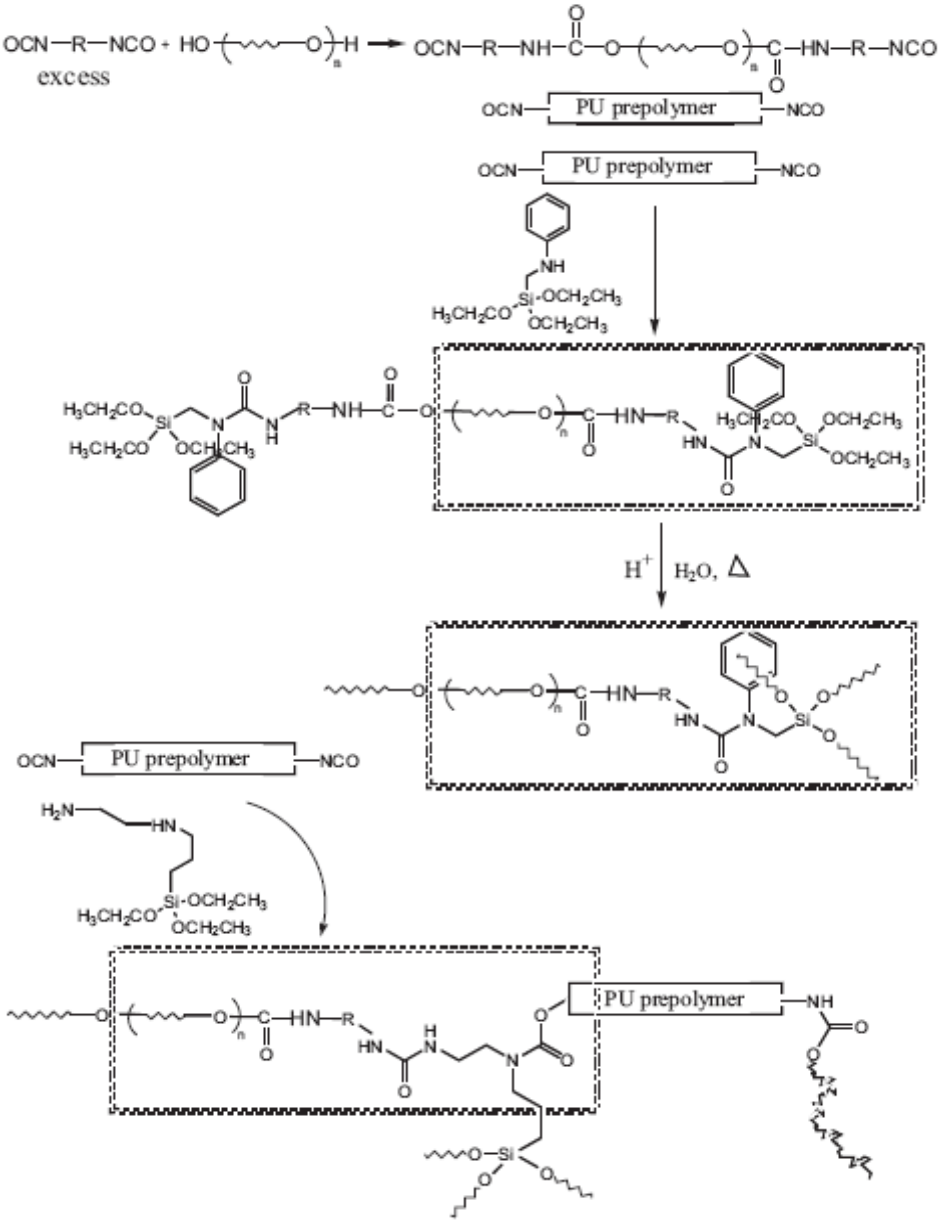

Scheme (1.11): Preparation of polymer sol–gel precursors and the sol–gel process to form organic–inorganic hybrid coatings.

1.2.5 Nanocomposite coatings

Polymer–clay nanocomposites are a new class of filled polymers in which clay platelets are dispersed in a polymer matrix at the nanometer scale. These silicate nanocomposite coatings possess several advantages, such as (i) lighter weight due to the low clay content (between 2 and 5wt%), which is economically interesting; (ii) improved mechanical behavior i.e., higher stiffness and strength [172],[173]; (iii) better barrier properties due to reduction in straight way movement of water and oxygen molecule; (iv) improved thermal properties, such as fire retardance and heat distortion temperature (HDT) [174] Several routes were developed to achieve a high degree of dispersion of the clay nanoplatelets: (i) in situ polymerization of monomers which were initially intercalated between silicate layers, (ii) melt intercalation and further exfoliation for thermoplastic polymers and (iii) combination with a polymer solution.. Depending on the nature of the components used (layered silicate, organic cation and polymer matrix) and the method of preparation, three main types of composites may be obtained when layered clay is associated with a polymer. When the polymer is unable to intercalate between silicate sheets, a phase-separated composite fig. (1.1a) is obtained, whose properties are in the same range as traditional microcomposites. However, this is not a nanocomposite. There are two possible types of nanocomposites with dispersion at the nanometer level. Fig. (1.1b) shows the intercalated structure, where a single (sometimes more than one) extended polymer chain is intercalated between the silicate layers resulting in a well ordered multilayer morphology with alternating polymeric and inorganic layers. When polymers intercalate layered silicates, the interlayer distance increases and the silicates are broken down into their nanoscale building blocks. When the silicate layers are completely and uniformly dispersed in a continuous polymer matrix, an exfoliated or delaminated structure is obtained fig (1.1c) [175],[176],[177] The delaminated structure is of particular interest because it makes the entire surface of clay layers available for the polymer and thereby maximizes polymer–clay interactions. In such an environment, the interfacial bonding between the polymer matrix and the reinforcing materials will be dramatically increased.[178],[179]

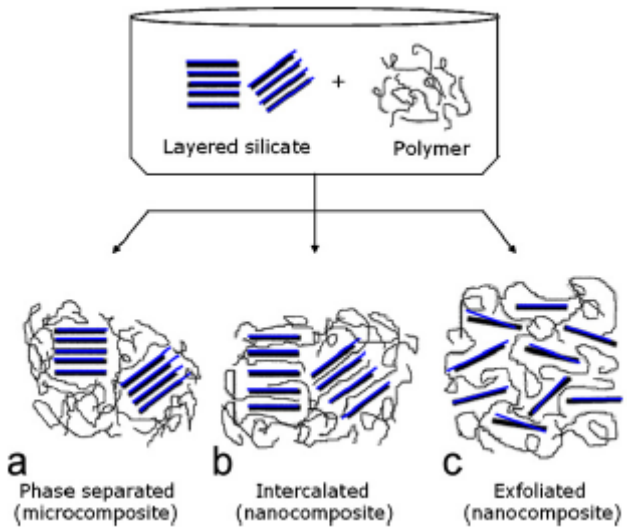

Figure (1.1): Different types of composite arising from the interaction of layered silicates and polymers: (a) conventional composites (microcomposites)-phase separated, (b) Intercalated nanocomposites, and (c) exfoliated nanocomposites.[175]

1.3 Anti-fog coating

1.3.1 Fog formation on plastic films

The term "fog" is used to describe the condensation of water vapour on the surface of a transparent plastic film in the form of small discrete droplets. Physical conditions leading to this phenomenon are:

1) Decrease in temperature on the inside of the film below the dew point of the enclosed air/water vapour mixture.
2) Cooling of the air near the film to a temperature at which it can no longer retain all water vapour; excess water condenses upon the film. Internal antifog agents are directly incorporated into plastics to achieve the spreading of condensed water droplets into a continuous and uniform layer of water on the fabricated film.

1.3.2 Principle of action

Polyolefins are hydrophobic and typically exhibit surface tensions around 30 mJ/m^2. When polyolefins are in contact with a polar liquid like water, which exhibits a higher surface energy (72 mJ/m^2), then liquid droplets are formed which do not spread as a uniform layer over the polyolefin surface. Internal anti-fog additives are surface active agents, which have a balanced incompatibility with the polymer matrix. They are added during the extrusion process in pure form, as concentrate or masterbatch. When the film is made they are uniformly dispersed throughout its thickness but they subsequently migrate to the film surface, where they increase the critical wetting tension. This is combined with a partial solubility of the anti-fog agent in water, which leads to a decrease in surface tension of the water, which will significantly diminish the difference between the surface tension of water and the polymer as illustrated in figure (1.2)

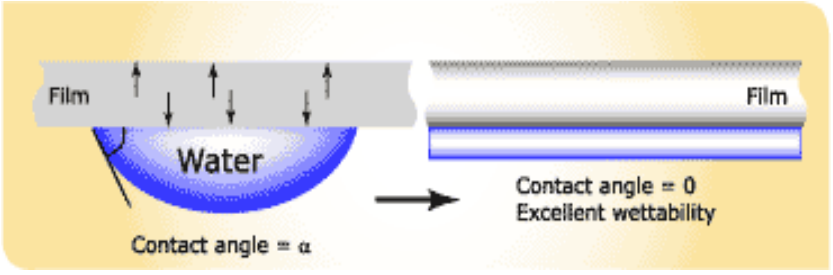

Figure (1.2): Migration of the anti-fog agent

The result is a reduction in contact angle between water and polymer surface, permitting the water to spread into a more uniform layer. The resulting transparency removes the optical barrier caused by the discrete droplets and overcomes the undesirable effects. The use of an internal additive, distributed throughout the thickness of the film, leads to a "reservoir" effect, which increases the useful life of thicker films for any specific concentration of anti-fog agent.

1.3.3 Consequences of fog formation

A number of undesirable effects may result from fog formation in agricultural, horticultural and food packaging applications. Where films are used as part of a greenhouse system or another aid of agricultural or horticultural control, the light transmission will be reduced. The following problems will result:

1) Slower plant growth rate.
2) Delayed crop maturity and hence delayed date sale.
3) Reduced crop yield per plant.

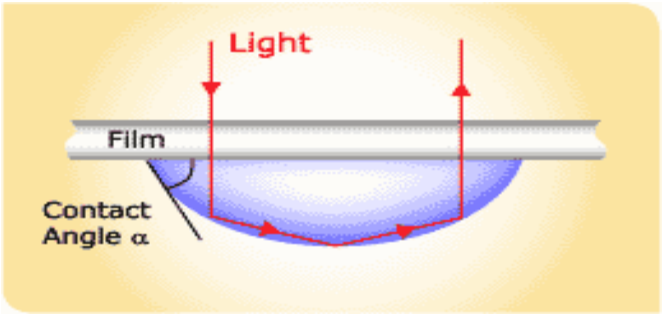

Figure (1.3): The shape of water droplets rather than their size is mostly responsible for changes in the light distribution.

The shape is determined by the contact angle between the water surface and the substrate surface the contact angle (α) is high, total internal reflection will lead to some of the incident light being returned through the film. The average light transmission will be seriously reduced. Light (and heat) transmission may be focused on delicate plant

tissue owing to water droplets acting as lenses, causing burning of the plants and crop spoilage.

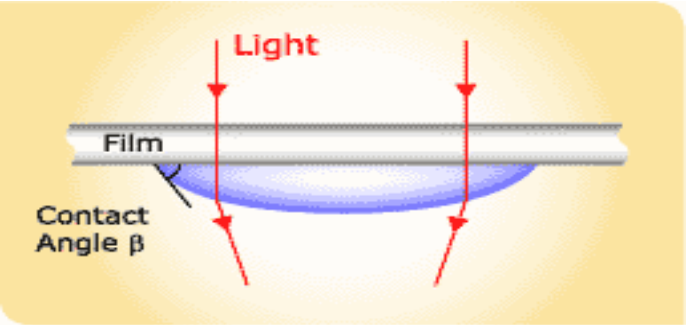

Figure (1.4): When the contact angle (β) is low, light is refracted at the water/air interface, giving an uneven distribution. In extreme cases, light may be focused because the water drop acts as a lens**.** The coalescence of small drops into larger ones will create dripping, allowed by an increase in plant diseases and plant damage (especially seedlings).

1.3.3 Foods wrap applications

Films are often used for food wrap, especially for wrapping items meant to be displayed or stored in refrigerated conditions. Fog reduces the films transparency.[180]

1.3.4 Anti-fog coatings based on UV-curable polymers

Fogging can be prevented by either modifying the surfaces to become very hydrophobic surfaces (preventing condensation of water or leading to immediate roll-off) [181] or modifying the surface to become very hydrophilic (such that the droplets spread to form smooth transparent film [182],[183]). The later is more common. More resistant coatings are needed for application such as industrial and sport safety lenses or visors [184], automotive windows, bathrooms mirrors and windows on the commercial freezers. These coatings have to fulfill the following requirements:

1) Droplets must spread
2) Spreading must be maintained after extended exposure to contaminating substrates.
3) The films must be still optically transparent.
4) The films must be mechanically stable.

Anti-fog coatings are usually used for transparent glass or plastic surfaces in optics, such as the mirrors, lenses, goggles, binoculars, camera objectives and windows. These coating mostly are based on the application of surfactant1[182] or hydrophilic Nanoparticles[185] to create a hydrophilic surface. They are available as spray solutions, gels, crèmes and wet tissues. Since they are not durable, they need to be reapplied regularly. To obtain durability, it is envisioned to make the coating UV-curable. Highly crosslinked polymers containing both hydrophilic and hydrophobic nanodomains should be used. These polymers contain olefinic repeat groups, which are crosslinked in a free radical polymerization in presence of photoinintiator.[186] UV-curable coatings can be easily applied many plastics substrates such as acrylics, polycarbonate (PC), polystyrene (PS) and polyvinyl chloride (PVC). UV-curable coatings were found be have abrasion resistance for superior to conventional acrylics and two components urethanes.[187] They perform well in long term weathering, impact resistance, chemical resistance, and scratch resistance.[188] The commonly used resins for UV-cured coatings are polyester, epoxy, and polyurethanes. Polyesters have low viscosity, moderate cost and little yellowing but they have poor surface cure (wrinkling and skin formation). They are often used as wood filler, primer, laminating adhesive, ink and paper coating. Epoxies are characterized by fast cure, good adhesion, good chemical resistance, and low cost. They produce hard films but the disadvantage of yellowing. The most important advantages of polyurethanes are flexibilites, toughness, abrasion resistance, and excellent weather ability for aliphatic types but they have yellowing for aromatic types. Therefore, the envisioned anti-fog coatings would be applied using polyurethanes with aliphatic types and as a thin films.

In recent years, there are significant progresses in the use of uv-curing waterborne polyurethane dispersions (UV-PUDs).[189],[190],[191],[192]

2 Preparation and Characterization of Thermal-Cured Anti-Fog Transparent Polyurethane Films

2.1 Materials

The materials and their chemical formulae used in this chapter are in the table 2.1

Table (2.1): The materials and their chemical formulae

N.	substance	Chemical formula	Supplier
1	Poly(ethylene glycol) PEG $_{1000}$,	$H(OCH_2CH_2)_nOH$, Mol. Wt. 950-1100	Merck
2	Isophorone diisocyanate (IPDI)	$OCNC_6H_7(CH_3)_3CH_2NCO$ Mol. Wt. 222.28	Merck
3	Dibutyltin dilaurate (DBTL)	$(CH_3CH_2CH_2CH_2)_2Sn[OCO(CH_2)_{10}CH_3]_2$ Mol. Wt. 631.56	Fluka
4	2-Hydroxyethyl acrylate (HEA)	CH_2=$CHCOOCH_2CH_2OH$ Mol. Wt.116.12	Alfa Aesar Gmb.
6	Azo bis iso butyronitrile (AIBN)	$(CH_3)_2C(CN)N$=$NC(CH_3)_2CN$ Mol. Wt.164.21	Aldrich
6	Aerosil R972		Degussa
7	Aerosil 200		Degussa
8	Laponite		Kockwood additives limited
9	(3-Aminopropyl)triethoxysila-ne (APTES)	$H_2N(CH_2)_3Si(OC_2H_5)_3$ Mol. Wt. 221.37	Aldrich

2.2 Experimental details

2.2.1 Preparation of polyurethane copolymer solution using PEG_{1000}: IPDI: HEA at ratios 1:2:2 (Acronym A)

Procedures

1- 70 g PEG_{1000} (0.07 mol) + 30 g acetone were mixed. The mixture fed into a three-necked flask equipped with a mechanical stirrer. The stirrer was operated at 100 rpm. A reflux condenser was employed. The temperature was 50 °C. The reaction was occurred under nitrogen atmosphere for 30 minutes.

2- 31.6 g (0.014 mol) IPDI + 50 mg DBTL were mixed. The mixture was slowly dropped into the reactor under the above conditions for 2.1/4 hours.

3- The system was further reacted under the above conditions for an additional 30 minutes.

4- 16.26 g (0.014 mol) HEA was added drop by drop to the reactor at 35 °C for 1.5 hours.

5- The reaction mixture was stirred for additional 30 minutes at 35 °C.

6- The resulting clear and viscous solution was diluted by using acetone to obtain a diluted polyurethane copolymer solution with 50% (w/w).

2.2.2 Preparation of polyurethane copolymer solution acronym using PEG_{1000}: IPDI: HEA at ratios 1:2.5:2.5 (Acronym B)

Procedures

1- 70 g (0.07 mol) PEG1000 + 30 g acetone were mixed. The mixture fed into a three-necked flask equipped with a mechanical. The stirrer was operated at 100 rpm. A reflux condenser was employed. The temperature was 50 °C. The reaction occurred under nitrogen atmosphere for 30 minutes.

2- 39 g (0.175 mol) IPDI + 70 mg DBTL were mixed. The mixture was slowly dropped into the reactor at the above conditions for 2 hours.

3- The system was further reacted under the above conditions for an additional 30 minutes.

4- 20.35 g (0.175 mol) HEA was added drop by drop to the reactor at 35 °C for 1 hour.
5- The reaction mixture was stirred for additional 1/2 hour at 35 °C.
6- The resulting clear and viscous solution was diluted by using acetone to obtain a diluted polyurethane copolymer solution with 50 % (w/w).

2.3.1 Preparation of anti-fog transparent polyurethane films by using a film applicator [193]

The polyurethane solution was diluted with acetone at different percentages. Different percentages of AIBN as a thermal initiator were added to the polyurethane solutions. Subsequently, the polyurethane solutions containing thermal initiator were cast by using the applicator at wet thicknesses of 120, 90, 60, and 30 μm. The film applicator (BYK Gardner 67299, cat. N. 2030) is made from hardened stainless steel with a flat edge beveled blade applicator body; The BYK 67299 applicator-frame is suitable for gelatin or other products with low viscosity. The product is applied on flat and relatively firm surfaces in a range of film widths. Supplied with a set of nineteen gauges from 30 to 1000 μm (1 to 40 mils) to accurately set the gap by vertical adjustment of the scraper as illustrated in Fig (2.1).

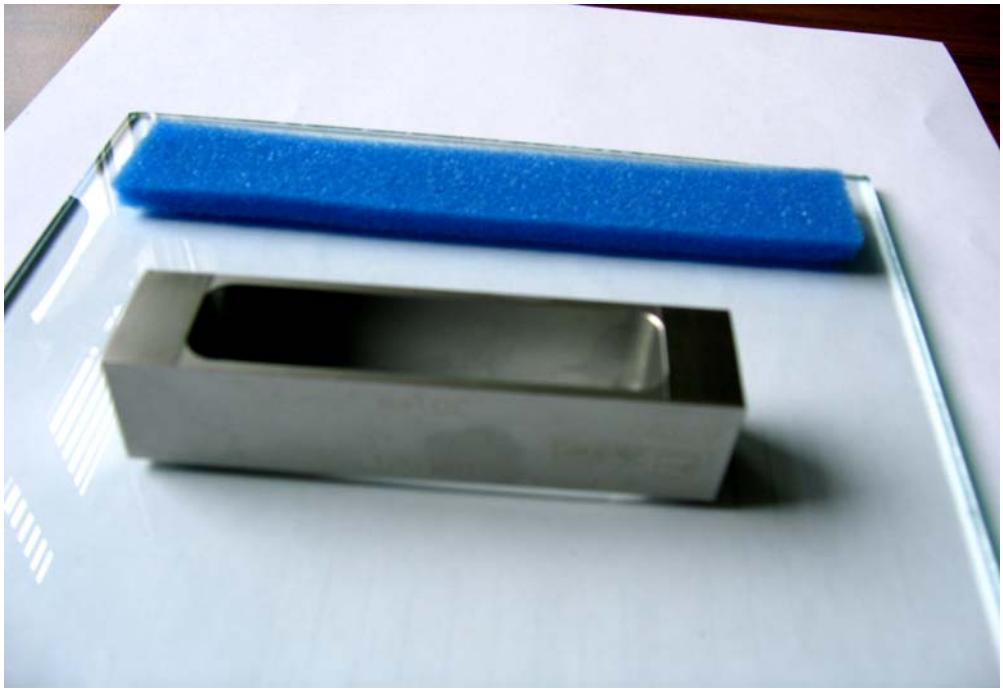

Fig. (2.1): The film applicator (BYK Gradner) .

The polyurethane films were left for 30 minutes allow for evaporation of the solvent. Subsequently, the polyurethane films were held in an oven at different temperatures. There were several factors changed such as temperature, holding time, percentage of AIBN as a thermal-initiator, and ramp or preheat method.

2.3.2 Preparation of anti-fog transparent nano-particles/polyurethane films on the glass substrate

The polyurethane solution was diluted at different percentages with acetone. Different percentages of AIBN were added as thermal-initiator as mentioned before. The Aerosil nano-particle was dispersed as nano-filler in the polyurethane solution by using a magnetic stirrer. Subsequently, the films were cast on the glass or polycarbonate substrate by using a film applicator at wet thicknesses of 120, 90, 60 and 30 μm.

2.3.3 Preparation of anti-fog transparent nano-particles/polyurethane on glass substrate by using APTES as adhesion promoter

Firstly, delamination is the separation of the polyurethane films from the glass surface. (3-Aminopropyl)triethoxysilane (APTES) was used as adhesion promoter to prevent the delamination of the polyurethane films. It is important to notice that the delamination does not occur on polycarbonate substrates. APTES was applied according to the following two methods.

In the first method, APTES was swept on the glass surface using fine special paper to make a thin layer from the APTES on the glass surface before casting the polyurethane films. The glass substrate was left to dry for about 30 minutes. Subsequently the polyurethane films were cast on APTES thin layer.

In the second method, a few drops from APTES were added to the polyurethane solution. Subsequently the polyurethane solution containing APTES was cast on the glass substrate. On the other hand, the APTES as adhesion promoter does not affect the hardness of the polyurethane films. APTES is a silane coupling agent and works synergistically with nano-fillers. The polyurethane films which cast according to the second method are smoother than those were cast according to the first method, and the second method is easier than the first method to apply in industry.

2.3.4 Thermal curing for anti-fog transparent polyurethane films

The polyurethane films were held in an oven at different temperatures, different holding times and, also at different heating methods (either ramp or preheat method). These factors were changed for the different series of polyurethane films in order to find suitable conditions for producing anti-fog transparent polyurethane films.
Thermal curing for anti-fog transparent polyurethane films was achieved by two different methods.

The first method is a preheat method. The temperature was adjusted at the holding temperature before putting the films into the oven

The second is a ramp method. The films were put into the oven. Subsequently, the temperature was increased gradually until the holding temperature was reached as illustrated in the following figure (2.2)

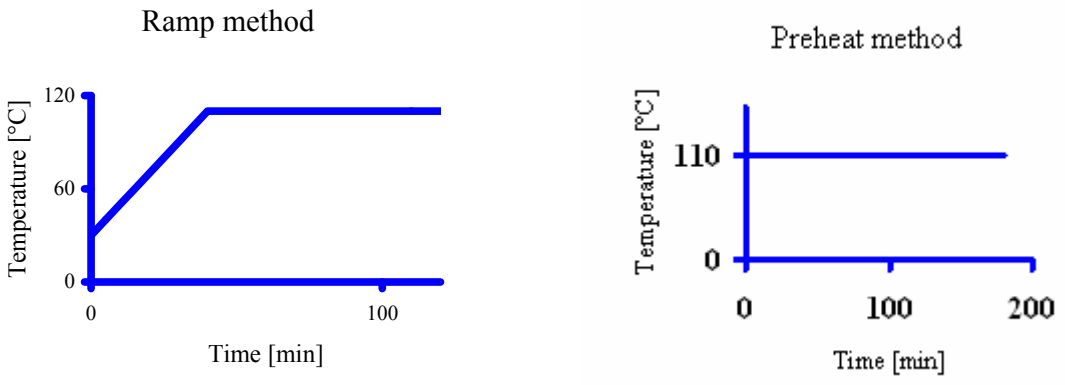

Fig. (2.2): Ramp and preheat method

2.4 Tests and Characterization

2.4.1 The anti-fog test of thermal-curable transparent polyurethane films

The water bath was heated at 80 °C. The films were placed above the bath, facing down. This way, they were exposed to water vapor. The distance between the film and the water surface water 7 cm.

2.4.2 The hardness test of thermal-curable anti-fog transparent polyurethane films

The hardness is a characteristic of a solid material expressing its resistance to permanent deformation. Hardness can be measured by various scales. Some of these scales are used for indentation hardness in engineering.[194] Among of these scales is the pencil hardness tester. There two series of pencils to determine the hardness.

The first series is used for investigation soft materials. They are characterized by the letter B. The second series which is used for investigation hard materials. They are characterized by letter H as following order.

(Hard series) 9H, 8H,…. ... , 2H, H, F, HB, B, 2B,…. ... , 8B, 9B (Soft series)

Where 9H is the hardest, 9B is the softest. Table (2.2) represents the hardness for some different coatings.[195]

Table (2.2): The hardness for some different coatings:

Type of coatings	Pencil Hardness
Catalyzed polyester	9H
Catalyzed polyurethane	9H
Catalyzed Modified Acrylic polyurethane	4H
Catalyzed Acrylic polyurethane	2H
Water-based polyurethane	3H
Water-based urethane/ Isocyanate Catalyst	2H
Conversion varnish	4H
Low VOC Catalyzed laquer [24 hrs]	2H
Low VOC laquer	3H
Urethane/Nitrocellulose laquer [24 hrs}	F
Water reducible laquer	2H
Tung oil/polyurethane wipe-on finish	2H
Water-based polyurethane wipe-on finish	HB-F
Aerosol precat	3B
Aerosol water clear acrylic	3B
Aerosol clear shellac	3B
Aerosol nitrocellulose/ polyurethane	HB
Aerosol nitrocellulose	3B
Amber (orange) Shellac 1 lb. cut	3B

Pencil hardness tester (wolf-wilburn), BYK additives & instruments, Cat No. PH- 5800 was used in our project Fig. (2.2).[193]

Hard series 1H-9H Soft series 1B-9B

Fig (2.3): The pencil hardness tester and the pencils hardness (Wolf-Wilburn).

2.4.3 The delamination of thermal-curable anti-fog transparent polyurethane films

Delamination is a mode of failure of laminated composite materials. Repeated cyclic stresses, impact, and so on can cause layers to separate, with significant loss of the mechanical toughness.[194]

2.4.4 The haziness of the thermal-curable anti-fog transparent polyurethane films

Generally, haze is use to describe turbidity in clear transparent glass or transparent plastic as a percent value.[194]

2.4.5 The tackiness measuring of thermal curable anti-fog transparent polyurethane by using Texture Analyzer

The texture analyzer is an instrument that measures the response of a sample to compressive or tensile force. It can do this by movement and measuring force, or by applying force and measuring movement as a function of time or distance Fig. (2.4).

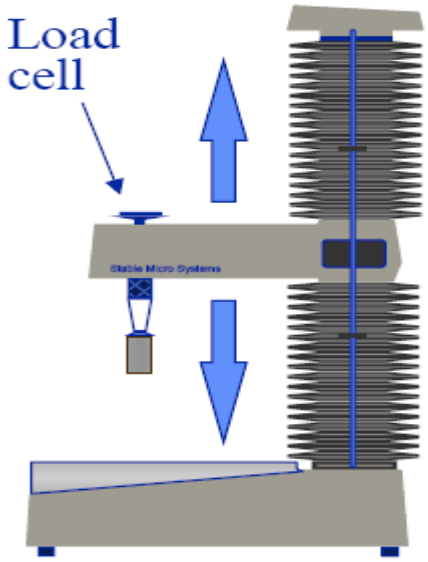

Fig. (2.4): The Texture analyzer

Basic principle of texture analyzer to measure the tackiness of the coatings

First step:

Probe begins to move from start point towards down sample pre-test speed. It can be used different pre-test speeds. As illustrated in the Fig. (2.5).

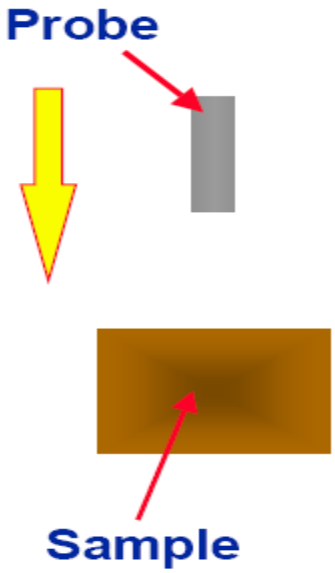

Fig.(2.5): The beginning movement of the probe

Second step:

When the probe registers a force equal to trigger force, the speed changes to the test speed and the system starts to collect the data for the sample which is clamped and to start presentation the relationship between the force versus the time or the distance. When the probe registers a force is equal to the trigger force, the speed changes directly to the test speed and the system starts to collect the data. The test should start when the probe and product have full contact as illustrated in Fig. (2.6).

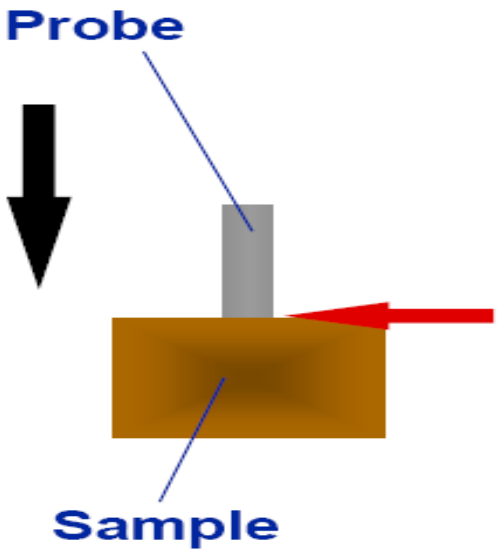

Fig. (2.6): The probe at full contact with the sample

Third step:

Probe continues to move into the sample body at the test speed until the test is complete as illustrated in Fig. (2.7), the system will directly produce the diagram of force versus time or distance.

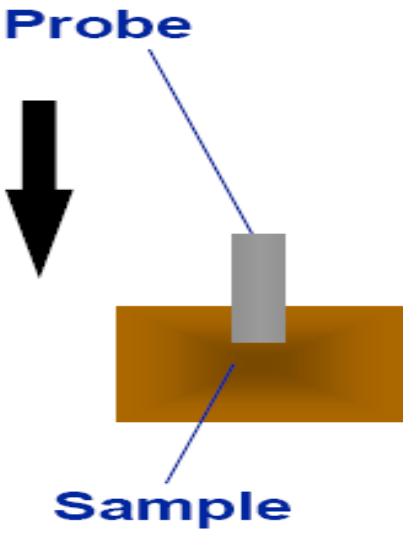

Fig. (2.7): The probe moving into the sample body

Fourth step:

When test is finished, the probe begins to move away from sample at post-test speed. The probe stops once it is back at the start point as illustrated in Fig. (2.8).

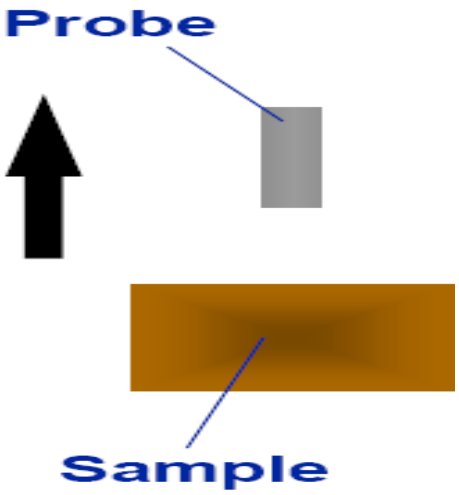

Fig. (2.8): The probe moving away from the sample.

The texture analyzer is usually use for texture analysis of many products, among these products are adhesives and also used to measure tackiness and peel strength.[196]

2.4.5 The purpose of using of the texture analyzer in our project

The Texture Analyzer was used to develop a method to test the adhesiveness of polyurethane films on either glass or polycarbonate substrate. The texture analyzer was used to determine the tackiness (debonding energy) of the curable anti-fog transparent polyurethane coating and also to monitor the success of thermal or UV-curing.

2.4.6 The methods of using of the texture analyzer

The stable micro systems-texture exponent 32-Analyzer was used to quantify the adhesive characteristics. After the polyurethane films were cast on the glass substrate, they were cured by thermal or UV curing. The glass plate was clamped down and pulled back the force applied was measured versus the distance. A punch probe of 5 mm diameter was used. The probe was lowered 5000 g of force until it reached to the film surface. When the repulsive force exerted by the exceeded 500 g, the work was reversed. The speed was 5 mm/sec. The force required to pull the probe away was recorded and plotted versus the distance. The tackiness (debonding energy) was measured for 10 times at different areas for the same polyurethane film. The average was also calculated.

2.4.8 The measurements of the texture analyzer

The maximum amount of (peak) force required to remove the probe from the sample was reported as the tack or adhesive strength of the formulation. The resulting value of the system measurement indicated the adhesive work. Finally, the distance to peak force was reported as stringiness. These parameters are important to compare the variables formulations and their effect on the different polyurethane films. As illustrated in the Fig. (2.9), the integrated force of detachment ($A_{det.}$) is represented by the integrated area under the curve. The area (A_{punch}) of the punch is equal to (πr^2) where r is the radius of the probe. Then the resulting work is equal to ($A_{det.}$)/ (A_{punch}).

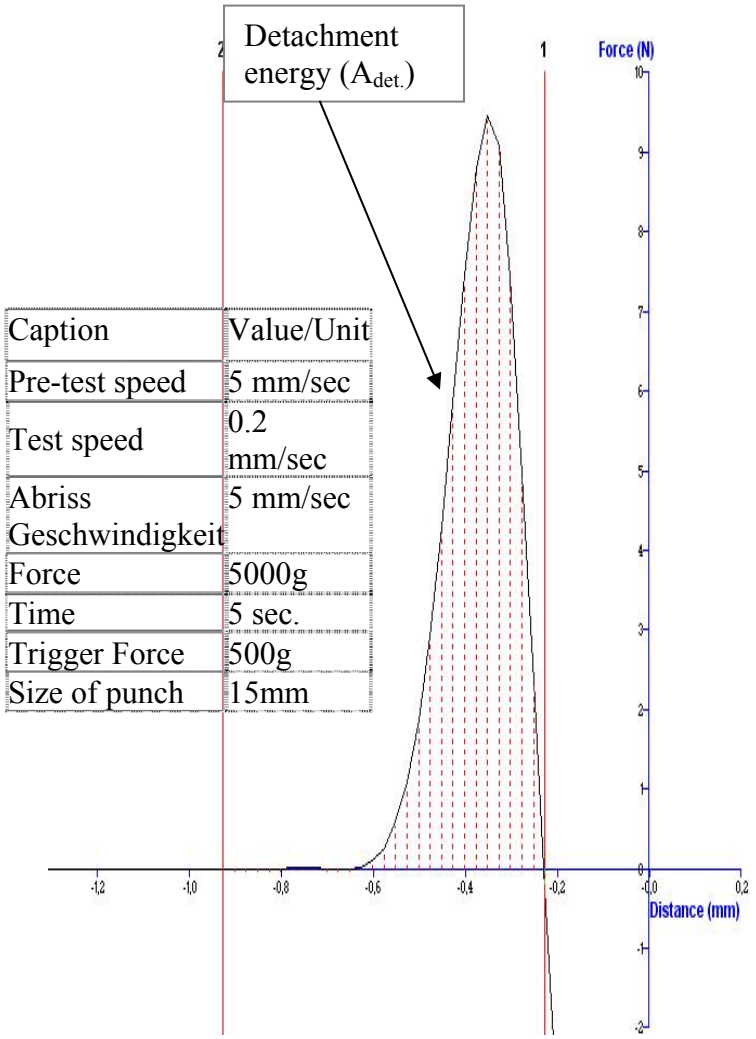

Caption	Value/Unit
Pre-test speed	5 mm/sec
Test speed	0.2 mm/sec
Abriss Geschwindigkeit	5 mm/sec
Force	5000g
Time	5 sec.
Trigger Force	500g
Size of punch	15mm

Fig. (2.10): The texture analyzer and the recording force versus distance diagram

2.5 Results and Discussions

2.5.1 Preparation of thermal-curable anti-fog transparent polyurethane acrylate based on polyethylene glycol (PEG1000)

Generally, the concept for the anticipated anti-fog coating on glass or polycarbonate is as follows:

A tough and scratch resistance coating shall be achieved using a polyurethane resin consisting of flexible short and highly crosslinkable chains. Hardness is achieved by inorganic nano- fillers. Easy curing is achieved due to the thermal crosslinking of acrylate groups at the end of the polyurethane chains. For the synthesis of the resin we have selected as a polyol the difunctional polyethylene glycol with an average molecular weight of 1000 g/mol. At this molecular weight the polyethylene glycol is markedly hydrophilic.

As the aliphatic diisocyanate, we have chosen isophorone diisocyanate (IPDI). IPDI is used for many applications, such as enamel coatings which are resistant to abrasion and degradation from ultraviolet light. These properties are particularly desirable for the applications.

In the first step, the addition reaction takes place in presence of DBTL as orgnometallic catalyst between PEG_{1000} and IPDI to form urethane preolymer.

A thermally-crosslinkable or UV-crosslinkable monomeric unit, HEA was used for polyurethane chains capping. This acrylate was already been used for improving adhesion and resistant against corrosion, fogging, and abrasion; end applications include adhesives, coatings, sealants and thermosetting paints.

In the second step, the addition reaction takes place between the resulting urethane prepolymer (from the first step) and HEA. The urethane prepolymer is capped by HEA to form polyurethane chains which are terminated by double bonds. At this stage the reaction mixture is very sensitive to polymerization of the acrylate groups. A gel is formed in a fast process for this reason in the second step. The reaction temperature was primarily kept below 45 °C for acronym (A) and acronym (B) preparation to avoid thermal polymerization of acrylate groups[197] for acronym (A) or (B).

So far we did not add any inhibitor to the mixture because this inhibitor would remain in the final product and would thus inhibit the thermally-initiated free radical polymerization.

2.5.2 Thermal curing of the anti-fog transparent polyurethane films

Azo compounds containing a nitrogen atom connected to a carbon and a nitrogen atom through a single and a double bond respectively can be used as thermal initiators. However, the driving force for the azo-type initiator is not the dissociation energy but the stable nitrogen formed in the dissociation reaction.[198]

The thermal curing of the films on the glass substrate was achieved at temperatures up to

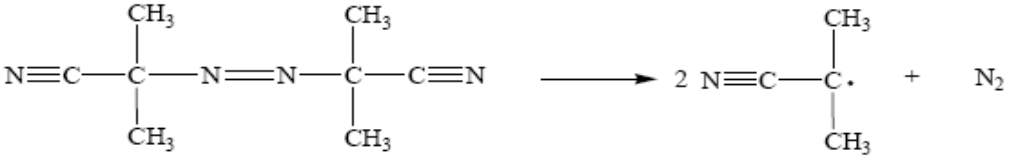

90, 100, 110 °C in presence of thermal initiator AIBN. The achieved degree curing depends on the AIBN content, the film thickness, the holding temperature, the holding time and the heating method (either ramp or preheat method) as illustrated in the table's series (2.3 to 2. 14).

Table (2.3): The recipes and characterization of series (1) of thermal-curable anti-fog PU films at different conditions which prepared from acronym (A)

Wet thickness [µm]	30	60	90	120
Substrate	glass			
Concentration of PU in acetone (w %)	40			
AIBN (wt.%, PU)	1.25			
Heating Method	ramp			
Holding Time (hour)	1			
Holding Temperature (°C)	110			
Anti-Fog Test	very good			
Delamination Occurred	No	No	No	No
Pencil Hardness Tester	4B	4B	4B	4B

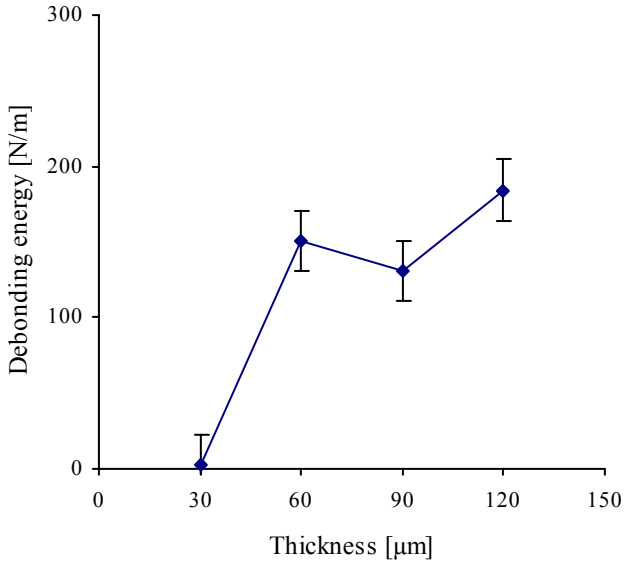

Fig. (2.11): Debonding energy versus thickness for series (1)

Table (2.4): The recipes and characterization of series (2) of thermal-curable anti-fog PU films at different conditions which prepared from acronym (A)

Wet thickness [µm]	30	60	90	120
Substrate	glass			
Concentration of PU in acetone (w %)	40			
AIBN (wt.%, PU)	1.25			
Heating Method	preheat			
Holding Time (hour)	1			
Holding Temperature (°C)	110			
Anti-fog Test	very good			
Delamination Occurred	No	Yes	Yes	No
Pencil Hardness Tester	3B	3B	3B	3B

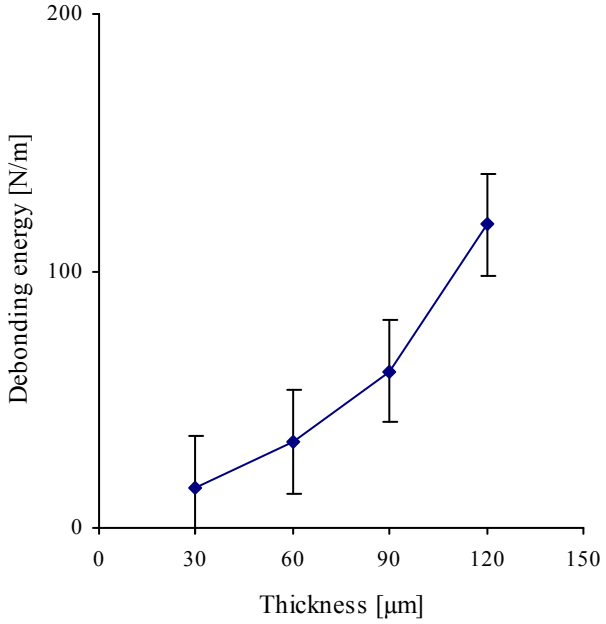

Fig. (2.12): Debonding energy versus thickness for series (2)

Table (2.5): The recipes and characterization of series (3) of thermal-curable anti-fog PU films at different conditions which prepared from acronym (A)

Wet thickness [µm]	30	60	90	120
Substrate	glass			
Concentration of PU in acetone (w %)	40			
AIBN (wt.%, PU)	5.00			
Heating Method	ramp			
Holding Time (hour)	1			
Holding Temperature (°C)	110			
Anti-fog Test	very good			
Delamination Occurred	Yes	No	No	Yes
Pencil Hardness Tester	4B	4B	5B	5B

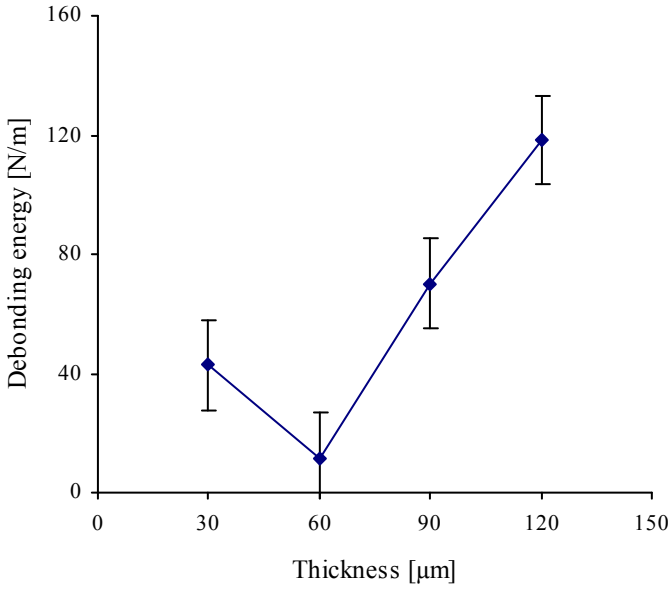

Fig. (2.13): Debonding energy versus thickness for series (3)

Table (2.6): The recipes and characterization of series (4) of thermal-curable anti-fog PU films at different condition which prepared from acronym (A)

We thickness [µm]	30	60	90	120
Substrate	glass			
Concentration of PU in acetone (w %)	40			
AIBN (wt.%, PU)	5.00			
Heating Method	preheat			
Holding Time (hour)	3			
Holding Temperature (°C)	90			
Anti-fog Test	very good			
Delamination Occurred	No	Yes	No	No
Pencil Hardness Tester	3B	4B	3B	3B

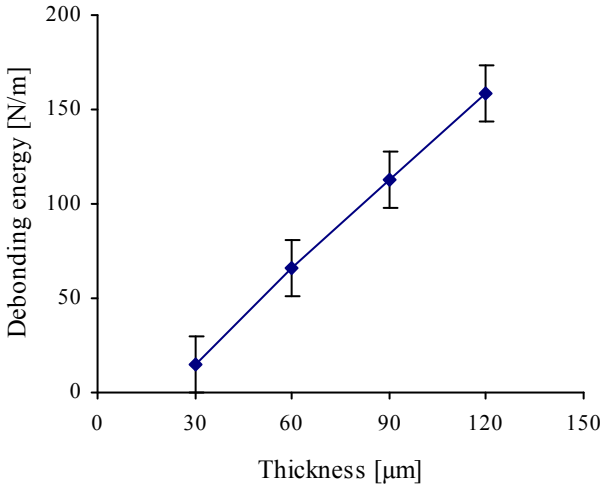

Fig. (2.14): Debonding energy versus thickness for series (4)

Table (2.7): The recipes and characterization of series (5) of thermal-curable anti-fog PU films at different conditions which prepared from acronym (A)

Wet thickness [µm]	30	60	90	120
Substrate	glass			
Concentration of PU in acetone(w %)	20			
AIBN (wt.%, PU)	5.00			
Heating Method	Preheat			
Holding Time (hour)	3			
Holding Temperature (°C)	110			
Anti-fog Test	very good			
Delamination occurred	No	No	Yes	No
Pencil Hardness Tester	2B	2B	2B	2B

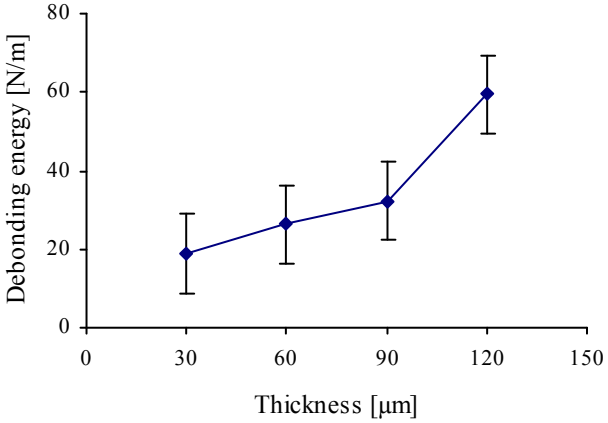

Fig. (2.15): Debonding energy versus thickness for series (5)

Table (2.8): The recipes and characterization of series (6) of thermal-curable anti-fog PU films at different conditions which prepared from acronym (A)

Wet thickness [µm]	30	60	90	120
Substrate	glass			
Concentration of PU in acetone (w %)	40			
AIBN (wt.%, PU)	2.50			
Heating Method	Preheat			
Holding Time (hour)	1.45			
Holding Temperature (°C)	110			
Anti-fog Test	very good			
Delamination occurred	No	partially	Yes	No
Pencil Hardness Tester	5B	5B	5B	Tacky

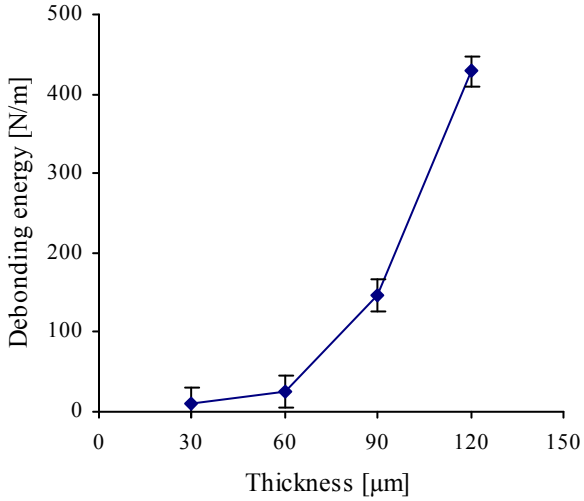

Fig. (2.16): Debonding energy versus thickness for series (6)

Table (2.9): The recipes and characterization of series (7) of thermal-curable anti-fog PU films at different conditions which prepared from acronym (A)

Wet thickness [µm]	30	60	90	120
Substrate	glass			
Concentration of PU in acetone(w %)	40			
AIBN (wt.%, PU)	2.50			
Heating Method	ramp			
Holding Time (hour)	3			
Holding Temperature (°C)	110			
Anti-fog Test	very good			
Delamination occurred	No	partially	partially	partially
Pencil Hardness Tester	4B	4B	5B	tacky

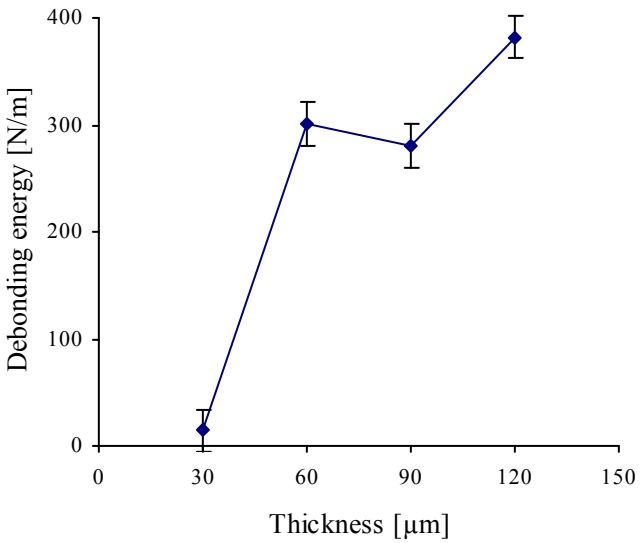

Fig. (2.17): Debonding energy versus thickness for series (7)

Table (2.10): The recipes and characterization of series (8) of thermal-curable anti-fog PU films at different conditions which prepared from acronym (A)

Wet thickness [µm]	30	60	90	120
Substrate	glass			
Concentration of PU in acetone (w %)	20			
AIBN (wt.%, PU)	2.50			
Heating Method	ramp			
Holding Time (hour)	1			
Holding Temperature (°C)	110			
Anti-fog Test	very good			
Delamination occurred	No	No	No	Yes
Pencil Hardness Tester	2B	2B	2B	3B

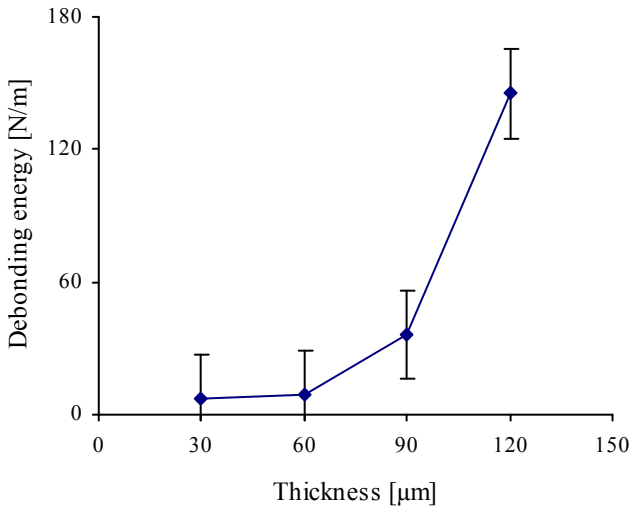

Fig. (2.18): Debonding energy versus thickness for series (8)

Table (2.11): The recipes and characterization of series (9) of thermal-curable anti-fog PU films at different conditions which prepared from acronym (A)

Wet thickness [µm]	30	60	90	120
Subsrate	glass			
Concentration of PU in acetone (w %)	20			
AIBN (wt.%, PU)	2.50			
Heating Method	preheat			
Holding Time (hour)	1			
Holding Temperature (°C)	110			
Anti-fog Test	very good			
Delamination occurred	Yes	No	No	Yes
Pencil Hardness Tester	3B	3B	4B	4B

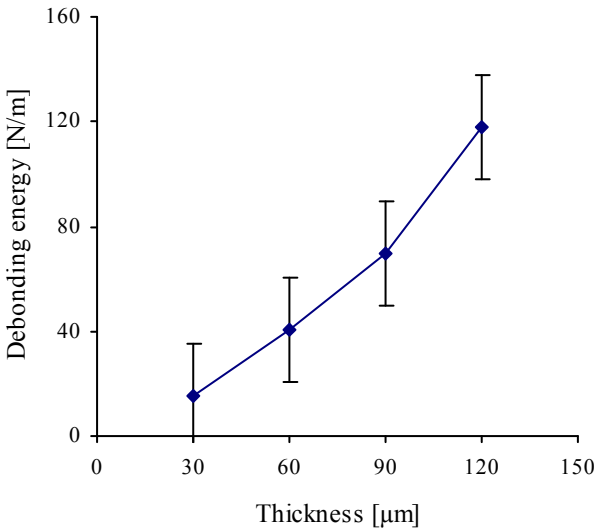

Fig. (2.19): Debonding energy versus thickness for series (9)

Table (2.12): The recipes and characterization of series (10) of thermal-curable anti-fog PU films at different conditions which prepared from acronym (A)

Wet thickness [µm]	30	60	90	120
Substrate	glass			
Concentration of PU in acetone (w %)	20			
AIBN (wt.%, PU)	5.00			
Heating Method	ramp			
Time (hour)	3			
Holding Temperature (°C)	110			
Anti-fog Test	very good			
Delamination occurred	No	partially	partially	partially
Pencil Hardness Tester	3B	4B	4B	4B

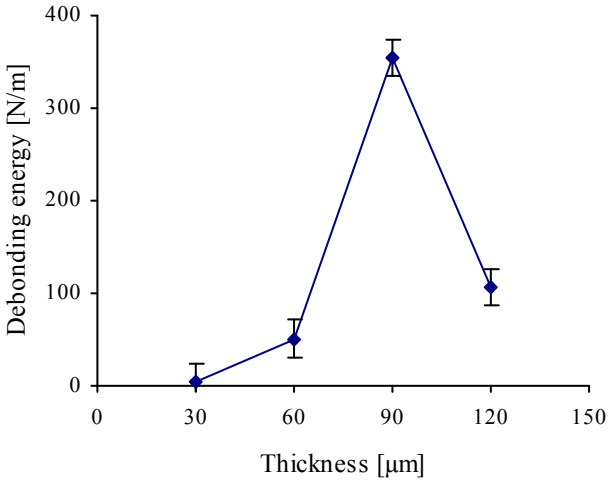

Fig. (2.20): Debonding energy versus thickness for series (10)

Table (2.13): The recipes and characterization of series (11) of thermal-curable anti-fog PU films at different conditions which prepared from acronym (A)

Wet thickness [µm]	30	60	90	120
Substrate	glass			
Concentration of PU in acetone (w %)	20			
AIBN (wt.%, PU)	10.00			
Heating Method	Half ramp			
Time (hour)	2			
Holding Temperature (°C)	110			
Anti-fog Test	very good			
Delamination occurred	No	No	No	partially
Pencil Hardness Tester	3B	3B	3B	4B

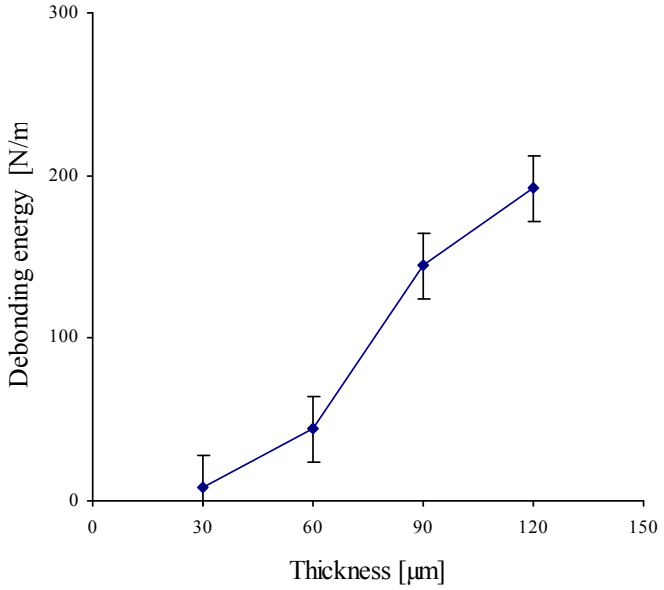

Fig. (2.21): Debonding energy versus thickness for series (11)

Table (2.14): The recipes and characterization of series (12) of thermal-curable anti-fog PU films at different conditions which prepared from acronym (A)

Wet thickness [µm]	30	60	90	120
Substrate	glass			
Concentration of PU in acetone (w %)	20			
AIBN (wt.%, PU)	10.00			
Heating Method	ramp			
Time (hour)	2			
Holding Temperature (°C)	110			
Anti-fog Test	very good			
Delamination occurred	No	No	No	No
Pencil Hardness Tester	3B	3B	3B	tacky

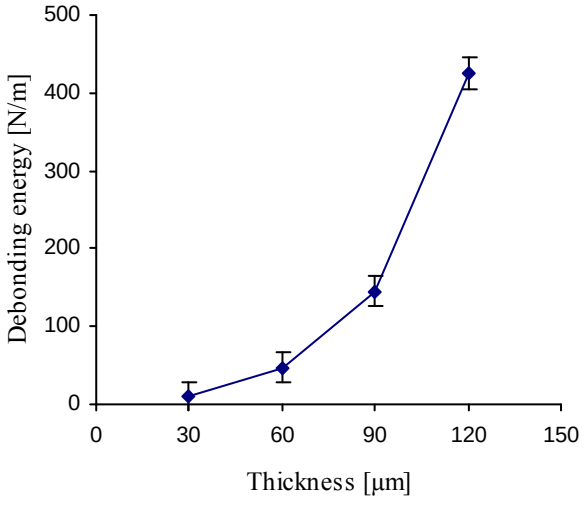

Fig. (2.22): Debonding energy versus thickness for series (12)

2.6 Thermal curable anti-fog transparent polyurethane films characterization

2.6.1 The anti-fog test

A water bath was heated to 80 °C. The films were placed above the bath (faced down) to receive the evaporated water, All polyurethane films displayed anti-fog property.

2.6.2 The hardness test

Hardness is the characteristic of a solid material expressing its resistance to permanent deformation. Hardness values of polyurethanes films were variable as we can see in above series as presented in tables (2.3 to 2.14). The hardness values of the films are the following descending order for the prvious series (S_n):

S_5, S_8 (2-3B) > S_2, S_{12} (3B) > S_1, S_4, S_9, S_{10}, S_{11} (3-4B) > S_3, S_7 (4-5) >S_6 (5B).

The hardness value depends on the conditions of the thermal-curing (percentage of the thermal-initiator, thickness of the film, holding temperature and holding time in the oven).

Series (S_5) has the highest hardness value (2B), at 5% wt., AIBN of polyurethane; preheat method for 3 hour at 110 °C and the series (S_8) has also hardness value (2-3B) at 2.5% wt. AIBN of polyurethane, ramp method for 1 hour at 110 °C.

Series (S_2) has hardness value (4-3B) at 1.25% wt., AIBN of polyurethane; preheat method for 1 hour at 110 °C and also series (S_{12}) has the same hardness value at 10 % wt., PU AIBN, ramp method for 2 hour at 110 °C. Generally, the hardness values of resulting thermal-curable anti-fog polyurethane films indicate to the polyurethane films are classified as softer films accodrding to the softer hardness pencil series. There is inverse relationship between the hardness and the tackiness of the thermal –curable polyurethane films.

2.6.3 The delamination test of thermal-curable anti-fog polyurethane films

Delamination occurred for some polyurethane films on glass substrates although these films have the same formulation and underment the same curing thermal conditions. The delamination occurred of the films for the series as the following descending order:

$$S_1, S_5, S_{12} > S_4, S_8, S_{11} > S_2, S_3, S_6, S_9 > S_7, S_{10}$$

The delamination of polyurethane films did not occur on the polycarbonate substrate nor, did occur with polyurethane films on glass substrate at 110 °C holding temperature. The heating improves the adhesion of polyurethane films on the glass substrate.

2.6.4 The appearance of the yellowish color in thermal-curable anti-fog polyurethane films

Series S_4, S_5, S_7 and S_{10} have got yellow color. This is attributed to long holding time in the oven. The yellowish color may be attributed to the degradation of diisocynate in the polymer network.

2.6.5 The measuring of tackiness (debonding energy)

The tackiness (debonding energy) of thermal-curable films was measured 10 times at different spots for the same film. The average and the standard deviation were calculated. The measurements indicated the tackiness of the polyurethane films after thermal curing. The tackiness of the films represented is illustrated in the Fig. series (2.11 to 2.22). As we can see in the figures, there is proportionality between the tackiness and the thickness of the film. With increasing the thickness, the tackiness also increases. There is anticorrelation between the tackiness of the film and the film hardness.

2.6.6 Preparation of thermal-curable anti-fog Aerosil-particles/polyurethane on the glass substrate

Different percentages of Aerosil R972 (hydrophobic) were disperesed as nano-filler in the polyurethane solution in presence of AIBN by using a magnetic stirrer. Subsequently the nano-particles/polyurethane dispersion was cast on the glass substrate at the wet thicknesses of 120, 90, 60 and 30 μm. After the evaporation of the acetone solvent at room temperature, polyurethane films were placed in an oven. The details of the method and characterization of the films were inserted in the table's series (2.15 to 2.16). There is a positive correlation between the film thickness and the tackiness. The filler increases the hardness of the polyurethane films but causes haziness for thermal-curable polyurethane films. Thermal-curable Aerosil/polyurethane films have tackiness values lower than thermal curable polyurethane films (without Aerosil). The

formulations and characterization of thermal-curable anti-fog nano-particles/polyurethane are shown in table series (2.23) to (2.24).

Table (2.15): The recipes and characterization of series (13) of thermal-curable anti-fog PU films at different conditions which prepared from acronym (A)

Wet thickness [µm]	30	60	90	120
Substrate	glass			
Concentration of PU in acetone(w%)	20			
AIBN (wt.%, PU)	2.50			
Aerosil (R972) (wt.%, PU)	2.50			
Heating Method	preheat			
Holding Time (hour)	2			
Holding Temperature (°C)	110			
Anti-Fog Test	very good			
Delamination Occurred	partially	No	No	No
Pencil Hardness Test	B	2B	2B	2B

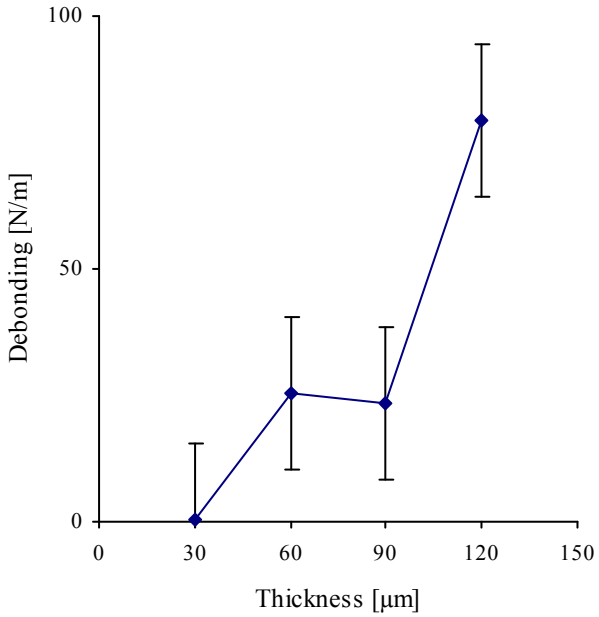

Fig. (2.23): Debonding energy versus thickness for series (12)

Table (216): The recipes and characterization of series (14) of thermal-curable anti-fog PU films at different conditions which prepared from acronym (A)

Wet thickness [µm]	30	60	90	120
Substrate	glass			
Concentration of PU in acetone (w %)	20			
AIBN(wt.%, PU)	2.50			
Aerosil (R972) (wt.%, PU)	5.00			
Heating Method	preheat			
Holding Time (hour)	1			
Holding Temperature(°C)	110			
Anti-Fog Test	very good			
Delamination Occurred	No	No	No	Yes
Pencil Hardness Test	B	HB	HB	HB

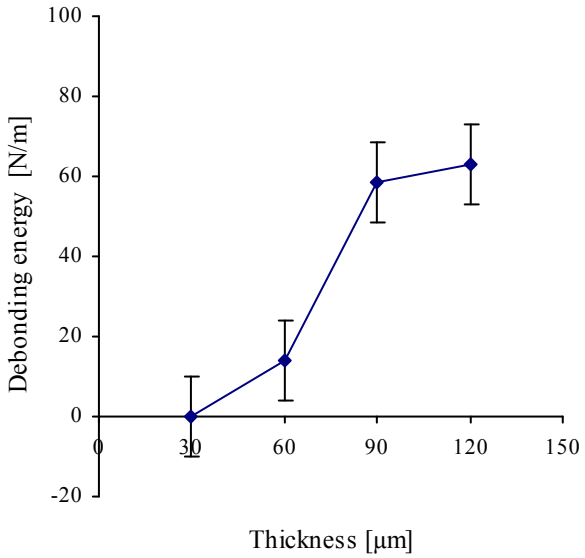

Fig. (2.24): Debonding energy versus thickness for series (12)

2.6.7 Preparation of thermal-curable anti-fog nano-particles/polyurethane on polycarbonate or glass substrate by using adhesion promoter

APTES has the ability to form a durable bond between organic and inorganic materials. APTES was used as adhesion promoter of the polyurethane films on glass substrates to prevent the delamination. It is important to remember that the delamination of the polyurethane did not occur on the polycarbonate substrate.

APTES was applied by two methods;

In the first method, APTES was swept on the glass by using fine special paper to make thin layer from APTES on the glass substrate. The glass was left for 1/2 hour to dry and subsequently the polyurethane films were cast on it.

In the second method, a few drops of APTES were directly added to the polyurethane solution and subsequently the polyurethane solution cast on the glass substrate. The formulation and characterization of thermal-curable anti-fog polyurethane films are tabulated in table (2.17)

Table (2.17): Thermal-curable of anti-fog laponite/polyurethane on either glass or polycarbonate substrate

Wet thickness [μm]	60	30			30	60
Substrate	glass	glass			polycarbonate	
Concentration of PU in acetone (w/w %)	20	20			20	
AIBN (Wt.%, PU)	5.00	5.00			5.00	
Laponite (Wt. %, PU)	3.00	3.00			3.00	
Heating Method	preheat	preheat			preheat	
Holding Time (hour)	2	2		1	1	
Holding Temperature(°C)	110	110		110	110	
Anti-Fog Test	very good	very good		very good	very good	
Adhesion promoter	--		APTES	APTES	---	
Delamination Occurred	Yes	Yes	No	No	No	No

As we can see delamination occurred for the thermal-curable anti-fog polyurethane films on the glass substrate in absence of APTES as adhesion promoter. When APTES is used as adhesion promoter, the delamination of thermal-curable anti-fog polyurethane did not occur. The delamination did not occur for thermal-curable anti-fog polyurethane films on the polycarbonate substrate.

2.6.8 The freezer test for thermal-curable anti-fog transparent polyurethane films

The thermal-curable transparent polyurethane films are still good anti-fog even after holding the polyurethane films in the freezer (under °C) for 24 hours either on glass or polycarbonate substrate.

The delamination of thermal-curable polyurethane films did not occur on polycarbonate substrate after the freezer test.

The delamination of thermal-curable polyurethane films did not occur on glasse substrate when APTES used as adhesion promoter after the freezer test.

Table (2.18): Freezer test for thermal curable of anti-fog polyurethane on either glass or polycarbonate substrate

Wet thickness [μm]	60	90	60	90	30	60	30	60
Substrate	PC				Glass			
Concentration of PU in acetone (w/w %)	20				20			
AIBN (wt.%, PU)	3.00				3.00			
Heating Method	preheat				preheat			
Holding Time (hour)	1h.				1h			
Holding Temperature (°C)	110				110			
Holding Time (hour) in freezer	24				24			
Anti-fog Test	Very good				Very good			
Delamination Occurred	No	No	No	No	No	Yes	No	Yes

2.7 Conclusions

- The polyurethane acrylate films based on polyethylene glycol mol. wt 1000 displayed a very good anti-fog property and were transparent.

- Delamination takes place on glass substrate while it does not occur on polycarbonate substrates.

- Delamination on glass substrates can be prevented by using ATPES as adhesion promoter.

- Upon increasing the holding time in the oven to around 3 hours, the tackiness comes back and the yellow color appears in the films.

- All polyurethane films display anti-fog properties even after holding them in the freezer for 24 hours.

- The tackiness of thermal-curable polyurethane films indicates incomplete curing of polyurethane prepared from acronym (A) or (B) (in the beginning of this chapter). This is attributed to residual momomers.

3 Preparation and characterization of UV-curable anti-fog transparent polyurethane films

3.1 Materials

In addition to the chemicals which were used in the second chapter, Irgacure 184 (1-hydroxycyclohexyl phenyl ketone) was also used in this chapter.

3.2 Experimental details

In addition to the acronyms (A) and (B) in the second chapter, the polyurethane acronyms (C), (D) and (E) were prepared and characterized in this chapter.

3.2.1 Preparation of polyurethane copolymer solution using PEG_{1000}: IPDI: HEA at ratios 1:2.2:2.2 (Acronym C)

Procedures:

1- 70g (0.07 mol) PEG_{1000} and 30 g acetone were mixed. The mixture was fed into a three-necked flask equipped with a mechanical stirrer. The stirrer was operated at 150 rpm. A reflux condenser was employed. The temperature was 60 °C. The reaction occurred under nitrogen atmosphere for 30 minutes.

2- 34.23 g (0.154 mol) IPDI and 0.34 g DBTL were mixed. The mixture was slowly dropped into the reactor under the above conditions for 2.1/2 hours.

3- The system was further reacted under the above conditions for one additional hour.

4- 17.88 g (0.154 mol) HEA was added drop by drop to the reactor under the above conditions for 1 hour.

5- The reaction mixture was stirred for one additional hour under the above conditions.

6- The resulting clear and viscous solution was diluted using acetone to obtain a diluted polyurethane copolymer solution with 50% (w/w).

3.2.2 Preparation of polyurethane copolymer solution using PEG_{1000}: IPDI: HEA at ratios 1:2.5:2.5 (Acronym D)

Procedures:

1- 70 g (0.07 mol) PEG_{1000} and 30 g acetone were mixed. The mixture was fed into a three-necked flask equipped with a mechanical stirrer. The stirrer was operated at

150 rpm. A reflux condenser was employed. The temperature was 60 °C. The reaction occurred under nitrogen atmosphere for 30 minutes.

2- 38.9 g (0.154 mol) IPDI and 0.34 g DBTL were mixed. The mixture was slowly dropped into the reactor under the above conditions for 2.1/2 hours.

3- The system was further reacted under the above conditions for one additional hour.

4- 20.32 g (0.154 mol) HEA was added drop by drop to the reactor under the above conditions for 1 hour.

5- The reaction mixture was stirred for an additional 1 hour under the above conditions.

6- The resulting clear and viscous solution was diluted by using acetone to obtain a diluted polyurethane copolymer solution with 50% (w/w).

3.2.2 Preparation of polyurethane copolymer solution using PEG_{1000}: IPDI: HEA at ratios 1:3:3 (Acronym E)

Procedures:

1- 70 g (0.07 mol) PEG_{1000} and 30 g acetone were mixed. The mixture was fed into a three-necked flask equipped with a mechanical stirrer. The stirrer was operated at 150 rpm. A reflux condenser was employed. The temperature was 60 °C under nitrogen atmosphere for 30 minutes.

2- 46.7 g (0.21 mol) IPDI and 0.5 g DBTL were mixed. The mixture was slowly dropped into the reactor under the above conditions for 2.1/2 hours.

3- 10 g acetone was added to dilute the viscosity of the resulting prepolymer.

4- The system was further reacted under the above conditions for one additional hour.

5- 24.4 g (0.21 mol) HEA was added drop by drop to the reactor under the above conditions for one hour.

6- The reaction mixture was stirred for one additional hour under the above conditions.

7- The resulting clear and viscous solution was diluted using acetone to obtain a diluted polyurethane copolymer solution with 50% (w/w).

3.3.1 Preparation of UV-curable films by using film applicator

The polyurethane solution was diluted to various percentages by using acetone. Different percentages of Irgacure 184 were dissolved in several drops of acetone and were subsequently mixed with the polyurethane solutions at room temperature. The polyurethane solutions containing the photo-initiator were cast on either the glass or the polycarbonate substrates by using the applicator at the wet thicknesses of 120, 90, 60 and 30 μm. The films were left for about 1/2 hour at room temperature to evaporate the solvent. The films were exposed to the UV-lamp to cure. The following several factors were changed, different polyurethane acronyms, types of polyurethanes depending on the variable formulations, preparation conditions, concentrations of polyurethane in acetone, percentages of Irgacure 184, film thicknesses and UV-curing time.

3.3.2 Preparation of UV-curable anti-fog transparent nano-particles/polyurethane dispersion by using Ultra-Turrax homogenizer

Different percentages from several types of nano-particles were dispersed into the polyurethane solution in presence of a photo-initiator (Irgacure 184). The Ultra-Turrax T25 Digital homogenizer was used to disperse the nano-particles in the polyurethane solution at high speed rotation of 24.000 rpm for 1 minute for all the polyurethane recipes, subsequently the nano-particles/polyurethane dispersion was cast on either the glass or the polycarbonate substrates at different wet thicknesses.

3.3.3 UV lamp [199]

Total operational device for use in existing transport facility, consisting of a UV lamp unit with pneumatic locking system and a power supply , designed for continuous operation in the small print area of paper, flat glass, plastics, foils, metals etc. The UV radiation is located in an air-cooled lamp housing with aluminum reflector. The UV radiation is ozone free (arc length of 70 mm, performance 120 W/cm) as illustrated in Fig. (2.10). Power supply network with switches, lamp On/Off, air access, network cables, etc.

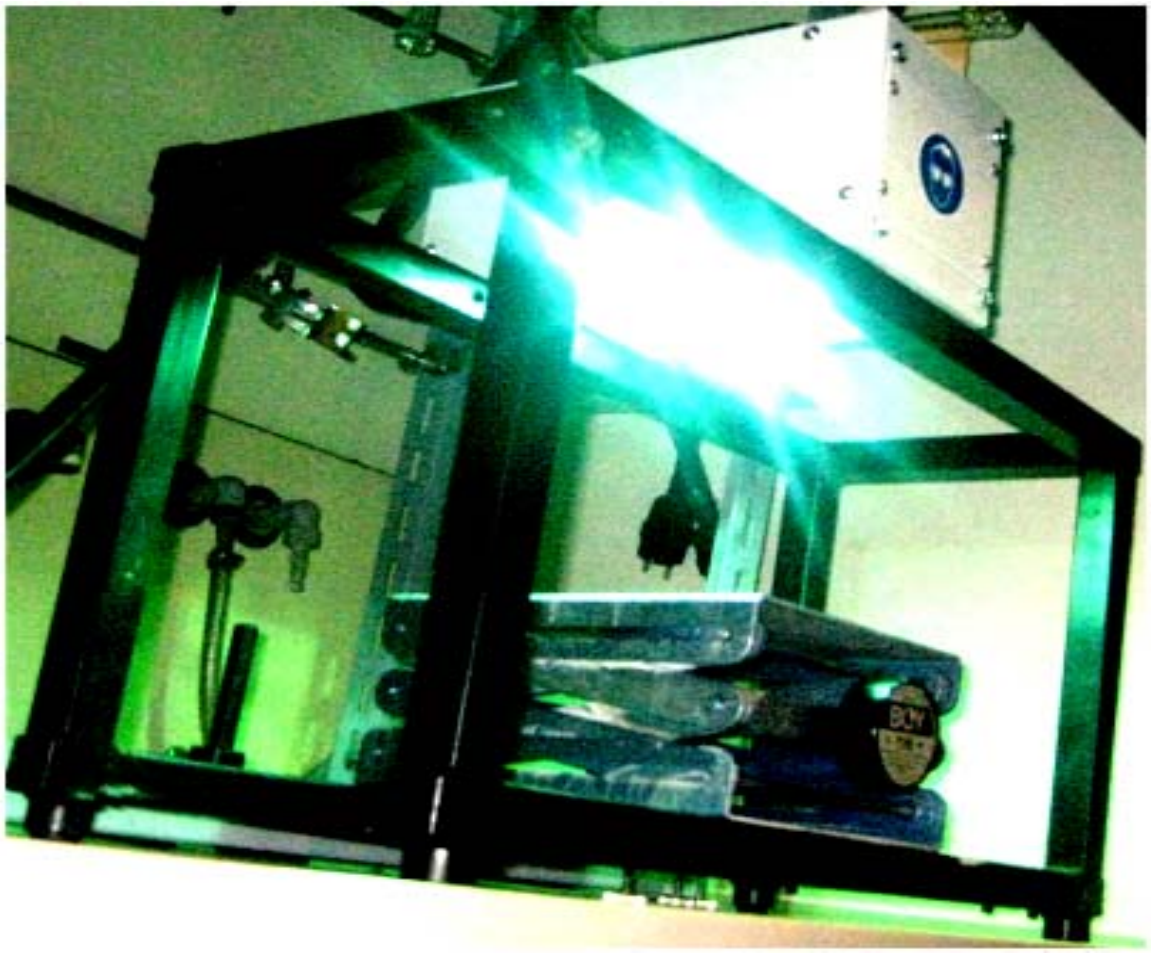

Fig. (3.1): UV-lamp, Arc length = 70 mm, 120 W / cm

3.4 Results and Discussions

3.4.1 UV-curable anti-fog transparent polyurethane films with or without tackiness

The negative value of the tackiness (debonding energy) for the polyurethane films means that the film does not have any tackiness and behaves like the blank substrate figures (3.5 to 3.7). The tackiness of the different polyurethane films is illustrated in figures (3.2 to 3.7). A large tackiness implies that the film has monomers. The polyurethane films in series (1 to 3) have tackiness values higher than in series (5 to 6). The tackiness of these series (1 to 3) is attributed to the existence of some residual monomer in these films depending on the conditions of polyurethane acronym (A) or (B) which the addition reaction between PEG_{1000} and IPDI in the first step achieved at lower temperature (50 °C) and also lower percentage of the catalyst (then the reaction between PEG_{1000} and IPDI is incomplete at lower temperature and also at lower percentage of the catalyst than those in polyurethane acronyms (C), (D) and (E) at 60 °C at both first and second steps of the reaction).

On another hand, the addition reaction between the urethane prepolymer and HEA in the second step was achieved at lower temperature (35 °C then, the capping of urethane prepolymer by HEA was incomplete) than those in polyurethane acronyms (C), (D) and (E). Subsequently, the crosslinking of polyurethane chains was fully completed especially with increasing of diisocynate ratio at higher percentage of the catalyst the polyurethane acronym (D) and (E). An increasing of ratio diisocynate to polyol led to an increase of the allophonate linkages in the polyurethane network at higher temperature. Then polyurethane preparation must be at 60 °C in both steps with optimizing the catalyst percetange and ratios of isocyanate to polyol.

3.4.2 The hardness of the UV-curable anti-fog transparent polyurethane films

The hardness values of UV-curable polyurethane films were tabulated in the table (3.1 to 3.6). Almost, there is a unity of the hardness values in the same series because the thicknesses of the films are close to each other. The nano-particles increase the hardness values from B (blank) to HB (with laponite), but the laponite causes hazy problem in the resulting polyurethane films.

3.4.3 Delamination of UV-curable Anti-fog transparent polyurethane films on the glass substrate

Delamination occurred for all UV-curable polyurethane films on glass substrate at either short or long UV-curing time, but did not take place when APTES was used as adhesion promoter on the glass substrate. Delamination did not occur for polyurethane films which cast on the polycarbonate substrate.

Table (3.1): The recipes and characterization of series (1) of UV-curable anti-fog PU films at different conditions which prepared from acronym (A)

Wet thickness [µm]	30	60	90	120
Substrate	Glass			
Concentration (w %) in acetone	20			
Irgacure 184 (wt.%, PU)	5.00			
Adhesion promoter	---			
Laponite (wt. %)	---			
Curing time	6 minutes			
Anti-Fog Test	very good			
Pencil Hardness Test	B	B	B	B
Delamination Occurred	Yes			

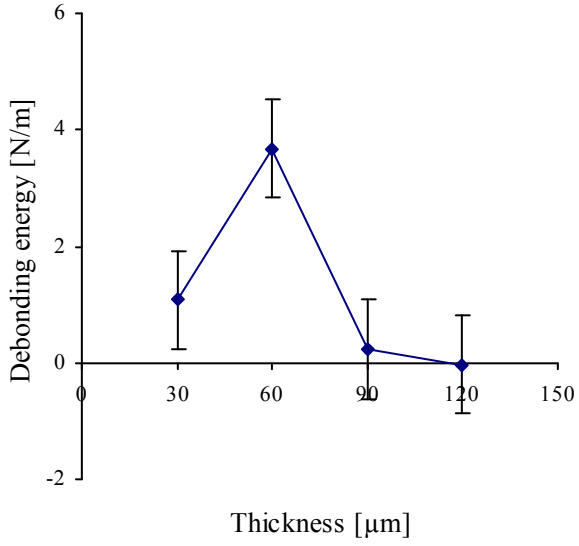

Fig. (3.2): Debonding energy versus thickness for series (1)

Table (3.2): The recipes and characterization of series (2) of UV-curable anti-fog PU films at different conditions which prepared from acronym (A)

Wet thickness [µm]	30	60	90	120
Substrate	Glass			
Concentration (w %) in acetone	20			
Irgacure 184 (wt.%, PU)	5.00			
Adhesion promoter	APTES			
Laponite (wt. %)	---			
Curing time	6 minutes			
Anti-Fog Test	very good			
Pencil Hardness Test	B	B	B	B
Delamination Occurred	No	No	No	No

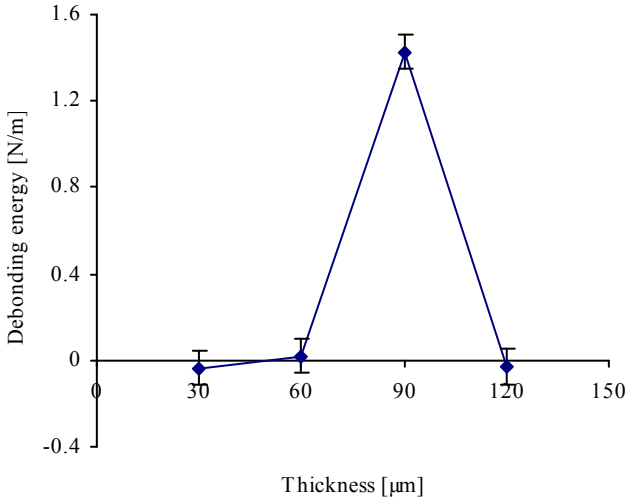

Fig. (3.3): Debonding energy versus thickness for series (2)

Table (3.3): The recipes and characterization of series (3) of UV-curable anti-fog PU films at different conditions which prepared from acronym (B)

Wet thickness [µm]	30	60	90	120
Concentration of PU in acetone(w %)	20			
Irgacure 184 (wt.%, PU)	5.00			
Adhesion promoter	---			
Substrate	Glass			
Laponite (wt. %)	---			
Curing time	6 minutes			
Anti-Fog Test	very good			
Pencil Hardness Test	B			
Delamination Occurred	No	Yes	Yes	Yes

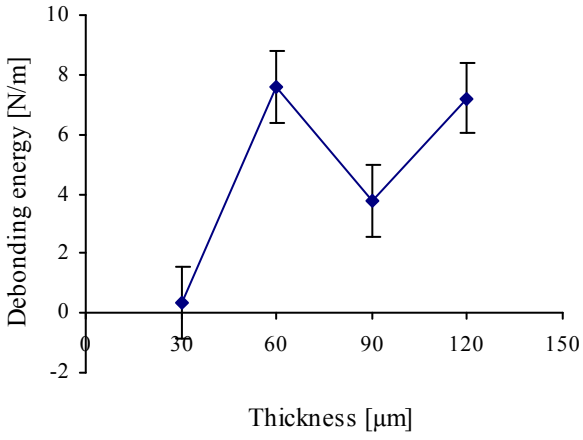

Fig. (3.4): Debonding energy versus thickness for series (3)

Table (3.4): The recipes and characterization of series (4) of UV-curable anti-fog PU films at different conditions which prepared from acronym (C)

Wet thickness [µm]	30	60	90	120
Substrate	Glass			
Concentration of PU in acetone (w %)	20			
Irgacure 184 (wt.%, PU)	5			
Adhesion promoter	APTES			
Laponite (wt. %)	5			
Curing time	6 minutes			
Anti-Fog Test	very good			
Pencil Hardness Test	B			
Delamination Occurred	No			

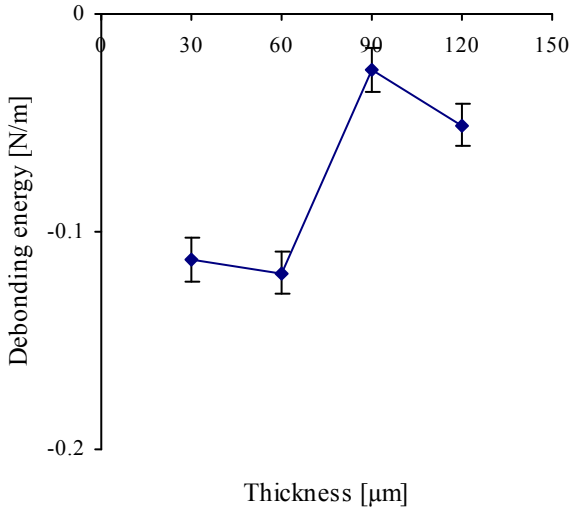

Fig. (3.5): Debonding energy versus thickness for series (4)

Table (3.5): The recipes and characterization of series (5) of UV-curable anti-fog PU films at different conditions which prepared from acronym (D)

Wet thickness [µm]	30	60	90	120
Substrate	Glass			
Concentration of PU in acetone (w %)	20			
Irgacure 184 (wt.%, PU)	5.00			
Adhesion promoter	APTES			
Laponite (wt. %)	5.00			
Curing time	6 minutes			
Anti-Fog Test	very good			
Pencil Hardness Test	HB			
Delamination Occurred	No			

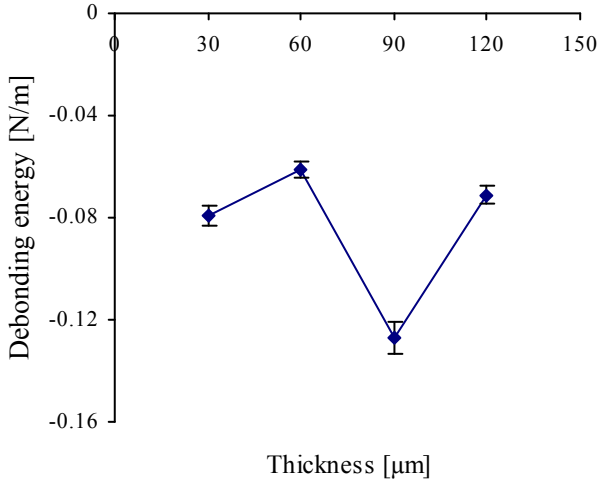

Fig. (3.6): Debonding energy versus thickness for series (5)

Table (3.6): The recipes and characterization of series (6) of UV-curable anti-fog PU films at different conditions which prepared from acronym (E)

Wet thickness [µm]	30	60	90	120
Substrate	Glass			
Concentration of PU in acetone (w %)	20			
Irgacure 184 (wt.%, PU)	5.00			
Adhesion promoter	APTES			
Laponite (wt. %)	5.00			
Curing time	6 minutes			
Anti-Fog Test	very good			
Pencil Hardness Test	HB			
Delamination Occurred	No			

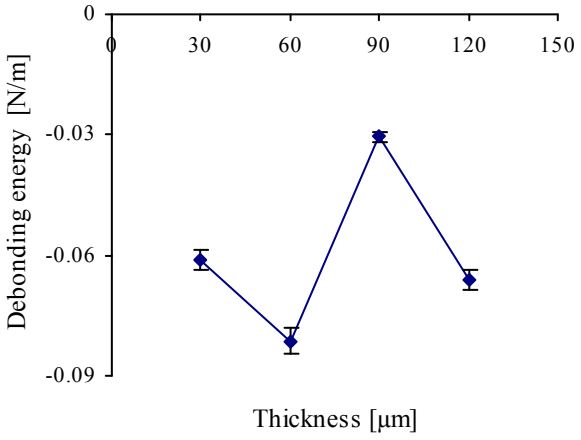

Fig. (3.7): Debonding energy versus thickness for series (6)

3.5 Comparison between two different polyurethane films which were cast from different polyurethanes acronyms.

The first acronym (A) was prepared from $PEG_{1000,}$: IPDI: HEA at the ratio 1:2:2, lower temperature (first step at 50 °C and the second step at 35 °C) of the reaction and also lower percentage of catalyst. Figure (3.8) presents the relationship between the irradiation times versus the tackiness for films which were cast from the polyurethane acronym (A). The tackiness of the resulting films was completely eliminated at irradiation time after five minutes, but the slight tackiness came back to the polyurethane films after about two days. This means that the polyurethane films have still some uncured monomers. The curing occurred for the top of the polyurethane films. There are still monomers in the bottom of the polyurethane films. After some time these monomers are going up to the top of the films causing the tackiness of the polyurethane film again.

The third acronym (C) was prepared from PEG_{1000}: IPDI: HEA at the ratio of 1:.2.2:2.2, at higher temperature (first step and the second step at 60°C) of the reaction and also at higher percentage of catalyst.

The fig (3.9) presents the relationship between the irradiation times versus the tackinesses of the polyurethane films which was cast from the polyurethane acronym (C). Whereas the tackiness of the polyurethane film was completely eliminated at irradiation time is one minute. The irradiation time for the polyurethane film which was cast from acronym (C) is shorter (1 minute) than time for polyurethane film (five minutes) that cast from acronym (A). And also the tackiness did not come back to the polyurethane film which was cast from acronym (C). The polyurethane film which was cast from the acronym (C) had more transparency and smoothness than the polyurethane film which was cast from polyurethane acronym (A). This means that the completely curing for the polyurethane films (which cast from polyurethane acronym (C)) leads to the smoothness of anti-fog polyurethane film surface without any wrinkling.

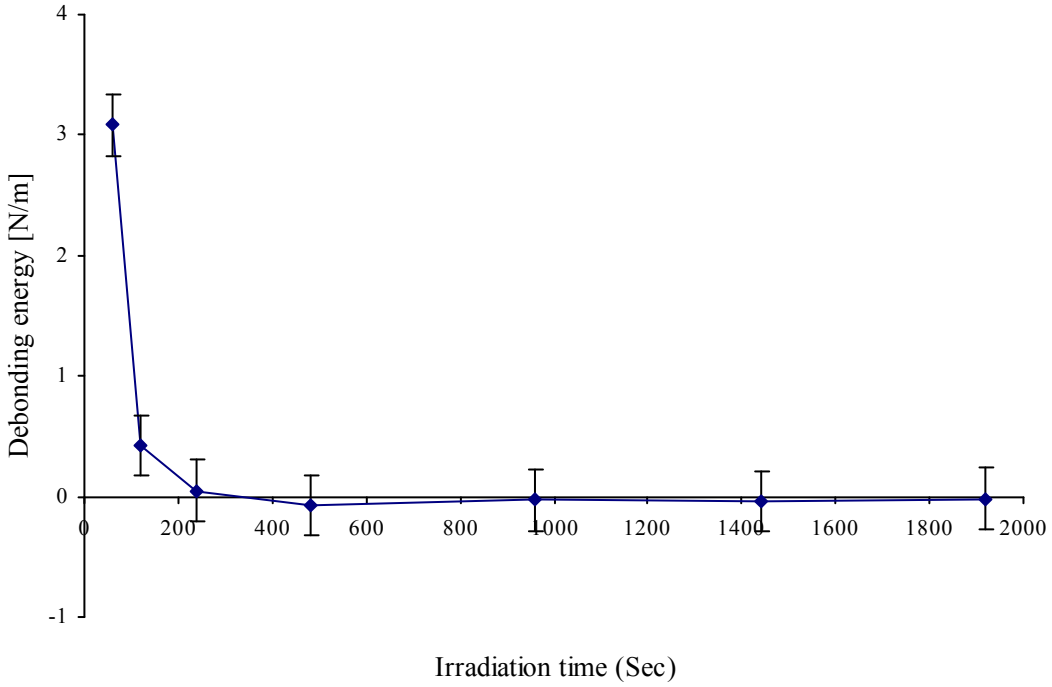

Fig (3.8): Irradiation time versus tackness for anti-fog PU film at 90 μm which was cast from polyurethane acronym (A)

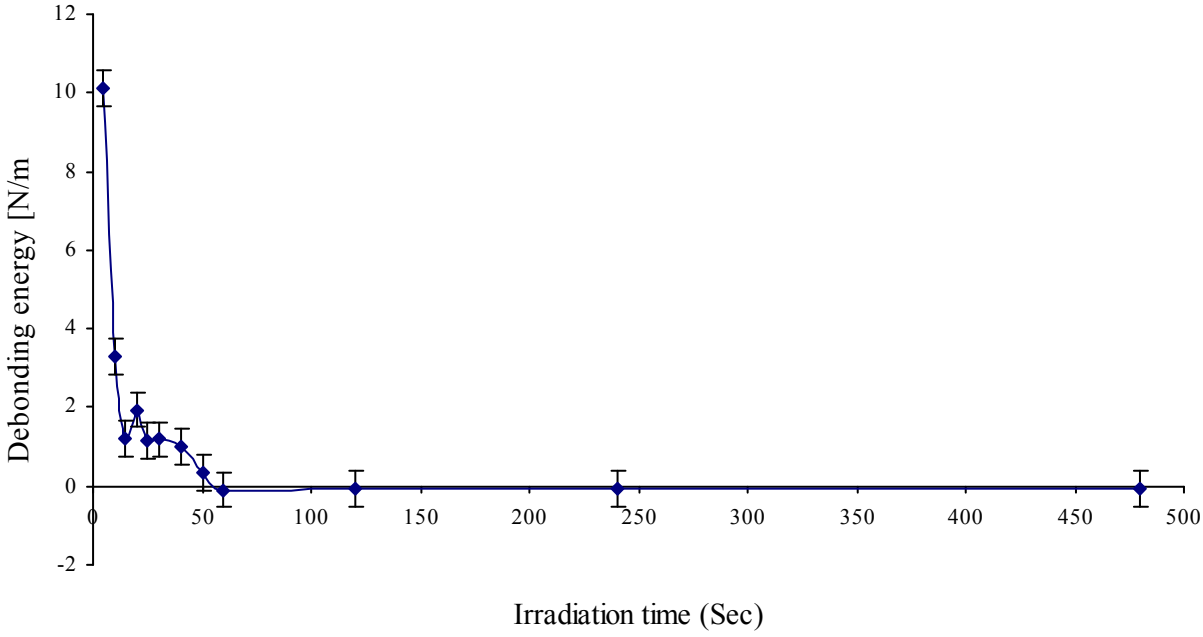

Fig.(3.9): Irradiation time versus tackiness for anti-fog PU film at 90 μm which was cast from polyurethane acronym (C)

3.6 The difference between thermal curing and UV-curing in the delamination and smoothness properties on glass substrate

The delamination did not occur for several thermal-cured anti-fog polyurethane films on glass substrates (without using APTES as adhesion promoter), but the delamination occurred for all UV-curable anti-fog polyurethane films (without using APTES as adhesion promoter). This is attributed to the heating process, which improves the adhesion of polyurethane films on glass surfaces.

Figure (3.10) represents the relationship between irradiation times and delamination times. Which the delamination occurred for all UV-curable polyurethane films around the same delamination times (13-20 sec). Delamination did not occur for UV-curable anti-fog polyurethane films on glass substrate when APTES was used as adhesion promoter. The delamination did not occur for neither UV-curable polyurethane films nor occur for thermal-curable polyurethane films on the polycarbonate substrate. The UV-curable polyurethane films were smoother than thermal-curable polyurethane films.

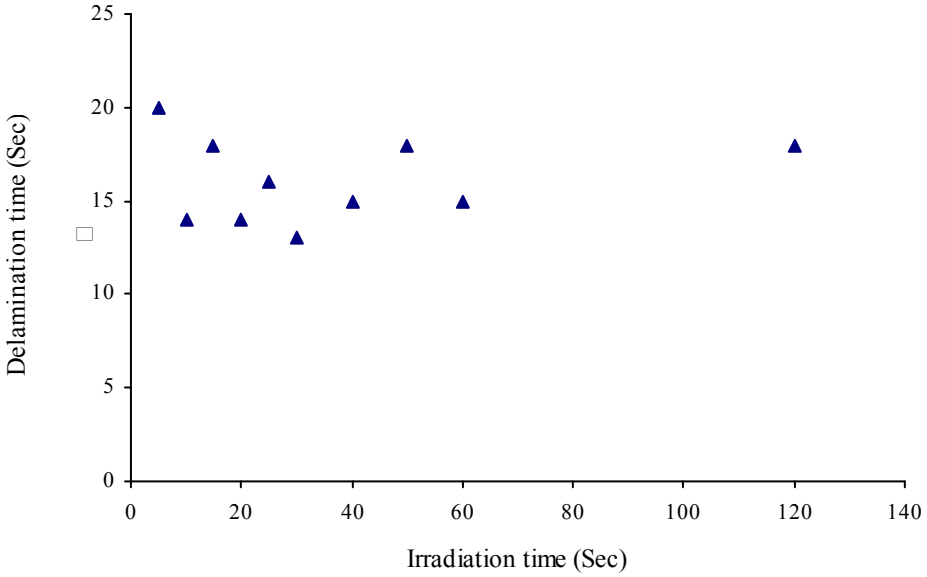

Fig. (3.10): Irradiation time versus delamination time for anti-fog PU film at 90 μm which were cast from polyurethane acronym (C)

3.7 Conclusions

- UV-curing has more advantages than thermal-curing like instant curing, ambient cure temperature, solvent free formations, in-line production, improved coating properties, low capital cost and energy efficiency.
- UV-curable anti-fog transparent polyurethane films have more smoothness; have no tackiness which cast from the acronyms C, D, and E depending on the preparation conditions of the polyurethane solution.
- The delamination occurred for all UV-curable anti-fog transparent polyurethane films which were cast on glass substrate while did not occur on polycarbonate substrate.
- The delamination takes place for UV-curable anti-fog transparent polyurethane films on the glass at lower or higher UV-curing time.
- APTES as adhesion promoter successfully overcomes on the delamination of UV-curable anti-fog transparent polyurethane films on the glass substrate.

4 Preparation and characterization of UV-curable anti-fog nano particles/ polyurethane films

4.1 Materials

In addition to the materials which were used in the previous chapters Köstrosol was used in this chapter as new nano-particles. Köstrosol is an aqueous dispersion of modified synthetic amorphous nanoscale silica particles with average diameter of around 20 nm. We have got the Köstrosol from GXC Company, Germany.

In our work, Köstrosol (silica nanoparticles dispersed in the water) was used after evaporation of the water to get the Köstrosol powder. Köstrosol poweder was dispersed in the polyurethane solution because the polyurethane solution forms gel with the water.

4.2 Experimental details

4.2.1 Preparation of polyurethane copolymer solution based on matrix from PEG_{1000} and PEG_{400} which the ratio between PEG_{1000} and PEG_{400} is (1:1) (Acronym F)

Procedures:

1- 50 g (0.05 mol) PEG_{1000} and 20 g (0.05 mol) PEG_{400} 30 g acetone were mixed. The mixture was fed into a three-necked flask equipped with a mechanical stirrer. The stirrer was operated at 150 rpm. A reflux condenser was employed. The temperature was 60°C under nitrogen atmosphere for 30 minutes.

2- 44.46 g (0.20 mol) IPDI and 0.44 g DBTL were mixed. The mixture was slowly dropped into the reactor under the above conditions for 2.1/3 hours.

3- The system was further reacted under the above conditions for an additional 1 hour.

4- 23.22 g (0.20 mol) HEA were added drop by drop to the reactor under the above conditions.

5- The reaction mixture was stirred for one additional hour under the above conditions.

6- The resulting clear and viscous solution was diluted by using acetone to obtain a diluted polyurethane copolymer solution with 50 % (w/w).

4.2.2 Preparation of polyurethane copolymer solution based on matrix from PEG_{1000} and PEG_{400} which the ratio between PEG_{1000} and PEG_{400} is (1:2) (Acronym G)

Procedures:

1- 80 g (0.08 mol) PEG_{1000} and 64 g (0.16 mol) PEG_{400} 30 g acetone were mixed. The mixture was fed into a three-necked flask equipped with a mechanical stirrer. The

stirrer was operated at 150 rpm. A reflux condenser was employed. The temperature was 60°C. The reaction occurred under nitrogen atmosphere for 1/2 hour.

2- 117.36 g (0.52 mol) IPDI and 1.17 g DBTL were mixed. The mixture was slowly dropped into the reactor under the above conditions for 2.1/4 hours.

3- 60 g Acetone was added to the reactor (to diluted the viscosity of the resulting urethane prepolymer)

4- The system was reacted further under the above conditions for additional 1.1/4 hours.

5- 61.30 g (0.52 mol) HEA was added drop by drop to the reactor for 1.1/2 hour under the above conditions.

6- The reaction mixture was stirred for one additional hour under the above conditions.

7- The resulting clear and viscous solution was diluted by using acetone to obtain a diluted polyurethane copolymer solution with 50 % (w/w).

4.2.3 Preparation of polyurethane copolymer solution based on a matrix from PEG_{1000} and PEG_{400} with a ratio between PEG_{1000} and PEG_{400} is 1:3 (Acronym H)

Procedures:

1- 70 g (0.07 mol) PEG_{1000} and 84 g (0.21 mol) PEG_{400} 30 g acetone were mixed. The mixture was fed into a three-necked flask equipped with a mechanical stirrer. The stirrer was operated at 150 rpm. A reflux condenser was employed. The temperature was 60°C. The reaction occurred under nitrogen atmosphere for 30 minutes.

2- 136.92 g (0.615 mol) IPDI and 1.4 g DBTL were mixed. The mixture was slowly dropped into the reactor under the above conditions for 2.1/2 hours.

3- 70 g acetone was added to the reactor (to dilute the viscosity of the resulting urethane prepolymer)

4- The system was reacted further under the above conditions for 1 hour.

5- 71.52 g (0.615 mol) HEA were added drop by drop to the reactor for 1.1/2 hour under the above conditions.

6- The reaction mixture was stirred for one additional hour under the above conditions.
7- The resulting clear and viscous solution was diluted by using acetone to obtain a diluted polyurethane copolymer solution with 50 % (w/w).

4.2.4 Preparation of anti-fog nano-filled/polyurethane dispersion by using Ultra-Turrax homogenizer

Different percentages from several types of nano-particles were dispersed into the polyurethane solution in presence of photoinitiator (Irgacure 184). The Ultra-Turrax T25 Fig. (4.1), digital homogenizer was used to completely disperse the nano-particles in the polyurethane solution at high speed rotation. 24.000 rpm for one minute were used for all the recipes, subsequently the nanoparticles/polyurethane dispersion was cast on either glass or polycarbonate substrate at different wet thicknesses.

4.2.4.1 Ultra-Turrax homogenizer

4.2.4.2

The homogenizer has high-speed, easy-to-operate disperser performs a variety of applications such as waste water samples, laboratory reactors, dispersion under vacuum/pressure, and sample preparation. Simply switch it on and choose your speed from 6,500 to 24,000 rpm. Overload protection turns unit off if the 300 W motor runs too high. Order strap clamp to stabilize your vessel, plate stand, and movable boss head to position the dispersing element and vessel holder separately below. The specifications of the Ultra-Turax homogenizer are the followsing:

Sample Volume:	1 to 2000 ml
Speed Range:	6,500 to 24,000 rpm
Dimensions:	2 3/4W x 8 3/4H x 2 1/2D"
Power:	115 V, 50/60 Hz

Fig. (4.1) **:** The Ultra-Turrax T25 Digital homogenizer

4.2.5 Optical imaging of UV-curable anti-fog nano-filled/polyurethane films by using (imaging equipment) canon camera looking into the microscope

UV-curable nano-filled/polyurethane films were clamped on the square line paper. The sides of the square are 5 mm long. By other meaning the square line paper was fixed underneath the glass as a background for the resulting images. The optical images of either polyurethane films or nano-filled/polyurethane films were imaged by using the canon camera which was fixed to look in the microscope. This is illustrated by the following optical imaging equipment Fig (4.1).

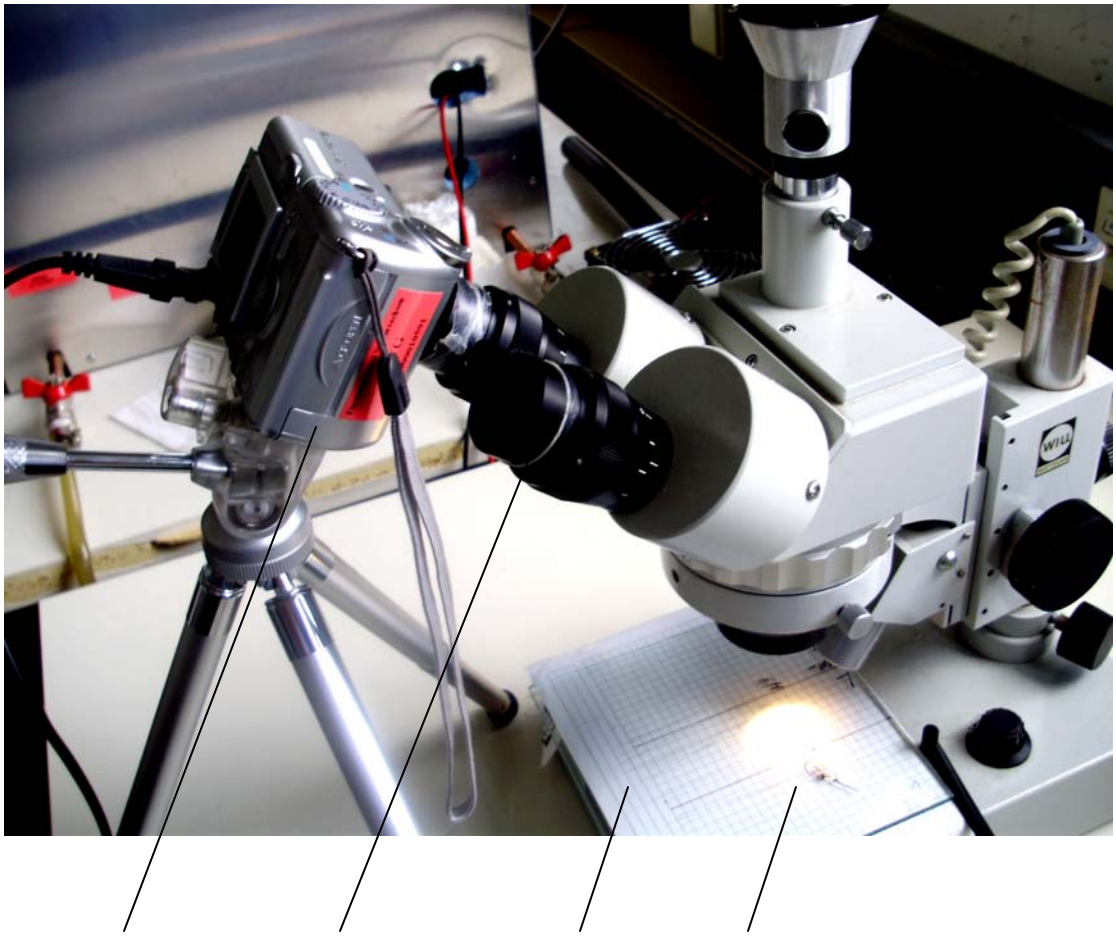

Fig. (4.2): The optical imaging equipment to image the nano-filled/polyurethane films

4.2.6 Glass transition temperatures of UV-curable anti-fog nano-filled/polyurethane films based on matrix from of PEG_{1000} and PEG_{400} at either ratio (1:3) or (1:2)

The glass transition temperature of UV-curable anti-fog polyurethane based on (PEG_{1000}/PEG_{400} = 1/3) or based on (PEG_{1000}/PEG_{400} = 1/2) were measured as blank films. The Aerosil R792/polyurethane based on (PEG_{1000} and PEG_{400}) either at ratio (1:2) or (1.3) at different percentages were measured as nano-filled films by Differential Scanning Calorimetry (DSC) using the DSC-7 instrument (Perkin Elmer) in the temperature range between (-100 and 100°C).

4.3 Results and discussion

4.3.1 The dispersion of nano-particles in the polyurethane solution

The Ultra-Trax homogenizer was used to disperse the nano-particles in the polyurethane solution. The resulting nano-particle/polyurethane dispersion was cast on the substrate subsequently to avoid the sedimentation of the nano-particles in polyurethane solution by the time, causing agglomeration technology problem. The resulting dispersion was physically unstable. Sedimentation was occured by time.

4.3.2 The hardness of UV-curable anti-fog nano-filled polyurethane based on matrix of PEG_{1000} and PEG_{400} at ratio (1:3)

The distribution of nano-particles in the anti-fog polyurethane films at a thickness of 30 or 90 μm increases the hardness values of the UV-curable anti-fog polyurethane films. Hardness values from B to HB or F were reached. The hardness values of the polyurethane films at different percentages of different nano-fillers were tabulated in the tables (4.1 to 4.3). On the other hand, the distribution of nano-particles in the polyurethane network did not decrease the anti-fog property of the polyurethane films.

4.3.3 The hardness of UV-curable anti-fog nano-filled polyurethane based on matrix of PEG_{1000} and PEG_{400} at ratio (1:2)

The hardness values of the polyurethane films at different percentages of different nano-fillers were tabulated in the tables (4.4 to 4.6). There is no difference between the hardness values of the UV-curable polyurethane films which were prepared based on

PEG_{1000} and PEG_{400} either at ratio (1:3) or (1:2). The structure of both polyurethane films are very close to each other.

4.3.4 Optical imaging of UV-curable anti-fog nano-filled polyurethane films based on matrix from of PEG_{1000} and PEG_{400} at either ratio (1:3) or (1:2) by using canon camera looking into the microscope or Confocal microscope

The images for UV-curable anti-fog polyurethane films (blank) and nano-filled polyurethane films at different nano-filler types, different percentages of these fillers and different thickness based on matrix from PEG_{1000} and PEG_{400} at ratio (1:3) were imaged by using our imaging equipment. The images are shown in the figures (4.3 to 4.8).
The images of UV-curable anti-fog nano-particles/polyurethane based on matrix from PEG_{1000} and PEG_{400} at ratio (1:3) at different percentages of Aerosil R792, Köstrosol or Laponite clay have agglomeration which is consider to be a nano-technology problem. This agglomeration increases by increasing the percentages of nano-filler in the polyurethane films. The agglomeration rate of the nano-particles /polyurethane films were ordered according to the following ascending order:

Aerosil R972/PU < Köstrosol/PU < Laponite/PU

UV-curable anti-fog AerosilR792/polyurethane films have lower agglomeration but the UV-curable polyurethane films also have haziness. The scattering of light by Aersoil R972 in the polyurethane films was lower than with Köstrosol or Laponite. The images showed that, increasing of nano-particles increases agglomeration in Köstrosol or laponite while in Aerosil R972/polyurethane films, increasing of nanoparticles increases of agglomeration at 0.5%, 1%, 2%, 3% (w/w) but at 5% or 7% the Nanoparticles are close packed. The scattering light was lower at higher percentages but the films were having haziness. The Aerosil/polyurethane dip films were imaged by confocal microscope Fig. (1.15). The confocal microscope emphasise the same behavour. UV-curable anti-fog Laponite/polyurethane films show higher agglomeration than Köstrosol/PU or Laponite/PU films. This may attributed to the significant chemical structure plates of the laponite clay. The images for UV-curable anti-fog polyurethane based on matrix from PEG_{1000} and PEG_{400} at ratio (1:2) at different thicknesses (blank) and UV-curable nano-filled/ polyurethane at different nano-filler type, different thicknesses or different percentages of nano-fillers were imaged and represented in figures (4.9 to 4.14). The nano-fillers have almost the same hardness values or agglomeration of UV-curable anti-fog polyurethane based on matrix from PEG_{1000} and PEG_{400} either at ratio (1:2) or (1:3). There is no big difference between the networks

which resulted from polyurethane based on PEG_{1000} and PEG_{400} either at ratio (1:2) or ratio (1:3). Which the structure of the both polyurethane networks based on PEG1000 and PEG_{400} either at ratio (1:3) or (1:2) are very close to each other.

Table (4.1, 2): The hardness values of UV-curable anti-fog Aerosil R972/PU or Köstrosol 2040/ PU films based on (PEG_{1000}/PEG_{400} = 1/3) at different percentages (w/w) on glass substrates

Samp. No	Nanopart-icles	Nanoparticles %(w/w)	Wet thickness μ m	Hardness
Blank 1		0	30	B
Blank 2			90	B
R1	Aerosil R972	0.5	30	HB
R2			90	HB
R3		1.0	30	HB
R4			90	HB
R5		2.0	30	HB
R6			90	HB
R7		3.0	30	F
R8			90	HB
R9		5.0	30	HB
R10			90	HB
R11		7.0	30	HB
R12			90	HB

Samp. No	Nanoparticles	Nanoparticles %(w/w)	Wet thickness μ m	Hardness
Blank 1		0	30	B
Blank 2			90	B
K1	Köstrosol 2040	0.5	30	HB
K2			90	HB
K3		1.0	30	HB
K4			90	HB
K5		2.0	30	HB
K6			90	HB
K7		3.0	30	F
K8			90	HB
K9		5.0	30	HB
K10			90	HB
K11		7.0	30	HB
K12			90	HB

Table (4.3): The hardness values of UV-curable anti-fog laponite/PU films based on (PEG_{1000}/PEG_{400} = 1/3) at different percentages (w/w) on glass substrates

Sample No	Nanoparticles	Nanoparticles %(w/w)	Wet thickness μ m	Hardness
Blank 1		0	30	B
Blank 2			90	HB
L1	Laponite	0.5	30	HB
L2			90	HB
L3		1.0	30	HB
L4			90	HB
L5		2.0	30	HB
L6			90	HB
L7		3.0	30	F
L8			90	HB
L9		5.0	30	HB
L10			90	HB
L11		7.0	30	HB
L12			90	HB

Fig. (4.3): The images of UV-curable anti-fog Aerosil R972/PU films based on (PEG_{1000}/PEG_{400} = 1/3) at different percentages (w/w) and at 30 μm (wet thickness) by using canon camera looking into the microscope on glass substrates

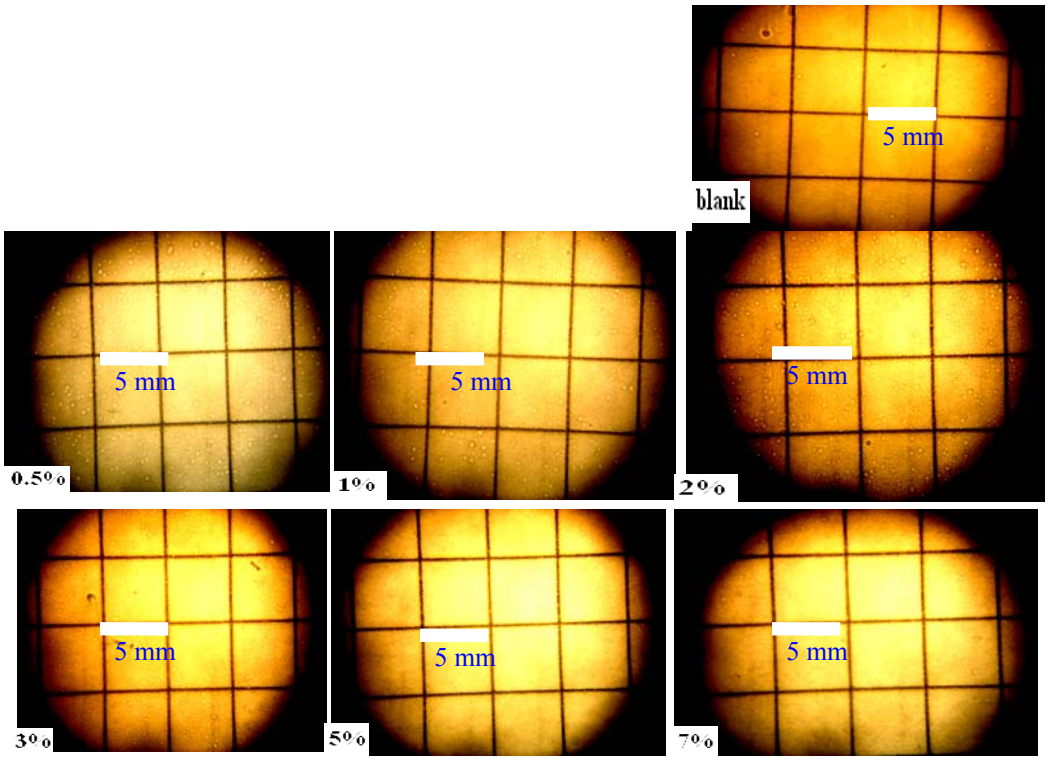

Fig. (4.4): The images of UV-curable anti-fog Aerosil R972/PU films based on (PEG_{1000}/PEG_{400} = 1/3) at different percentages (w/w) and at 90 μm (wet thickness) by using canon camera looking into the microscope on glass substrates

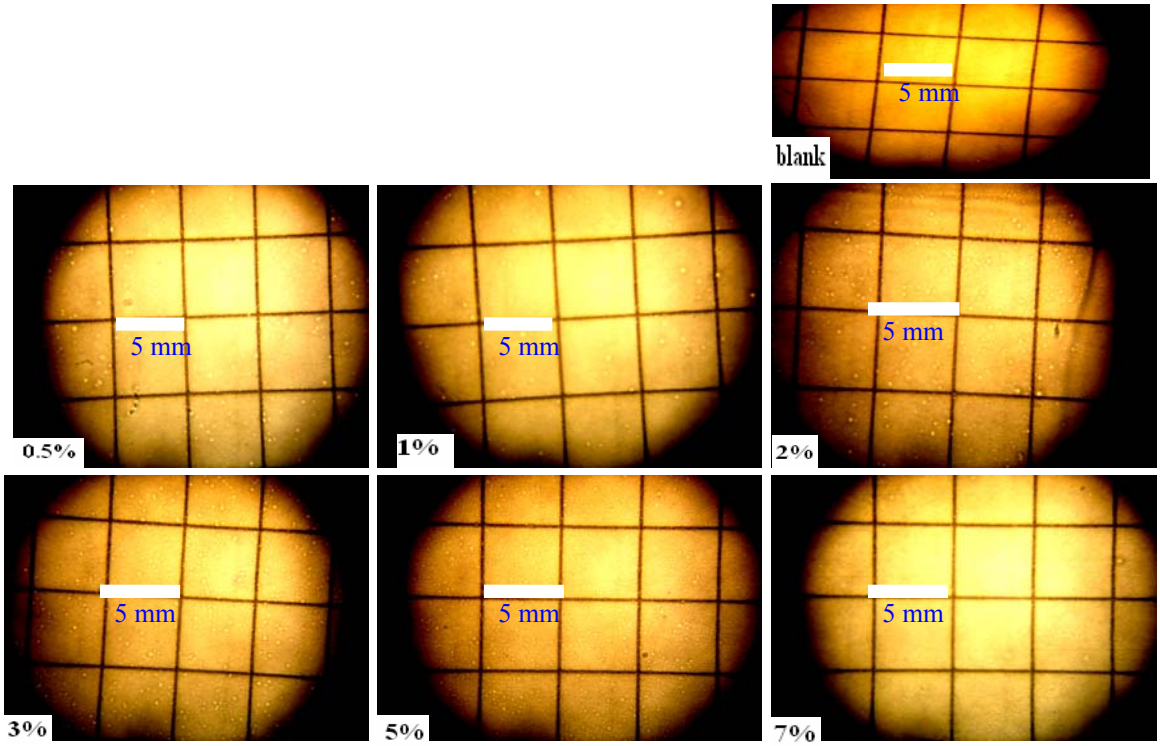

Fig. (4.5): the images of UV-curable anti-fog Köstroso/PU films based on (PEG_{1000}/PEG_{400} = 1/3) at different percentages (w/w) and at 30 μm (wet thickness) by using canon camera looking into the microscope on glass substrates

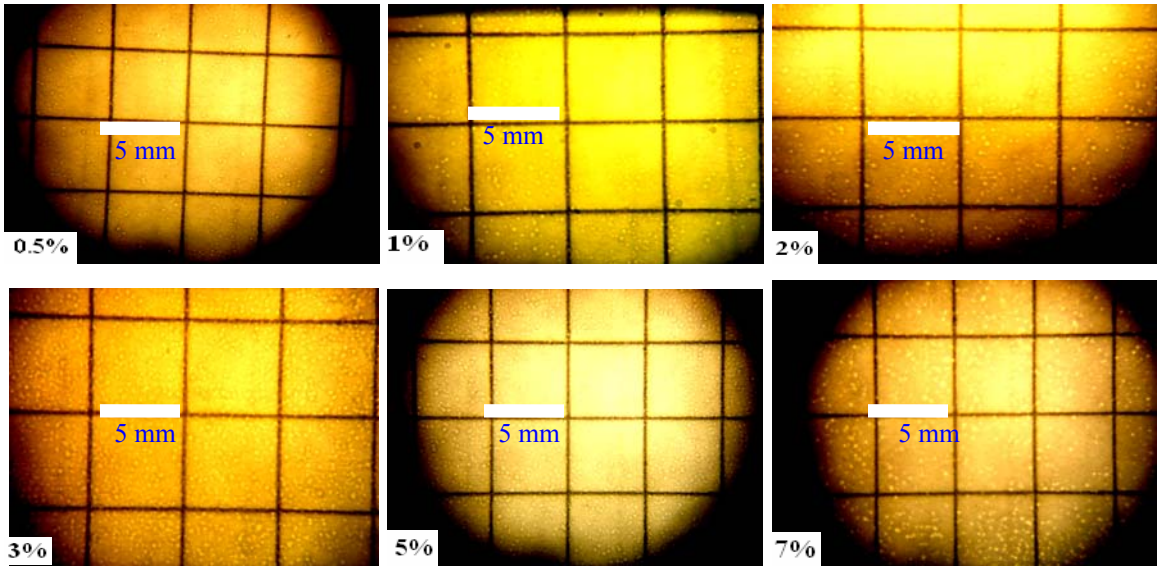

Fig. (4.6): The images of UV-curable anti-fog Köstrosol/PU films based on (PEG_{1000}/PEG_{400} = 1/3) at different percentages (w/w) and at 30 μm (wet thickness) by using canon camera looking into the microscope on glass substrates

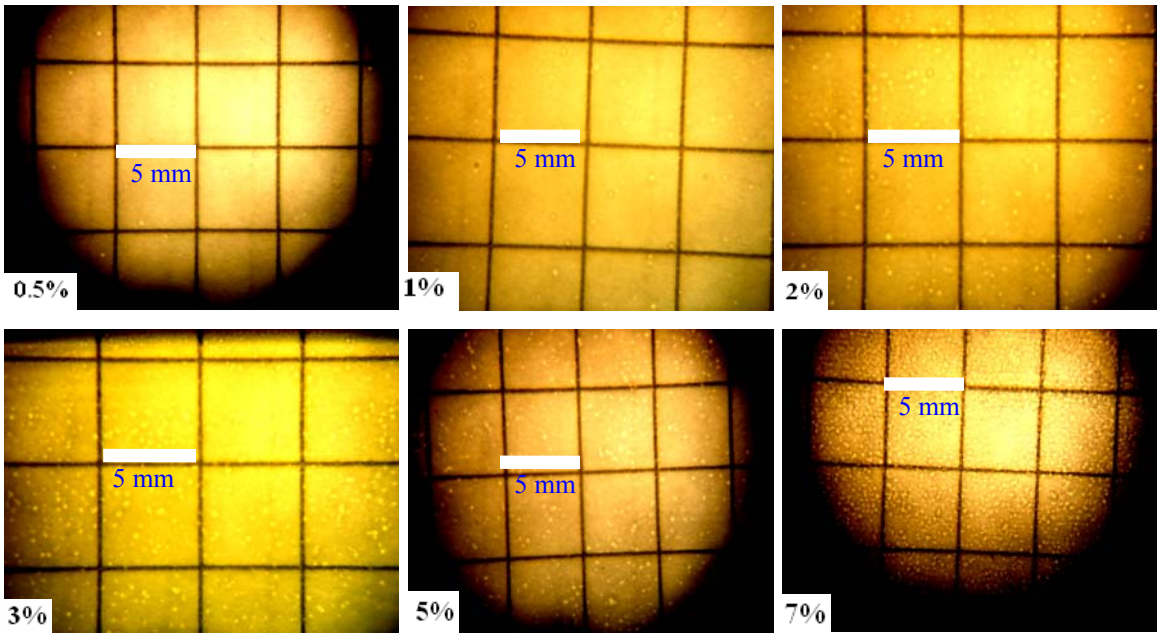

Fig. (4.7): The images of UV-curable anti-fog Laponite/PU films based on (PEG_{1000}/PEG_{400} = 1/3) at different percentages (w/w) and at 30 μm (wet thickness) by using canon camera looking into the microscope on glass substrates

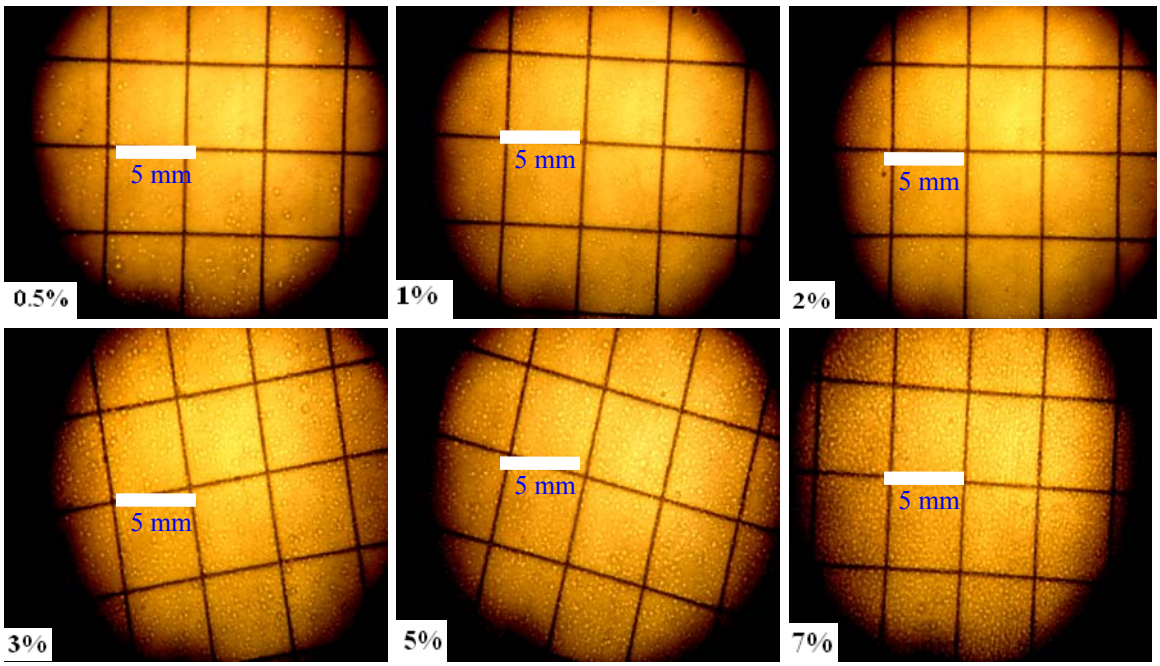

Fig. (4.8): The images of UV-curable anti-fog Laponite/ PU films based on (PEG_{1000}/PEG_{400} = 1/3) at different percentages (w/w) and at 90 μm (wet thickness) by using canon camera looking into the microscope on glass substrates

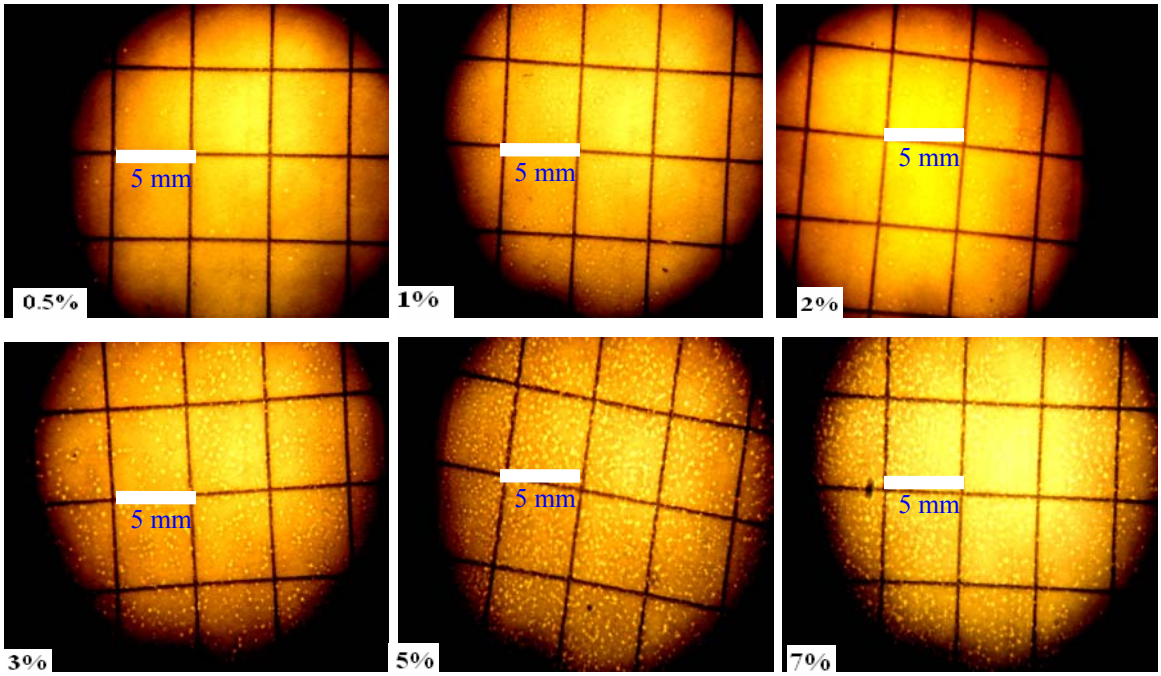

Table (4.4, 5): The hardness values of UV-curable anti-fog of Aerosil R972/PU or Köstrosol /PU films based on (PEG_{1000}/PEG_{400} = 1/2) at different percentages (w/w) on glass substrates

Samp. No	Nanoparticles	Nanoparticles %(w/w)	Wet thickness μ m	Hardness
Blank 1		0	30	B
Blank 2			90	B
R1	Aerosil R972	0.5	30	HB
R2			90	HB
R3		1.0	30	HB
R4			90	HB
R5		2.0	30	HB
R6			90	HB
R7		3.0	30	F
R8			90	HB
R9		5.0	30	HB
R10			90	HB
R11		7.0	30	HB
R12			90	HB

Samp. No	Nanoparticles	Nanoparticles %(w/w)	Wet thickness μ m	Hardness
Blank 1		0	30	B
Blank 2			90	B
R1	Köstrosol 2040	0.5	30	HB
R2			90	HB
R3		1.0	30	HB
R4			90	HB
R5		2.0	30	HB
R6			90	HB
R7		3.0	30	F
R8			90	HB
R9		5.0	30	HB
R10			90	HB
R11		7.0	30	HB
R12			90	HB

Table (4.6): The hardness of UV-curable anti-fog of laponite/PU films based on (PEG_{1000}/PEG_{400} = 1/3) at different percentages (w/w) on glass substrates

Sample No	Nanoparticles	Nanoparticles %(w/w)	Wet thickness μ m	Hardness
Blank 1		0	30	B
Blank 2			90	B
L1	Laponite	0.5	30	HB
L2			90	HB
L3		1.0	30	HB
L4			90	HB
L5		2.0	30	HB
L6			90	HB
L7		3.0	30	HB
L8			90	HB
L9		5.0	30	HB
L10			90	HB
L11		7.0	30	HB
L12			90	HB

Fig. (4.9): The images of UV-curable anti-fog Aerosil R972/PU films based on (PEG_{1000}/PEG_{400} =1/2) different percentages (w/w) and at 30 μm (wet thickness) by using canon camera looking into the microscope on glass substrates

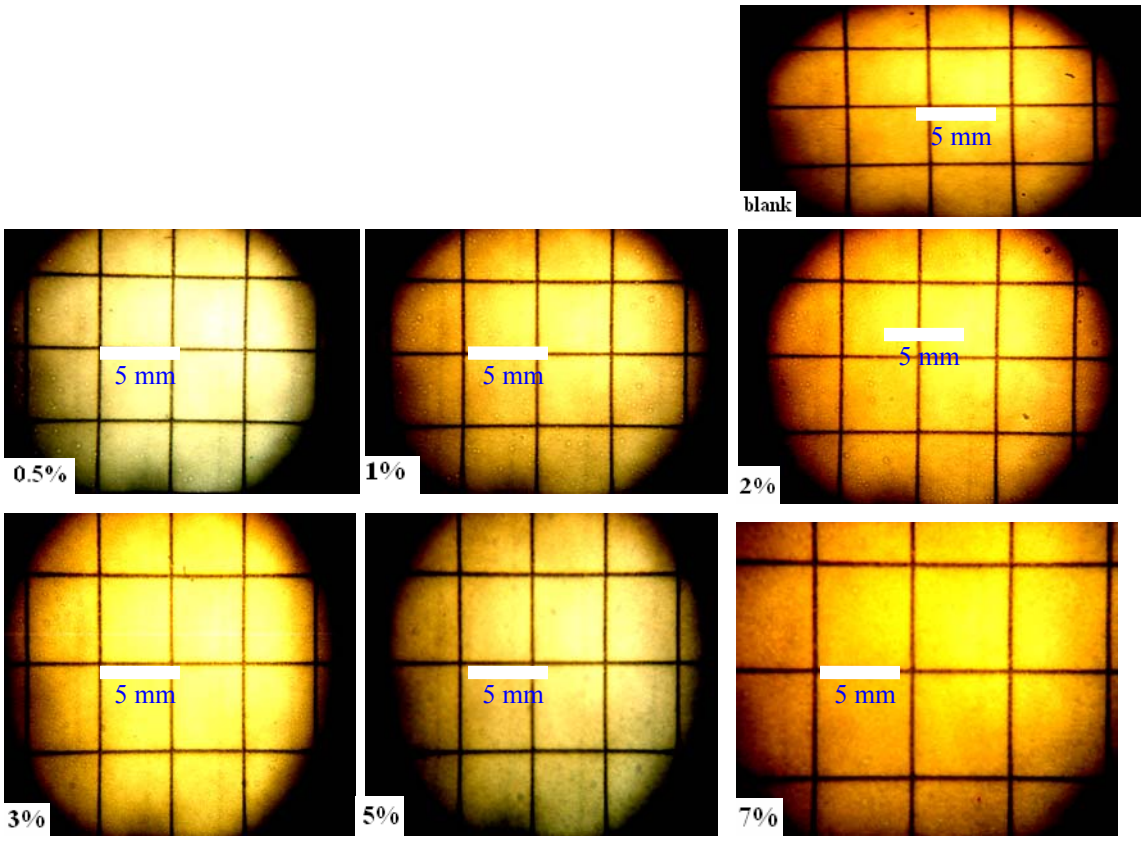

Fig. (4.10): The images of UV-curable anti-fog Aerosil R972/PU films based on (PEG_{1000}/PEG_{400} =1/2) at different percentages (w/w) and at 90 μm (wet thickness) by using canon camera looking into the microscope on glass substrates

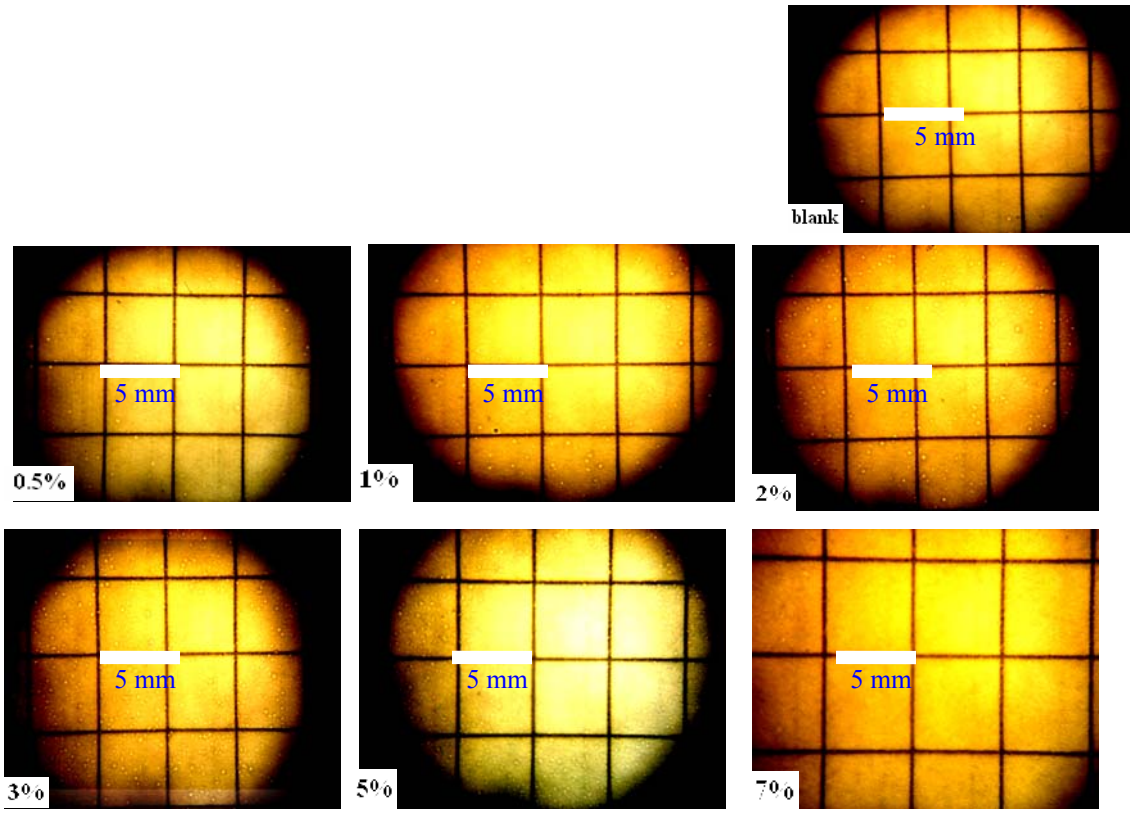

Fig. (4.11): The images of UV-curable anti-fog Köstrosol 2040/PU films based on (PEG_{1000}/PEG_{400} =1/2) at different percentages (w/w) and at 30 μm (wet thickness) by using canon camera looking into the microscope on glass substrates

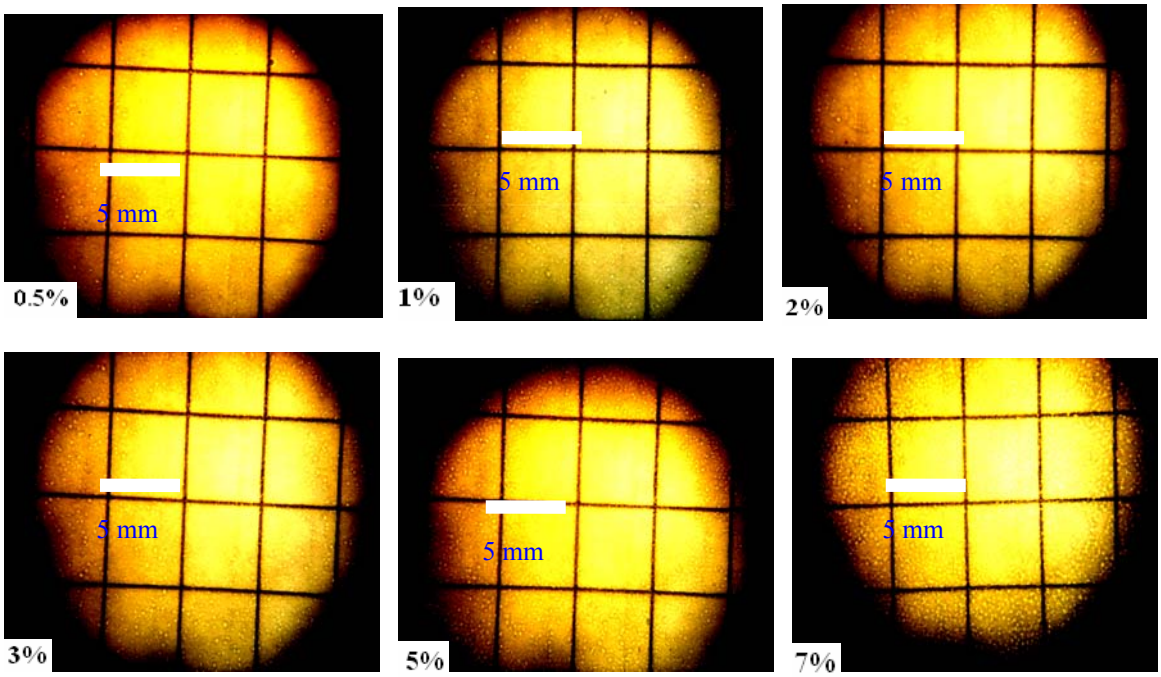

Fig. (4.12): The images of UV-curable anti-fog Köstrosol 2040/PU films based on (PEG_{1000}/PEG_{400} =1/2) at different percentages (w/w) and at 90 μm (wet thickness) by using canon camera looking into the microscope on glass substrates

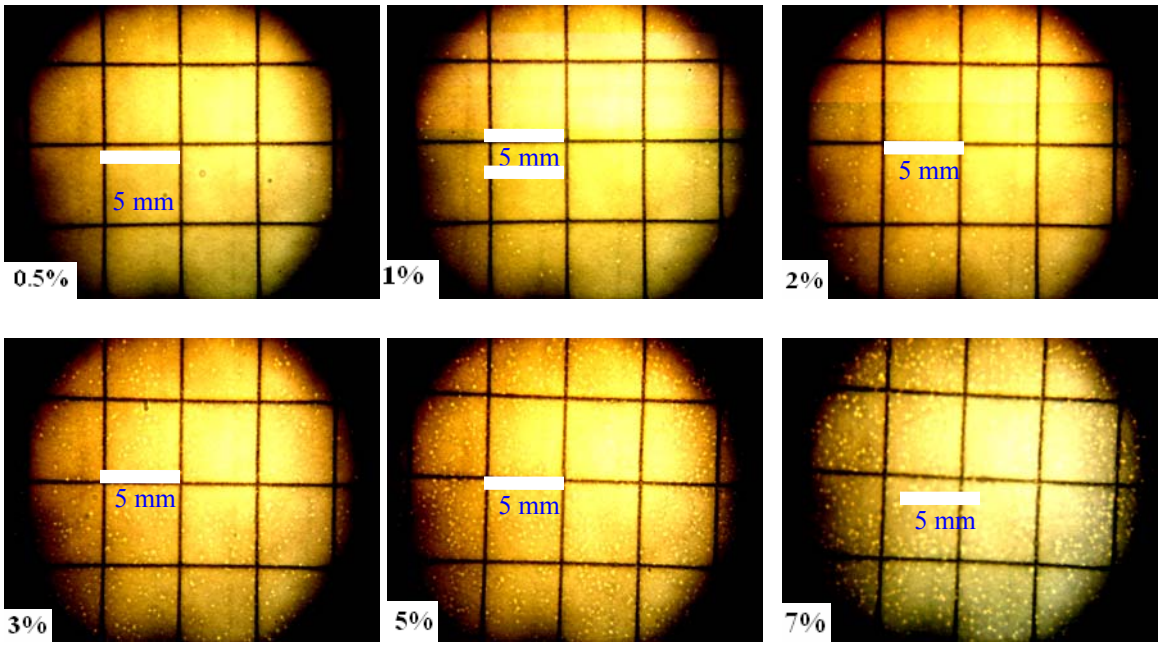

Fig. (4.13): The images of UV-curable anti-fog Laponite /PU films based on (PEG_{1000}/PEG_{400} =1/2) at different percentages (w/w) and at 30 μm (wet thickness) by using canon camera looking into the microscope on glass substrates

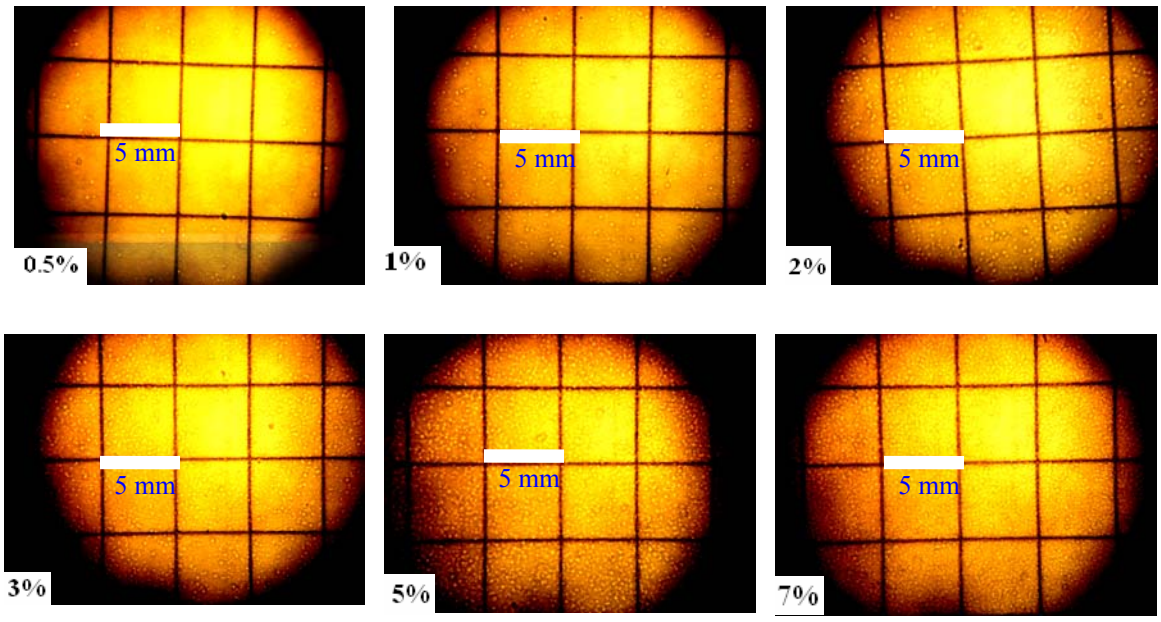

Fig. (4.14): The images of UV-curable anti-fog Laponite/PU films based on (PEG_{1000}/PEG_{400} =1/2) at different percentages (w/w) and at 90 μm (wet thickness) by using canon camera looking into the microscope on glass substrates

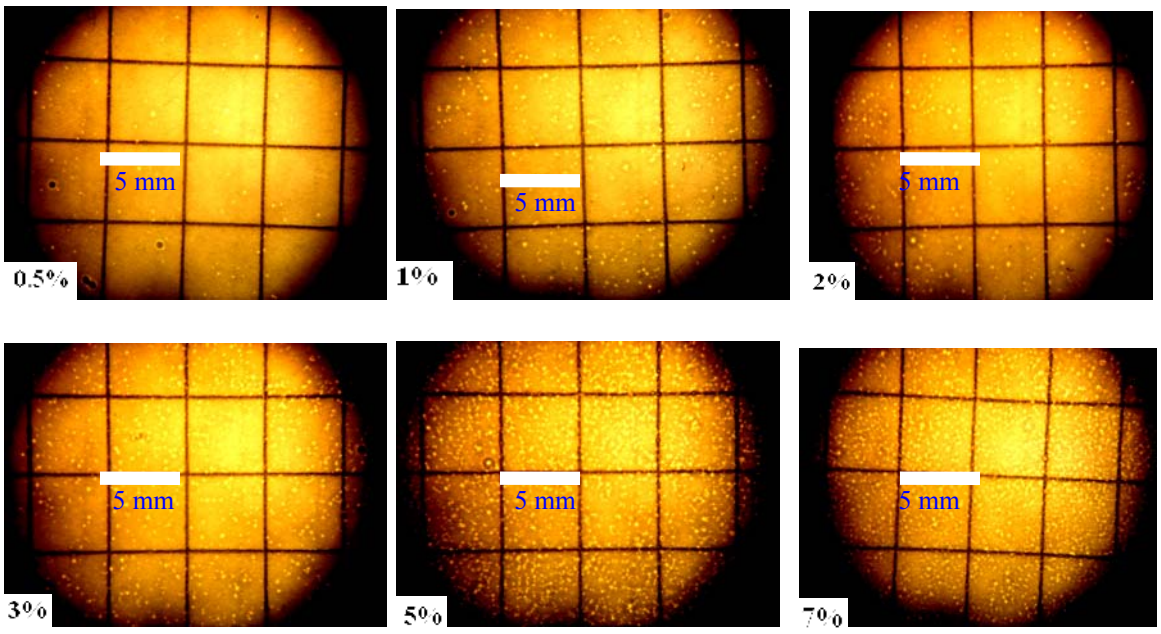

Fig. (4.15): An optical images of UV-curable anti-fog Aerosil R972 /PU dip films based on (PEG_{1000}/PEG_{400} =1/2) at different percentages of Aerosil R972 (w/w) by using Confocal microscope on glass substrates

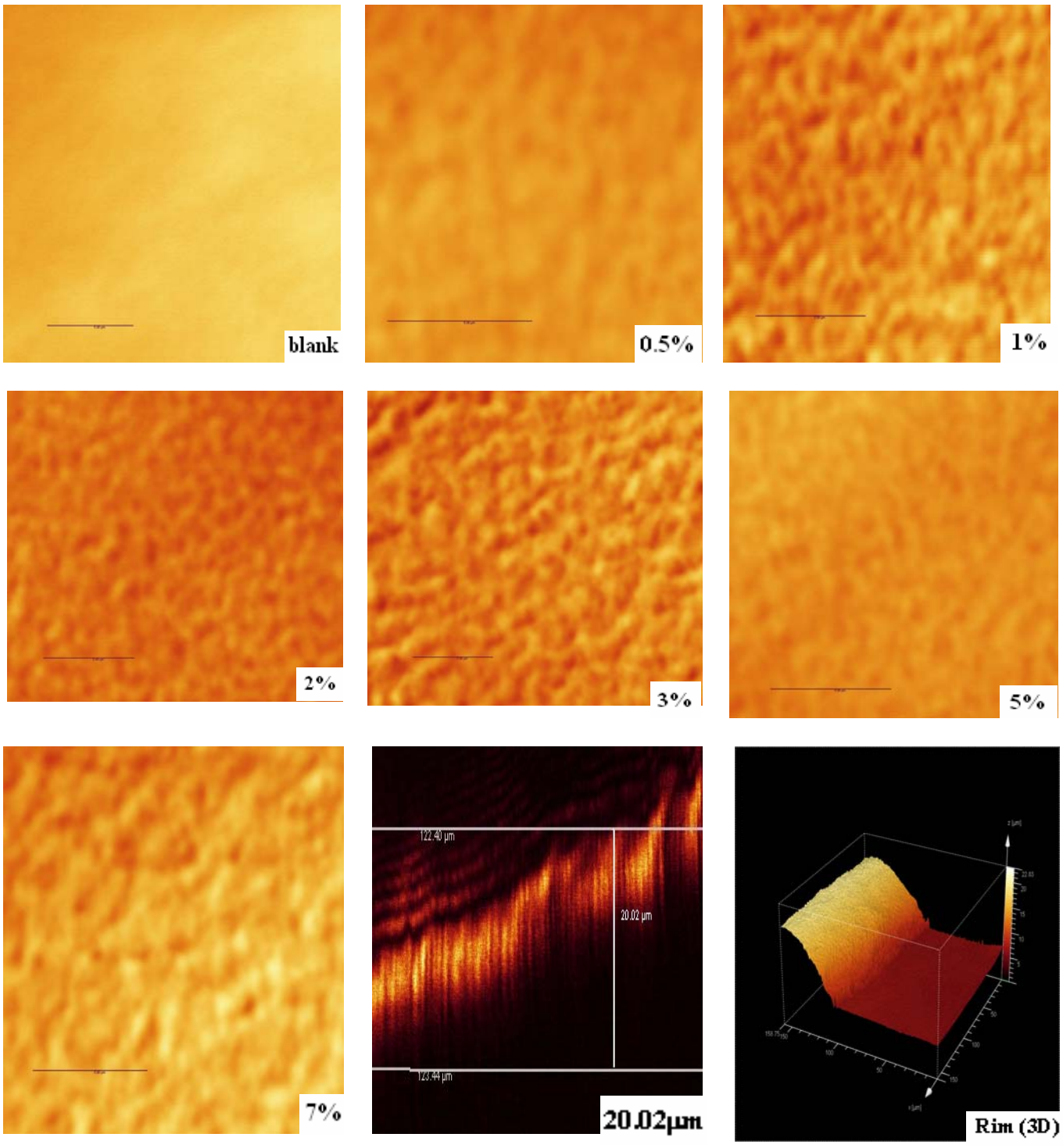

4.4 Glass transition temperatures of UV-curable anti-fog nano-filled/polyurethane films based on matrix from of PEG_{1000} and PEG_{400} at either ratio (1:3) or (1:2)

The glass transition temperatures of UV-curable anti-fog polyurethane films based on (PEG_{1000}/PEG_{400}) at either ratio (1:3) or (1:2) as a blank films and Aerosil R972/polyurethane films at different percentages are also measured by Differential Scanning Calorimetry (DSC). The data of the measurements were represented in figure (4.15 and 4.16). We have not seen any noticeable shift in the polymer after showing uniform distribution of sphere nano-silica and no agglomeration. Surprisingly, we found no relevant effects when increasing the filler content and this also agrees with Gonzalez-Irun Rodriguez et. al.[208]

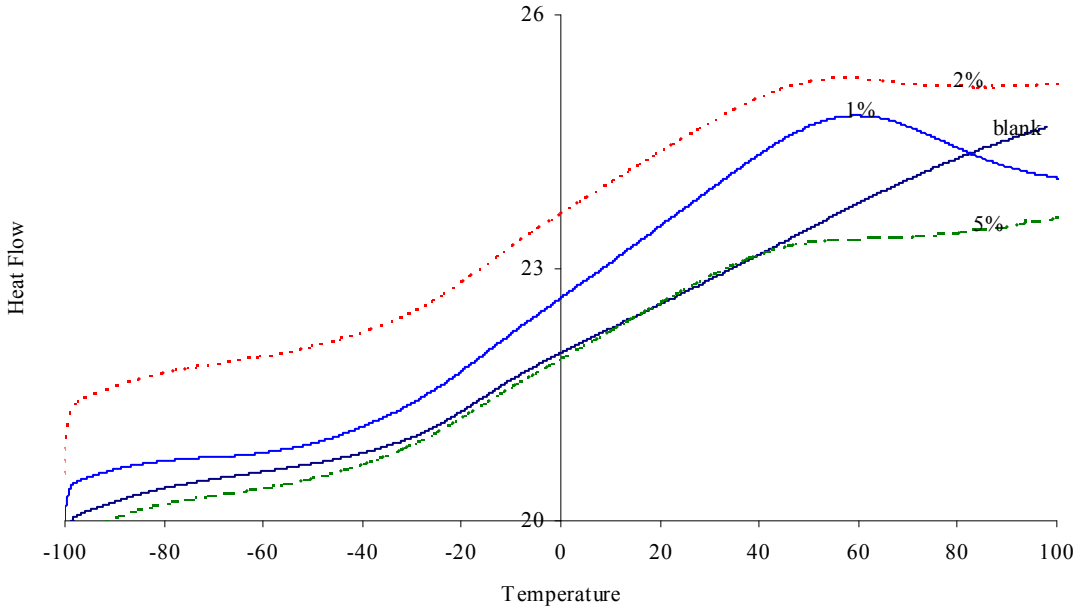

Fig. (4.15): The glass transition temperatures of UV-curable anti-fog Aerosil R792/PU films based on (PEG_{1000}/PEG_{400} =1/3) at different percentages of Aerosil R972

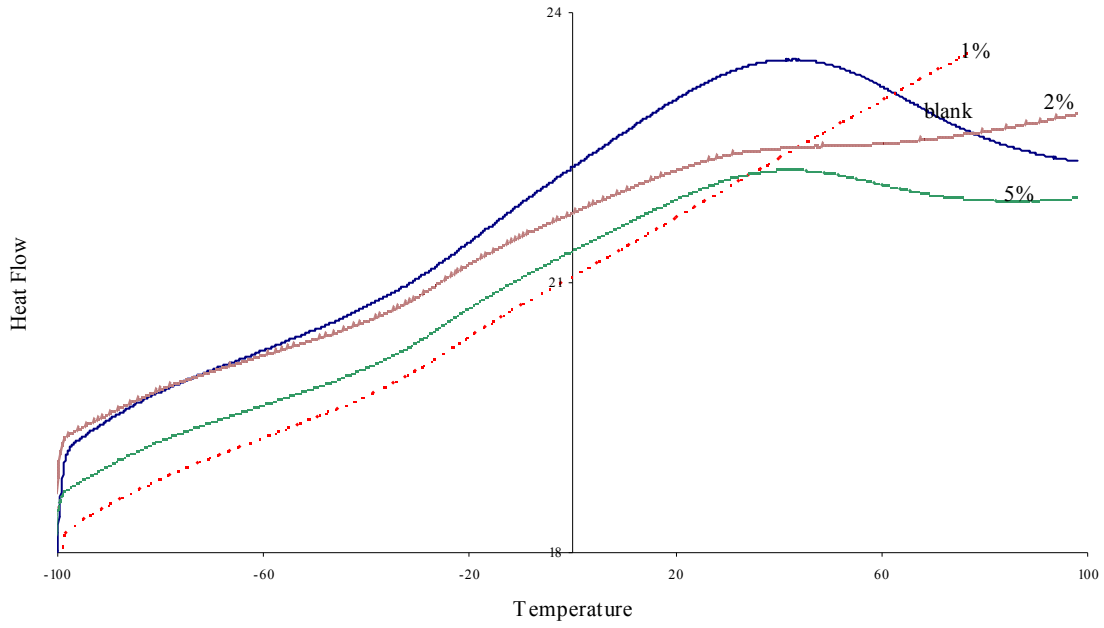

Fig. (4.16): The glass transition temperatures of UV-curable anti-fog Aerosil R792/PU films based on (PEG_{1000}/PEG_{400} =1/2) at different percentages Aerosil R972

4.5 Conclusions

- The nano-particles, Aerosil R792 (hydrophobic), Köstrosol 2040 and laponite clay increase the hardness values of UV-curable anti-fog polyurethane but not so much even at higher percentages and they do not effect on the anti-fog property of the resulting UV-curable polyurethane films.

- The previous nano-particles cause agglomeration nano-technology problem in the resulting UV-curable anti-fog polyurethane films. This leads to haziness in the resulting nano-particles/polyurethane films.

- There is no noticeable changing of glass transition temperatures of the nano-particles/polyurethane films.

5 Preparation and characterization of Stöber particles, UV-curable anti-fog Stöber particles/polyurethane films and preparation of Stöber particles/ polyurethane gel

5. 1 Introduction

The sol-gel process, as the name implies, involves the evolution of inorganic networks through the formation of a colloidal suspension (sol) and gelation of the sol to form a network in a continuous liquid phase (gel).[203] The precursors for synthesizing these colloids consist of a metal or metalloid element surrounded by various reactive ligands. Metal alkoxides are most popular because they react readily with water. The most widely used metal alkoxides are the alkoxysilanes, such as tetramethoxysilane (TMOS) and tetraethoxysilane (TEOS).

5.2 Base-Catalyzed Mechanism

Basic alkoxide oxygens tend to repel the nucleophile, -OH. However, once an initial hydrolysis has occurred, following reactions proceed stepwise, with each subsequent alkoxide group more easily removed from the monomer.[204] Therefore, more highly hydrolyzed silicones are more prone to attack. Additionally, hydrolysis of the forming polymer is more sterically hindered than the hydrolysis of a monomer. Although hydrolysis in alkaline environments is slow, it still tends to be complete and irreversible. [205] Thus, under basic conditions, it is likely that water dissociates to produce hydroxyl anions in a rapid first step. The hydroxyl anion then attacks the silicon atom. Again, an S_N2-type mechanism has been proposed in which the -OH displaces -OR with inversion of the silicon tetrahedron as illustrated in Fig. (5.1)

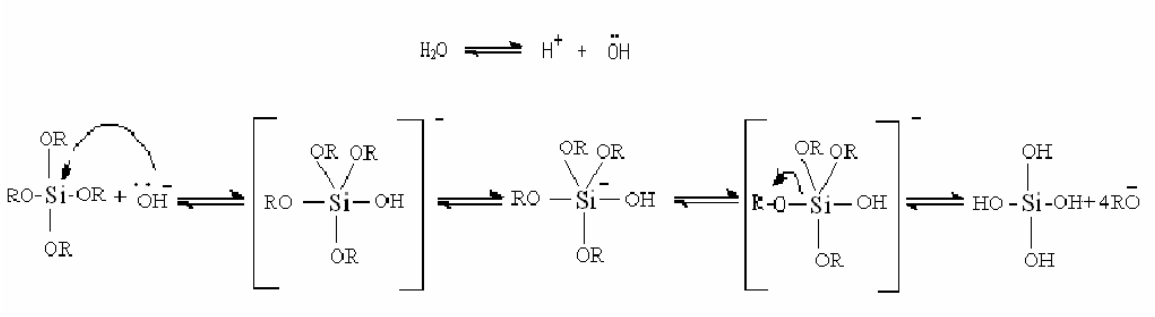

Fig (5.1): The base-catalysis hydrolysis

The most widely accepted mechanism for the base-catalyzed condensation reaction involves the attack of a nucleophilic deprotonated silanol on a neutral silicic acid.[206]

Fig. (5.2): The nucleophilic attack to form a siloxane bond

Generally, many factors affect on the resulting silica network, such as, pH, temperature and time of reaction, reagent concentrations, catalyst nature and the concentration, H_2O/Si molar ratio (R), aging temperature and time. The sol-gel derived silicon oxide networks, under acid-catalyzed conditions, yield primarily linear or randomly branched polymers which entangle and form additional branches resulting in gelation. Which silicon oxide networks derived under base-catalyzed conditions yield more highly branched clusters which do not interpenetrate prior to gelation and thus behave as discrete clusters as shown in Fig. (5.3).

Acid catalyzed

Yield primarily linear or randomly branched polymer

Based-catalyzed

Yield highly branched clusters

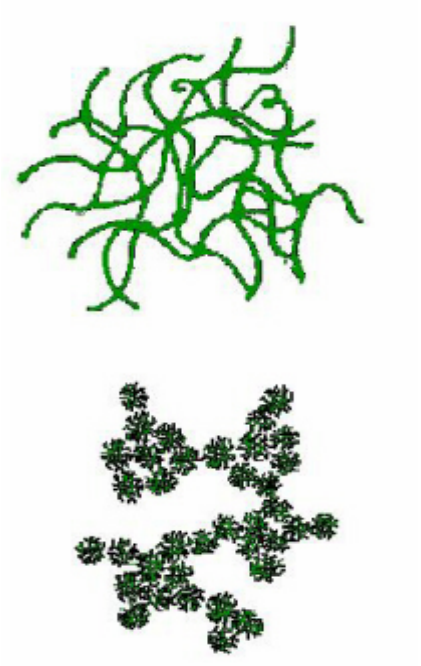

Fig. (5.3): The summary of acid/base sol-gel conditions.[207]

5.2 Materials

In addition to the materials which were used in the previous chapters, the chemicals which were used in this chapter are tabulated in the table (5.1).

Table (5.1): Materials and their chemical formulae

substance	Mol.Formula, M. wt.	supplier
Orthosilicic acid tetraethyl ester, Tetraethoxysilane (TEOS)	$Si(OC_2H_5)4$ Molecular Weight:208.33	Merck
(Triethoxysilyl)ethylene, Vinyltriethoxysilane (VTES)	$H_2C=CHSi(OC_2H_5)_3$ Mol. Wt. 190.31	Merck
Ethyl alcohol	CH_3CH_2OH Molecular Weight:46.07	Merck
Ammonia solution (28% wt.% ammonia)	NH_4OH Molecular Weight:35.05	Merck
Isopropanol	$(CH_3)_2CHOH$, Formula Weight: 60.10	Merck
Stearic acid (9)	Linear Formula: $CH_3(CH_2)_{16}COOH$ Molecular Weight: 284.48	Merck

5.3 Experimental details

5.3.1 The first method to prepare the Stöber particles:

Preparation of the pure silica particles (the ratio between TEOS and H_2O was 1/31)

The spherical silica particles were prepared by the modified Stöber method using TEOS as precursor [200] according to the following procedures:

1) 3.81 ml (28% wt.) Ammonia solution and 40.78 ml deionized water and 105.46 ml ethanol were mixed in the three necked flask at stirring 150 rpm under nitrogen atmosphere.

2) 16.75 ml TEOS and 133.25 ml ethanol were mixed, and subsequently were added drop by drop into the above mixture for 1/2 hour under the above conditions.

3) The stirring continued for 3 hours. The total volume of the resulting solution was about 300 ml and the final compositions of the solution are 0.25 M TEOS, 0.188 M ammonia, 8 M water and 13.6 M ethanol.

4) The particle diameter was determined by using Dynamic Light Scattering (DLS).

5) The stirring continued to modify the surface of Stöber particles according to the two following modification methods:

5.3.2 Preparation of modified-silica particles by either VTES or Stearic acid

a) The first modification of Stöber particles method:

To modify the Stöber particles surfaces, 0.54 ml VTES were added to the above prepared pure silica particles solution and the reaction was allowed to continue for an additional 19 hours under the above stirring. The silica particles were separated by centrifugation and washed with ethanol for three times.[201]

b) The second modification of Stöber particles method:

0.8 g stearic acid (as long chain fatty acid to modify Stöber particles surfaces) were added to the prepared pure silica particles solution and the reaction was allowed to continue for an additional 19 hours under the above stirring. The silica particles was also separated by centrifugation and washed with ethanol for at least three times. [202]

5.3.3 The second method to prepare Stöber particles:

Preparation of Stöber particles colloidal dispersion in acetone (the ratio between TEOS and H_2O was 1/4)

1) 60 g acetone and 12.4 g TEOS and 4 g ethanol and 4.3 g distilled water were mixed by magnetic stirrer.
2) 6 g (28% wt.) ammonia solution was added subsequently to the first mixture under the magnetic stirrer at 50°C.
3) The stirring continued for additional 2.1/2 hours to get the silica colloidal dispersion.

5.3.4 The third method to prepare Stöber particles:

Preparation of Stöber particle colloidal dispersion in acetone (the ratio between TEOS and H_2O was 1/4)

1) 60 g acetone and 12.4 g TEOS and 4 g ethanol and 4.3 g distilled water were mixed by magnetic stirrer
2) 6 g (28% wt.) ammonia solution was added to the first mixture under magnetic stirrer at 50°C.
3) The stirring continued for additional 10 minutes to get silica colloidal dispersion.

5.3.5 The fourth method to prepare Stöber particles:

Preparation of Stöber particles in mixture from Ethanol and methanol (the ratio between TEOS and H_2O was 1/21)

1) 43.9 g ethanol and 14.6 g methanol and 5.65 g TEOS and 10 g distilled water were mixed by magnetic stirrer
2) 2.9 g (28% wt) ammonia solution was added directly to the first mixture at 50°C under magnetic stirrer.
3) The stirring continued to additional 1/2 hour to get the silica colloidal dispersion.

5.3.6 The fifth method to prepare Stöber particles:

Preparation of Stöber particles in isopropanol (the ratio between TEOS and H_2O was 1/4)

1) 15 g acetone and 4.1 g TEOS and 1 g ethanol and 1.43 g distilled water were mixed by magnetic stirrer
2) 1.5 g (28% wt.) ammonia solution was added to the first mixture under the magnetic stirrer at 50°C
3) The stirring continued for additional 10 minutes to get silica colloidal dispersion.

5.3.7 Determination the particles diameter by using Dynamic Light Scattering (DLS)

The silica particles diameter was measured by dynamic light scattering DLS. The measurements were carried out at 25°C on an ALV/SLS system equipped with a

multi-τ digital correlator 5000E (ALV, Germany) at scattering angle of 90°. A solid state laser (ADLAS DPY 135, out put power = 100 mw, λ_0 = 632 nm) was used as the light source.

5.3.8 Preparations of anti-fog Stöber particles/polyurethane films based on (PEG_{1000} and PEG_{400})

a) The first method to prepare Stöber particles/polyurethane films:

Different percentages of modified Stöber particles (according to the first method of preparation of modified Stöber particles) were dispersed in the polyurethane solution by using the Ultra Turrax homogenizer. The resulting Stöber particles/polyurethane dispersion was cast by using applicator on either glass or polycarbonate substrate. The resulting Stöber particles/polyurethane films were left to evaporate the solvent for 1/2 hour. Subsequently, the films were exposed to UV-lamp to cure.

a) The second method to prepare Stöber particles/polyurethane films:

Different percentages of Stöber particles colloidal dispersion were dispersed in the polyurethane solution by vigorously checked which the Stöber particles. Stöber particles were easy dispersed in the polyurethane solution and were still dispersed in the polyurethane solution without any sedimentation according to this method. The resulting Stöber particles/polyurethane dispersion was cast by using applicator on either glass or polycarbonate substrate. Then the Stöber particles/polyurethane films were left to evaporate the solvent for 1/2 hour and subsequently the films were exposed to the UV-lamp to cure.

5.4 Results and discussion

5.4.1 Determination the particles diameter by using Dynamic Light Scattering (DLS)

The diameters of the silica particles were measured by using DLS as mentioned before and the results were inserted in table (5.2). The diameter of the silica particles was varied depending on the preparation method of the silica nano-particles. The diameter of silica particle can be ordered according to the type of the solvent as follows:

Ethanol/water < Acetone < Isopropanol < Ethanol/Methanol

Table (5.2): The silica particle diameters at different preparation methods

Preparation method	Used solvent	Particle diameter (nm)
First method	Ethanol/Water	177
Second method	Ethanol/Water	177
Third method	Acetone	200
Fourth method	Ethanol/Methanol	256
Fifth method	Isopropanol	248

5.4.2 Preparation of UV-curable anti-fog Stöber particles/polyurethane films based on (PEG_{1000}/PEG_{400} =1/3) according to the first or second preparation method of Stöber particles.

Accordingly to the first method of the preparation of modified Stöber particles the sedimentation took place for the resulting modified Stöber particles/polyurethane dispersion by time. The modified Stöber particles were separated from its colloid, and then dispersed in the polyurethane solution. The resulting UV-curable modified Stöber/polyurethane films showed also haziness. Then modified Stöber particles which were prepared accordingly to the first method caused the haziness of the resulting UV-curable anti-fog modified Stöber particles/polyurethane films. The Stöber particles/polyurethane dispersion which was prepared accordingly to the second method of preparation Stöber particles was very well dispersed in polyurethane solution without any sedimentation of the Stöber particles in the polyurethane solution. The Stöber particles colloid was dispersed in the polyurethane without separating of the Stöber particles from the colloid. But the resulting UV-curable anti-fog Stöber particles/polyurethane films also had haziness. This is attributed to the agglomeration of Stöber particles during the preparation of the Stöber particles according to the second method. The images of the UV-curable anti-fog Stöber particles/polyurethane films

based on (PEG1000/PEG400 =1/3) at two different percentages of Stöber particles (w/w) were imaged by Confocal –Laser-Scanning microscope. This prepared according to the second method preparation of Stöber particles. The agglomeration can be obviously seen in Fig. (5.4). On the left side, these images were imaged by the normal imaging method of confocal microscope method or in the right side which the images were imaged after making thin layers of water between the film and the lens of the microscope.

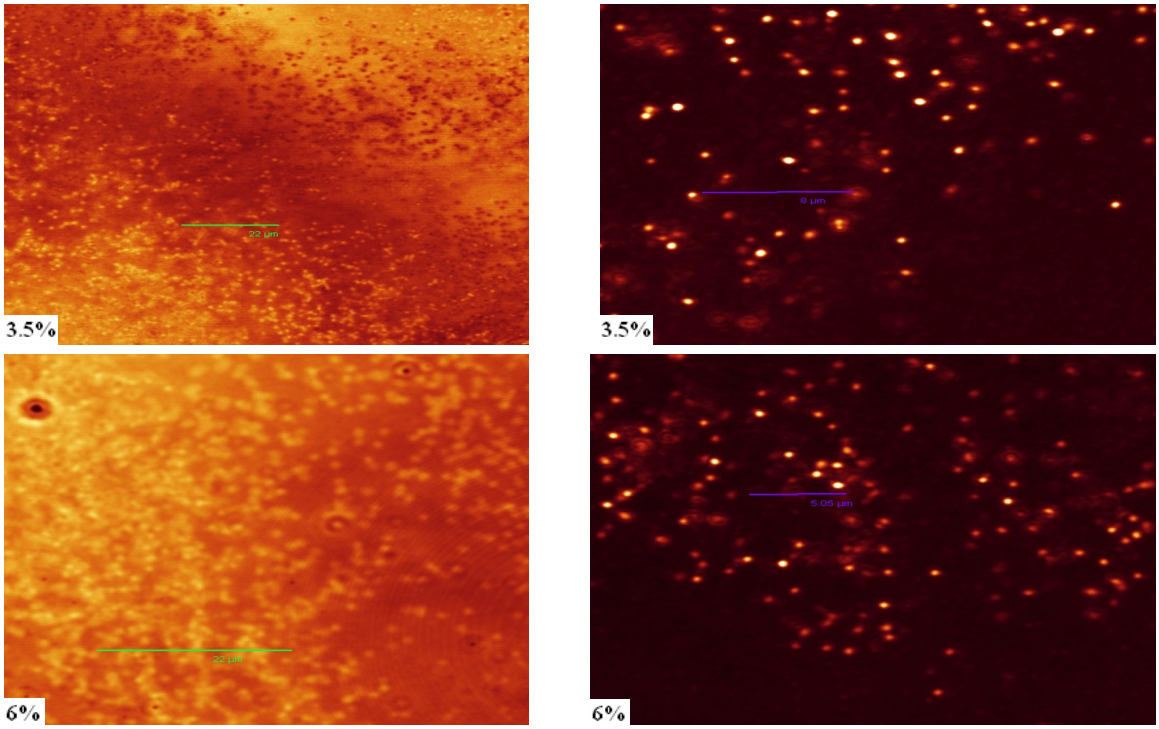

Fig. (5.4): The images of UV-curable anti-fog Stöber particles/polyurethane films based on (PEG1000/PEG400 =1/3) at different percentages (w/w) of Stöber particles at wet thickness 90 µm by using laser Confocal-Scanning Microscope on polycarbonate substrate

5.4.3 Preparation of UV-curable anti-fog Stöber particles/polyurethane films based on (PEG1000/PEG400 =1/3) at different Stöber particles without any agglomeration or even haziness in the resulting UV-curable Stöber particles/polyurethane films

This was achieved by using Stöber particles colloid which was prepared according to the third preparation method of Stöber particles. Stöber particles were prepared in acetone solvent and subsequently dispersed in the polyurethane solution (the Stöber particle diameter is 200 nm). The polyurethane solution was diluted by the same solvent (acetone) as well. The resulting Stöber particles/polyurethane colloidal dispersion according to this method was very physically stable without any sedimentation of Stöber particles in polyurethane solution. There is neither sedimentation nor agglomeration of the Stöber particles in polyurethane solution. The resulting UV-curable Stöber particles/polyurethane films did not have any haziness. The images of anti-fog UV-curable Stöber particles/polyurethane films based on (PEG1000/PEG400 =1/3) at different percentages (w/w) of Stöber particles and at 30 or 90 μm (wet thickess) were imaged by using a canon camera looking into the microscope on glass substrate were illustrated in the figures (5.5 and 5.6). The Stöber particles as a nano-filler increase the hardness values of the UV-curable anti-fog polyurethane films table (5.2) and it did not decrease the anti-fog property of the polyurethane films.

Table (5.3): The hardness values of UV-curable anti-fog Stöber particles/polyurethane films based on (PEG1000/PEG400 = 1/3) at different percentages of Stöber particles

Sample No	Nanoparticles	Nanoparticles %(w/w)	Wet thickness μ m	Hardness
Blank 1		0	30	B
Blank 2			90	B
S1	Stöber particles	0..62	30	HB
S2			90	HB
S3		1.23	30	HB
S4			90	HB
S5		1.84	30	HB
S6			90	HB
S7		2.43	30	F
S8			90	HB
S9		3.61	30	HB
S10			90	HB
S11		5.88	30	F
S12			90	HB

Fig(5.5): The images of UV-curable anti-fog Stöber particles /polyurethane films based on (PEG_{1000}/PEG_{400} =1/3) at different percentages (w/w) of Stöber particles and at 30 μm (wet thickess) by using canon camera looking into the microscope on glass substrates

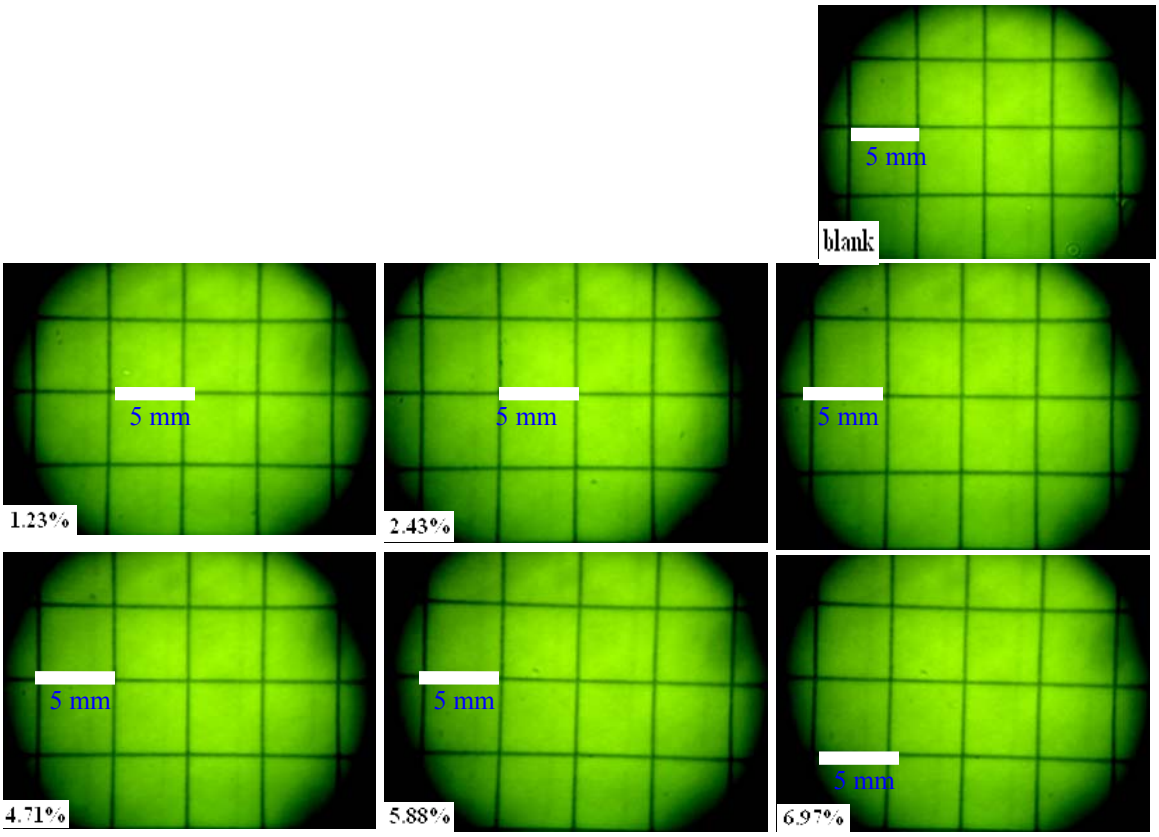

Fig(5.6): The images of UV-curable anti-fog Stöber particles/polyurethane films based on (PEG_{1000}/PEG_{400} =1/3) at different percentages (w/w) of Stöber particles and at 90 µm (wet thickess) by using canon camera looking into the microscope on glass substrate

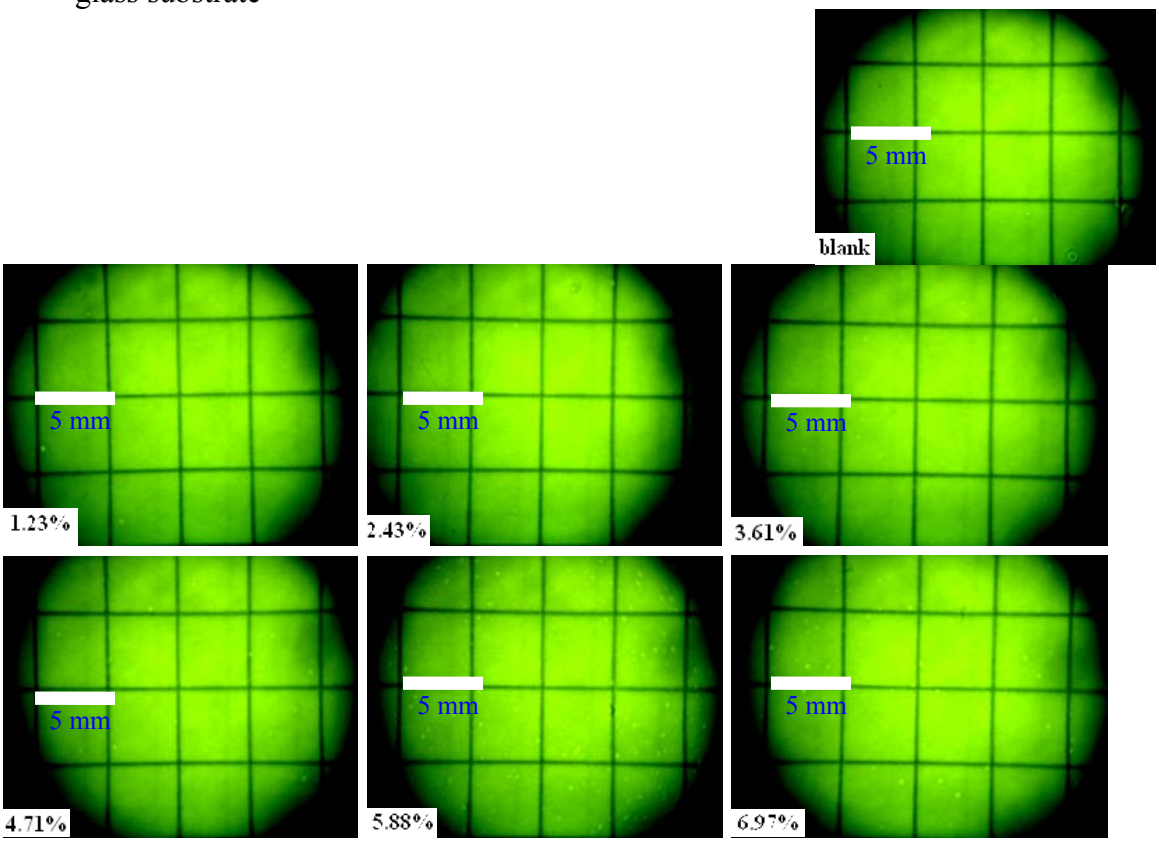

5.4.4 Glass transition temperatures of UV-curable anti-fog Stöber particles/ polyurethane films based on (PEG_{1000}/PEG_{400} = 1/3) at different percentahes of Stöber particles

The glass transition temperatures of UV-curable anti-fog polyurethane films based on (PEG_{1000}/PEG_{400} = 1/3) was measured as a blank film and UV-curable anti-fog Stöber particles /polyurethane films based on (PEG_{1000}/PEG_{400} = 1/3) at different percentages of Stöber particles were measured by Differential Scanning Calorimetry (DSC) at the scale temperature from (-100 to +100°C). The data of the measurements were represented in figure (4.14 and 4.15). While shifting of the glass transition has been reported by many authors, we have not seen any noticeable shift in the polymer after

showing uniform distribution of sphere nano silica and no agglomeration. Surprisingly, we found no relevant effects when increasing the filler content and this also agrees with Gonzalez-Irun Rodriguez et- al. [208]

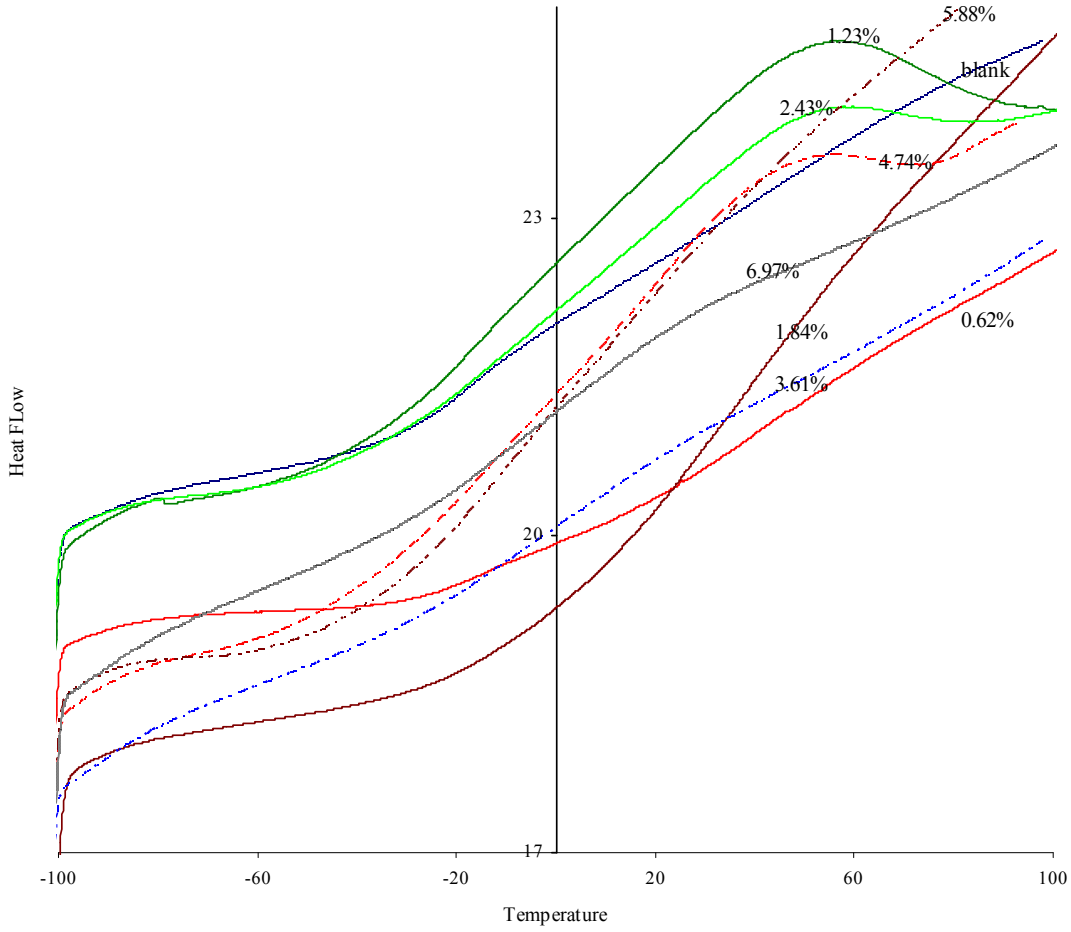

Fig (5.7): The glass transition temperature of UV-curable anti-fog Stöber particles/ polyurethane films based on (PEG_{1000}/PEG_{400} =1/3) at different percentages of Stöber particles (which prepared according to the third method).

5.4.5 The physical stability of Stöber particles/Polyurethane colloidal dispersion based on (PEG_{1000}/PEG_{400} =1/3) in acetone by the time

According to the third method to prepare Stöber particles, the Stöber particles were prepared in the acetone and polyurethane based on (PEG_{1000}/PEG_{400} =1/3) also prepared in the same solvent. Different percentages of Stöber particles (1%, 3% or 5% w/w) were dispersed in the polyurethane solution without any other additives as shown in figure (5.8). At 1% (w/w) Stöber particles/polyurethane dispersion, the Stöber particles is still physically stable without converting to a gel. Sedimentation of the Stöber particles did not occur in the dispersion until after four months as shown in figure (5.9). But at the following Stöber particles percentages 3% or 5% (w/w) of Stöber particles/polyurethane, the particles started to convert to a gel after few hours from dispersion process time. The gel was completely formed for 3% and 5% (w/w) after three days from the dispersion process time. This is indication to the completely distribution of Stöber particles in the network of the polyurethane polymer at higher percentages 3% and 5% (w/w). It means that Stöber particles formed the physical hydrogen bonding with the polyurethane polymer

Fig. (5.8): Different percentages of Stöber particles/polyurethane colloidal dispersion based on (PEG_{1000}/PEG_{400} =1/3) after the dispersion process directly.

Fig. (5.9): Different percentages of Stöber particles/polyurethane colloidal dispersion based on (PEG_{1000}/PEG_{400} =1/3) at 1% (w/w) Stöber particles after four months (from dispersion process time) without any physical changing.

5.4.6 The physical stability of Stöber particles/Polyurethane colloidal dispersion based on (PEG_{1000}/PEG_{400} =1/3) in isopropanol by time

According to the fifth method to prepare Stöber particles, the Stöber particles were prepared in isopropanol and polyurethane based on (PEG_{1000}/PEG_{400} =1/3) which also prepared in the same solvent. Different percentages (1%, 3% or 5% w/w) of Stöber particles were dispersed in the polyurethane solution without any other additives as shown in figure (5.10). At 1% (w/w) Stöber particles, the colloidal dispersion is still physically stable without any changing. Sedimentation of the Stöber particles did not occur in the polyurethane solution while at 3% or 5% Stöber particles of Stöber particles /polyurethane started to convert to a gel after few hours from the dispersion process time. The resulting gel was completely formed after three days from the dispersion process time as shown in figure (5.11). The resulting gel property of the Stöber particles/polyurethane in isopropanol seems to be like the Stöber particles/polyurethane in acetone, although the curing did not occur for the films which were cast from the Stöber particles/polyurethane in isopropanol.

Fig. (5.10): Different percentages of Stöber particles/polyurethane based on (PEG_{1000}/PEG_{400} =1/3) dispersion after the dispersion process directly

Fig. (5.11): 3% and 5% of Stöber particles (w/w) of Stöber particles/polyurethane based on (PEG_{1000}/PEG_{400} =1/3) gel (without any other additives)

5.5 Conclusions

- The dispersion of Stöber particles as a powder in the polyurethane solution leads to the agglomeration in the resulting UV-curable anti-fog polyurethane films while the dispersion of the Stöber colloid in the polyurethane solution (the same dispersed media) does not do.

- There is no noticeable shift in the polymer after showing uniform distribution of sphere Stöber particles.

- The Stöber particles/polyurethane colloidal dispersion at lower percentage (1% w/w) of Stöber particles in polyurethane dispersion is very physically stable without any changing for more than four months. At 3% or more than 3% (w/w) of Stöber particles, the colloidal dispersion completely converted to gel after three days.

6 Attachment of inorganic moieties onto polyurethane network

6.1 Introduction

Polyurethanes have been used in a series application due to basically their versatility in terms of controlling the behavior by altering basically the type of reagents used. Inorganic functionalities based on Si-O bonds were incorporated into polyurethane to produce structurally designed networks having controlled presence of inorganic entities. This type of structurally designed material may display controlled properties suitable for a series of important proposed applications such as high performance coating and foams with enhanced mechanical properties.[209]

In this chapter, the attachment of inorganic moieties onto the aliphatic polyurethane chains by 3-aminopropyl triethoxy silane (APTES). The urethane prepolymer was capped by APTES. This method increases the UV curing time to around one hour and decreased the transparency of the resulting films. The coherence of the casting films was not good.

When HEA was added to (PEG1000: IPDI: APTES) copolymer according to our preparation method, the UV-curing time for the resulting films decreased from one hour to the half hour. The transparency of the resulting films was not good.

The reaction between the diisocynate groups from the prepolymer (OCN-PEG-NCO) and the eithoxy groups from VTES did not occur when acetone is used to dilute of the resulting polyurethane solution but it did occur when water was used and the UV-curing time was small for this type of the copolymer.

6.2 Experimental details

6.2.1 Preparation of polyurethane based on (PEG_{1000}: IPDI: HEA) copolymer solution at ratios 1:3:3

Procedures:

1) 70 g (0.07 mol) PEG_{1000} and 30 g acetone were mixed. The mixture was fed into a three-necked flask equipped with a mechanical stirrer. The stirrer was operated at 150 rpm. A reflux condenser was employed. The temperature was 60°C .The reaction occurred under nitrogen atmosphere for 30 minutes.

2) 46.7 g (0.21 mol) IPDI and 0.5 g DBTL were mixed. The mixture was slowly dropped into the reactor under the above conditions for 2.1/4 hours.

3) 10 g acetone was added to the resulting viscous urethane prepolymer.

4) The system was further reacted under the above conditions for an additional1 hour.

5) 24.4 g (0.21 mol) HEA were added drop by drop to the reactor at the above conditions for one hour.

6) The reaction mixture was stirred for an additional 30 minutes under the above conditions.

7) The resulting clear and viscous solution was diluted by using acetone to obtain a diluted polyurethane copolymer solution with 50 % (w/w).

6.2.2 Preparation of polyurethane based on (PEG_{1000}: IPDI: APTES) copolymer solution at ratios 1:2:2

Procedures:

1) 20 g (0.02 mol) PEG_{1000} and 10 g acetone were mixed. The mixture was fed into a three-necked flask equipped with a mechanical stirrer. The stirrer was operated at150 rpm. A reflux condenser was employed. The temperature was 60°C under nitrogen atmosphere for 30 minutes.

2) 9.2 g (0.04 mol) IPDI and 0.09 g DBTL were mixed. The mixture was slowly dropped into the reactor under the above conditions for 30 minutes.

3) 10 g acetone was added to the resulting viscous urethane prepolymer.

4) The system was further reacted under the above conditions for an additional1 hour.

5) 9 g (0.04 mol) APTES were added drop by drop to the reactor for 30 minutes under the above conditions.
6) The reaction mixture was stirred for an additional 30 minutes under the above conditions.
7) The resulting clear and viscous solution was diluted by using acetone to obtain a diluted polyurethane copolymer solution with 50 % (w/w).

6.2.3 Preparation of polyurethane based on (PEG_{1000}: IPDI: APTES: HEA) copolymer solution at ratios 1:2:2:2

Procedures:

1) 20 g (0.02 mol) PEG_{1000} and 10 g acetone were mixed. The mixture was fed into a three-necked flask equipped with a mechanical stirrer at 150 rpm. A reflux condenser was employed. The temperature was 60°C. The reaction occurred under nitrogen atmosphere for 30 minutes.
2) 9.2 g (0.04 mol) IPDI and 0.09 g DBTL were mixed. The mixture was slowly dropped into the reactor under the above conditions for 30 minutes.
3) 10 g acetone was added to the resulting viscous urethane prepolymer.
4) The system was completed under the above conditions for additional1 hour.
5) 9 g (0.04 mol) APTES were added drop by drop to the reactor for 30 minutes under the above conditions.
6) The reaction mixture was stirred for an additional 15 minutes under the above conditions.
7) The resulting clear and viscous solution was diluted by using acetone to obtain a diluted polyurethane copolymer solution with 50 % (w/w).

6.2.4 Preparation of polyurethane based on (PEG_{1000}: IPDI: VTES) copolymer solution at ratios 1:3:3

Procedures:

1) 23.3 g (0.023 mol) PEG_{1000} and 20 g acetone were mixed. The mixture was fed into a three-necked flask equipped with a mechanical stirrer. The stirrer was operated at

temperature 150 rpm. A reflux condenser was employed. The temperature was 60°C under nitrogen atmosphere for 30 minutes.

2) 15.6 g (0.07 mol) IPDI and 80 mg DBTL were mixed. The mixture was slowly dropped into the reactor under the above conditions for 15 minutes.
3) The system was further reacted for an additional 30 minutes under the above conditions.
4) 13.3 g (0.07 mol) VTES were added drop by drop to the reactor for 15 minutes under the above conditions for 1 hour.
5) The reaction mixture was stirred for an additional 30 minutes under the above conditions.
6) The resulting clear and viscous solution was diluted by using acetone to obtain a solution with 50 % (w/w).

6.2.4 Preparation of polyurethane based on (PEG_{1000}: IPDI: VTES) copolymer solution at ratios 1:3:3

Procedures:

1) 23.3 g (0.023 mol) PEG_{1000} and 20 g acetone were mixed. The mixture was fed into a three-necked flask equipped with a mechanical stirrer. The stirrer was operated. A reflux condenser at 150 rpm. The temperature was 60°C. The reaction occurred under nitrogen atmosphere for 1/2 hour.
2) 15.6 g (0.07 mol) IPDI and 80 mg DBTL were mixed. The mixture was slowly dropped into the reactor under the above conditions for 15 minutes.
3) The system was further reacted for an additional 30 minutes under the above conditions.
4) 13.3 g (0.07 mol) VTES were added drop by drop to the reactor for 15 minutes under the above conditions for 1 hour.
5) The reaction mixture was stirred for an additional minutes under the above conditions.
6) The resulting clear and viscous solution was diluted by using distilled water to obtain a solution with 50 % (w/w).

6.3 Results and Discussion

According to the polyurethane preparation, in the first step, the addition reaction occurred between PEG_{1000} and IPDI to form urethane linkages and subsequently, in the second step, the resulting urethane prepolymer was capped by the silane 3-aminopropyle triethoxy silane (APTES) to form urea linkages. The anti-fog films which were prepared from this copolymer (PEG_{1000}: IPDI: APTES) needed too long time to cure under the UV-lamp (around one hour). This curing time is longer than the required curing time for the films which were prepared from polyurethane copolymer (PEG_{1000}: IPDI: HEA). Practically, this was not suitable to apply in industry. The transparency for the films which were prepared from (PEG_{1000}: IPDI: APTES) copolymer are not good.

When HEA was added to the (PEG_{1000}: IPDI: APTES) under the experimental conditions to get (PEG_{1000}: IPDI: APTES: HEA), the films which were cast from this copolymer needed to 1/2 hour under the UV-lamp to cure.

When the films were cast from (PEG_{1000}: IPDI: VTES) copolymer which were prepared in acetone, the resulting films did not cure under UV-lamp. This is attributed to the capping by VTES for the resulting prepolymer (OCN-PEG-NCO) did not occur because the films which prepared from this solution did not cure.

When the copolymer (PEG1000: IPDI: VTES) was diluted by water under the experimental conditions, the films which were prepared from this solution were successfully cured under the UV-lamp. This is attributed to the hydrolysis of VTES occurred in the presence of water to convert from vinyl triexothxy silane to vinyl trihydroxy silane then, the addition reaction occurred between the OH groups from VTES and -NCO groups from resulting urethane prepolymer. But the resulting films from this solution show wrinkling. The data of the above different copolymers were inserted in the table (6.1)

UV curing time of the copolymer (PEG_{1000}: IPDI: HEA) at a ratio 1:2:2 was about eight minutes. After changing the ratios to 1:3:3, the curing time decreased to about four minutes which the diisocyanates ratio increased the allophonate linkages in the polyurethane coating network.

The transparency and coherence of films which were cast from all the following copolymer, (PEG_{1000}: IPDI: APTES), (PEG_{1000}: IPDI: APTES: HEA) or (PEG_{1000}: IPDI: VTES) were lower than the transparency of the films which cast from (PEG_{1000}: IPDI: HEA) copolymer. The curing times and casting properties of the previous copolymers were tabulated in the table (6.1).

Table (6.1): Formulation of different copolymer and their curing time

No	Copolymer	Ratio	Solvent	Curing time min	Casting film	Transparency
1	PEG_{1000}: IPDI: HEA	1:3:3	Acetone	3.1/2	Coherent film	Very good
2	PEG_{1000}: IPDI: APTES	1:2:2	Acetone	>50	Coherent film	bad
3	PEG_{1000}:IPDI:APTES:HEA)	1:2:2:2	Acetone	30	Coherent film	bad
4	PEG_{1000}: IPDI: VTES	1:3:3	Acetone	No reaction	---	----
5	PEG_{1000}: IPDI: VTES	1:3:3	H_2O	8	No Coherent film	bad

6.4 Conclusions

- The attachment of inorganic moieties in the anti-fog polyurethane chains leads to less transparency, less coherent of the resulting UV-curable anti-fog polyurethane films.

7 References

[1] Bayer O. The diisocyanate polyaddition process (polyurethanes). Description of a new principle for building up high-molecular compounds. Angew Chem 1947; A59:257.

[2] Wang F. Doctoral dissertation; polydimethylsiloxane modification of segmented thermoplastic polyurethanes and polyureas. Virginia Polytechnic Institute and StateUniversity; 1998.

[3] Saunder s JH, Frisch KC. Polyurethanes: chemistry and technology, vol. XVI. High polymers, Part I. New York: Wiley; 1962.

[4] Narayan R, Chattopadhyay DK, Sreedhar B, Raju KVSN, Mallikarjuna NN, Aminabhavi TM. Synthesis and characterization of crosslinked polyurethane dispersions based on hydroxylated polyesters. J Appl Polym Sci 2006;99:368–80.

[5] Levchik SV, Weil ED. Thermal decomposition, combustion and fire-retardancy of polyurethanes a review of the recent literature. Polym Int 2004;53:1585–610.

[6] Janischewski K, Reichel D. Aqueous two component polyurethane coatings, preparation thereof and use thereof. US patent 6048926, 2000.

[7] Wicks Jr ZW. Blocked isocyanates. Prog Org Coat 1975;3:73–99.

[8] Wicks Jr ZW. New developments in the field of blocked isocyanates. Prog Org Coat 1981; 9:3–28.

[9] Blencowe A, Clarke A, Drew MGB, Hayes W, Slark A, Woodward P. Alternative syntheses of linear polyurethanes using masked isocyanate monomers. React Funct Polym 2006; 66:1284–95.

[10] Schollenberger CS, Dinbergs KJ. Thermoplastic urethane molecular weight-property relations. J Elastoplast 1973; 5:222–51.

[11] Aneja A, Wilkes GL. On the issue of urea phase connectivity in formulations based on molded flexible polyurethane foams. J Appl Polym Sci 2002; 85:2956–67.

[12] Aneja A, Wilkes GL, Rightor EG. Study of slabstock flexible polyurethane foams based on varied toluene diisocyanate isomer ratios. J Polym Sci Part B: Polym Phys 2003; 41:258–68.

[13] Smith CH, Petersen CA. Effect of diisocyanate structure on load-bearing properties of flexible urethane foams. SPE J 1962;18/4:455–9.

[14] Sung CSP, Schneider NS. Infrared studies of hydrogen bonding in toluene diisocyanate based polyurethanes. Macromolecules 1975; 8:68–73.

[15] Nierzwicki W, Walczynski B. Study of toluene diisocyanate- based polyurethanes of various isomer ratios. J Appl Polym Sci 1990; 41:907–15.

[16] Barbeau P, Gerard JF, Magny B, Pascault JP. Effect of the diisocyanate on the structure and properties of polyurethane acrylate prepolymers. J Polym Sci: Part B: Polym Phys 2000; 38:2750–68.

[17] Lipatova TE, Shilov VV, Minenko NN. The heterogeneous structure of polyurethane networks. Angew Makromol Chem 1981; 100:99–115.

[18] Adsuar MSS, Papon E, Villenave JJ. Influence of the synthesis conditions on the properties of thermoplastic polyurethane elastomers. J Appl Polym Sci 2000; 76:1590–5.

[19] Rogulska M, Podkos´ cielny W, Kultys A, Pikus S, Poz´ dzik E. Studies on thermoplastic polyurethanes based on new diphenylethane-derivative diols. I. Synthesis and characterization of nonsegmented polyurethanes from HDI and MDI. Eur Polym J 2006; 42:1786–97.

[20] Prisacariu C, Olley RH, Caraculacu AA, Bassett DC, Martin C. The effect of hard segment ordering in copolyurethane elastomers obtained by using simultaneously two types of diisocyanates. Polymer 2003; 44: 5407–21.

[21] Polyurethane Elastomers book, second ed. C. Helpburn BT37 0QB, UK

[22] Guo SH. Hydroxy-functional acrylate resins. US patent 5571884, 1996 and US patent 5525693, 1996.

[23] Wamprecht C, Sonntag M. Polyester polyols and their use as a binder component in two-component polyurethane coating compositions. US patent 6423816, 2002.

[24] Santos D, Manuel A. Polyester polyols and their use as the polyol component in two-component polyurethane paints. US patent 6184332, 2001.

[25] Brown DW, Lowry RE, Smith LE. Kinetics of hydrolytic aging of polyester urethane elastomers. Macromolecules 1980; 13:248–52.

[26] Pegoretti A, Fambri L, Penati A, Kolarik J. Hydrolytic resistance of model poly(ether urethane ureas) and poly(ester urethane ureas). J Appl Polym Sci 1998; 70: 577–86.

[27] Burdeniuc JJ, Kamzelski AZ. Blowing catalyst compositions containing hydroxyl and surface active groups for the production of polyurethane foams. European patent 1702913, 2006.

[28] Roy S, Majumdar KK. Preparation of organo-tin catalyst useful for preparation of polyurethanes. Indian patent 194604, 2004.

[29] Caillaud JL, Deguillaume S, Vincent M, Giannotta JC, Widmaier JM. Influence of a metallic filler on polyurethane formation. Polym Int 1996; 40:1–7.

[30] Cooper SL, Tobolsky AV. Anomalous depression of rubbery modulus through crosslinking. J Appl Polym Sci 1967; 11:1361–9.

[31] Dzierza W. Mechanical properties of crosslinked polyurethanes. J Appl Polym Sci 1978; 22:1331–42.

[32] Britain JW, Gemeinhardt PG. Catalysis of the isocyanatehydroxyl reaction. J Appl Polym Sci 1960; 4:207–11.

[33] Lenz RW. Organic chemistry of synthetic high polymers. New York: Interscience; 1967 [Chapter 7].

[34] Sasaki N, Yokoyama T, Tanaka T. Properties of isocyanurate- type crosslinked polyurethanes. J Polym Sci: Polym Chem Ed 1973; 11:1765–79.

[35] Hepburn C. Polyurethane elastomers, 2nd ed. London, New York: Elsevier; 1992

[36] Mayr AE, Cook WD, Edward GH, Murray GJ. Cure and properties of unfoamed polyurethanes based on uretonimine modified methylene-diphenyl diisocyanate. Polym Int 2000; 49:293–301.

[37] (a) ASTM Standard D16-00. Technology for paint, related coatings, materials, and applications; (b) Dieterich D, Grigat E, Hahn W, Hespe H, Schmelzer HG. Principles of polyurethane chemistry and special applications. In: Oertel G, editor. Polyurethane handbook. Munich: Hanser Publishers; 1993. p. 11–53.

[38] Seymour RW, Cooper SL. Viscoelastic properties of polyurethane block polymers. Adv Urethane Sci Technol 1974; 3:66–80.

[39] Cooper SL, Tobolsky AV. Properties of linear elastomeric polyurethanes. J App Polym Sci 1966;10:1837–44.

[40] Schollenberger CS. Simulated vulcanizates of polyurethane elastomers. US patent 2871218, 1959.

[41] Koutsky JA, Hien NV, Cooper SL. Some results on electron microscope investigations of polyether-urethane and polyester–urethane block copolymers. J Polym Sci: Part B: Polym Lett 1970;8:353–9

[42] (a) Miller JA, Lin SB, Hwang KKS, Wu KS, Gibson PE, Cooper SL. Properties of polyether-polyurethane block copolymers: effects of hard segment length distribution. Macromolecules 1985; 18:32–44 (b) Sanchez-Adsuar MS, Papon E, Villenave JJ. Influence of the synthesis conditions on the properties of thermoplastic polyurethane elastomers. J Appl Polym Sci 2000; 76:1590–5.

[43] Paik Sung CS, Hu CB, Wu CS. Properties of segmented poly(urethaneureas) based on 2,4-toluene diisocyanate. 1. Thermal transitions, X-ray studies, and comparison with segmented poly(urethanes). Macromolecules 1980; 13:111–6.

[44] Sung CSP, Smith TW, Sung NH. Properties of segmented polyether poly (urethaneureas) based of 2,4-toluene diisocyanate. 2. Infrared and mechanical studies. Macromolecules 1980; 13:117–21.

[45] Adhikari R, Gunatillake PA, McCarthy SJ, Meijs GF. Mixed macrodiol-based siloxane polyurethanes: effect of the comacrodiol structure on properties and morphology. J Appl Polym Sci 2000; 78:1071–82.

[46] Martin DJ, Meijs GF, Gunatillake PA, McCarthy SJ, Renwick GM. The effect of average soft segment length on morphology and properties of a series of polyurethane elastomers. II. SAXS-DSC annealing study. J Appl Polym Sci 1997; 64:803–17.

[47] Wang CB, Cooper SL. Morphology and properties of segmented polyether polyurethaneureas. Macromolecules 1983; 16:775–86.

[48] Aitken RR, Jeffs GMF. Thermoplastic polyurethane elastomers based on aliphatic diisocyanates: thermal transitions. Polymer 1977; 18:197–8.

[49] Seymour RW, Cooper SL. Thermal analysis of polyurethane block polymers. Macromolecules 1973; 6:48–53.

[50] Leung LM, Koberstein JT. DSC annealing study of microphase separation and multiple endothermic behaviors in polyether-based polyurethane block copolymers. Macromolecules 1986;19:706–13.

[51] Yoo S, Lee HS, Seo SW. Orientation and phase separated structure of polyurethanes having various chemical structures. Pollimo 1997; 21:459–67.

[52] Van Bogart JWV, Gibson PE, Cooper SL. Structure– property relationships in polycaprolactone-polyurethanes. J Polym Sci: Polym Phys Ed 1983; 21:65–95.

[53] Hartmann B, Duffy JV, Lee GF, Balizer E. Thermal and dynamic mechanical properties of polyurethaneureas. J Appl Polym Sci 1988; 35:1829–52.

[54] Frontini PM, Rink M, Pavan A. Development of polyurethane engineering thermoplastics. II. Structure and properties. J Appl Polym Sci 1993; 48:2023–32.

[55] Stanford JL, Still RH, and Wilkinson AN. Effects of softsegment prepolymer functionality on structure–property relations in RIM copolyurethanes. Polymer 2003; 44: 3985–94.

[56] Camargo RE, Macosko CW, Tirre UM, Wellinghoff ST. Phase separation studies in rim polyurethanes catalyst and hard segment crystallinity effects. Polymer 1985; 26:1145–54.

[57] Nishimura H, Kojima H, Yarita T, Nishiro M. Phase structure of polyetherpolyol-4,4 prime –diphenylmethane diisocyanate-based reaction injection molded (rim) polyurethanes. Polym Eng Sci 1986; 26:585–92.

[58] Markovs RA. Effect of polyol structure in diamine extended rim systems. J Cell Plast 1985; 21:326–31.

[59] Petrovic ZS, Javni I. The effect of soft-segment length and concentration on phase separation in segmented polyurethanes. J Polym Sci: Part B: Polym Phys 1989; 27:545–60.

[60] Stanford JL, Still RH, Wilkinson AN. Effects of soft segment prepolymer functionality on structure development in RIM copolymers. Polymer 1995; 36:3555–64.

[61] Paul CJ, Nair MGR, Koshy P, Idage BB. Segmented block copolymers of natural rubber and bisphenol A-toluene diisocyanate oligomers. J Appl Polym Sci 1999; 74:706–21.

[62] Pandya MV, Deshpande DD, Hundiwale DG. Effect of diisocyanate structure on viscoelastic, thermal, mechanical and electrical properties of cast polyurethanes. J Appl Polym Sci 1986; 32:4959–69.

[63] Schneider NS, Sung CSP, Matton RW, Illinger JL. Thermal transition behavior of polyurethanes based on toluene diisocyanate. Macromolecules 1975; 8:62–7.

[64] Speckhard RA, Strate GV, Gibson PE, Cooper SL. Properties of polyisobutylene-polyurethane block copolymers: I. Macroglycols from ozonolysis of isobutyleneisoprene copolymer. Polym Eng Sci 1983; 23:337–49.

[65] Chang SL, Yu TL, Huang CC, Chen WC, Linliu K, Lin TL. Effect of polyester side chains on the phase segregation of polyurethanes using small-angle X-ray scattering. Polymer 1998; 39:3479–89.

[66] Blackwell J, Nagarajan MR, Haitink TB. Structure of polyurethane elastomers: effect of chain extender length on the structure of MDI/diol hard segments. Polymer1982;23:950–6.

[67] Hong JL, Lillya CP, Chein JCW. Degree of phase separation in polyether-polyurethane copolymers with different chemical structures of hard segments. Polymer 1992; 33:4347–51.

[68] Pandya MV, Deshpande DD, Hundiwale DG. Thermal behavior of cast polyurethane elastomers. J Appl Polym Sci 1988; 35:1803–15.

[69] Vlajic M, Enes T, Aisa S, Vahid S. Chemical structure and properties of polyurethane elastomers II. The effects of the chain extenders and crosslinkers on the properties of thermoplastic and thermosetting elastomers. Polimeri 1990; 11:15–8.

[70] Petrovic ZS, Javni I, Divjakovic V. Structure and physical properties of segmented polyurethane elastomers containing chemical crosslinks in the hard segment. J Polym Sci: Part B: Polym Phys 1998; 36:221–35.

[71] Liaw DJ. The relative physical and thermal properties of polyurethane elastomers: Effect of chain extenders of bisphenols, diisocyanate, and polyol structures. Appl Polym Sci 1997; 66:1251–65.

[72] Blackwell J, Nagarajan MR. Conformational analysis of poly(mdi-butandiol) hard segment in polyurethane elastomers. Polymer 1981;22:202–8

[73] Blackwell J, Quay JR, Nagarajan MR, Born L, Hespe H. Molecular parameters for the prediction of polyurethane structures. J Polym Sci: Polym Phys Edu 1984; 22: 1247–59.

[74] Auten KL, Petrovic ZS. Synthesis, structural characterization, and properties of polyurethane elastomers containing various degrees of unsaturation in the chain extenders. J Polym Sci: Part B, Polym Phys 2002; 40:1316–33.

[75] Barikani M, Barmar M. Thermoplastic polyurethane elastomers: synthesis, and study of effective structural parameters. Iran Polym J 1996; 5:231–5.

[76] Zawadski SF, Akcelrud L. HTPB-based polyurethanes: a correlation study between morphology and mechanical behaviour. Polym Int 1997; 42:422–8.

[77] Minoura Y, Yamashita S, Okamoto H, Matsuo T, Izawa M, Kohmoto SI. Crosslinking and mechanical property of liquid rubber. I. Curative effect of aliphatic diols. J Appl Polym Sci 1978; 22:1817–44.

[78] Siegmann A, Cohen D, Narkis M. Polyurethane elastomers containing polybutadiene and aliphatic diols: Structure- property relationships. Polym Eng Sci 1987; 27: 1187–94.

[79] Yen MS, Chen PY, Tsai HS. Synthesis, properties, and dyeing application of nonionic waterborne polyurethanes with different chain length of ethyldiamines as the chain extender. J Appl Polym Sci 2003; 90:2824–33.

[80] Ahn TO, Jung SU, Jeong HM, Lee SW. Properties of polyurethanes with mixed chain extenders and mixed soft segments. J Appl Polym Sci 1994; 51:43–9.

[81] Masiulanis B, Zielinski R. Mechanical, thermal, and electric properties of polyurethaneimide elastomers. J Appl Polym Sci 1985; 30:2731–41.

[82] Smith TL, Magnusson AB. Diisocyanate-linked polymers. III. Relationships between the composition and ultimate tensile properties of some polyurethane elastomers. J Appl Polym Sci 1961; 5:218–32.

[83] Haska SB, Bayramli E, Pekel F, Ozkar S. Mechanical properties of HTPB-IPDI based elastomers. J Appl Polym Sci 1997; 64:2347–54.

[84] Kothandaraman H, Venkatarao K, Thanoo BC. Preparation, properties, and crosslinking studies on polyurethane elastomers. Polym J 1989; 21:829–39.

[85] Kothandaraman H, Venkatarao K, Thanoo BC. Crosslinking studies of polyether-ester-based polyurethane systems. J Appl Polym Sci 1990; 39:943–54.

[86] Consaga JP, French DM. Properties of hydroxyl-terminated polybutadiene-urethane systems. J Appl Polym Sci 1971; 15:2941–56.

[87] Spirkova M, Matejka L, Hlavata D, Meissner B, Pytela J. Polybutadiene-based polyurethanes with controlled properties: properties: preparation and characterization. J Appl Polym Sci 2000; 77:381–9.

[88] Kontou E, Spathis G, Niaounakis M, Kefalas V. Physical and chemical cross-linking effects in polyurethane elastomers. Colloid Polym Sci 1990; 268:636–44.

[89] Desai S, Thakore IM, Sarawade BD, Devi S. Effect of polyols and diisocyanates on thermo-mechanical and morphological properties of polyurethanes. Eur Polym J 2000; 36:711–25.

[90] Paulmer RDA, Shah CS, Patni MJ, Pandya MV. Effect of crosslinking agents on the structure and properties of polyurethane millable elastomer composites. J Appl Polym Sci 1991; 43:1953–9.

[91] Chiou BS, Schoen PE. Effects of crosslinking on thermal and mechanical properties of polyurethanes. J Appl Polym Sci 2002; 83:212–23.

[92] Thomas O, Priester Jr RD, Hinze KJ, Latham DD. Effect of cross-link density on the morphology, thermal and mechanical properties of flexible molded polyurea/urethane foams and films. J Polym Sci: Part B: Polym Phys 1994; 32:2155–69.

[93] Dounis DV, Wilkes GL. Influence of diethanolamine on hard segment ordering in flexible polyurethane foams. J Appl Polym Sci 1997; 65:525–37.

[94] Petrovic ZS, Ilavsky M, Dus¡;ek K, Vidakovic M, Javni I, Banjanin B. Effect of crosslinking on properties of polyurethane elastomers. J Appl Polym Sci 1991; 42:391–8.

[95] Petrovic ZS, Javni I, Banhegy G. Mechanical and dielectric properties of segmented polyurethane elastomers containing chemical crosslinks in the hard segment. J Polym Sci: Part B: Polym Phys 1998; 36:237–51.

[96] Studer K, Decker C, Beck E, Schwalm R. Overcoming oxygen inhibition in UV-curing of acrylate coatings by carbon dioxide inerting, Part I. Prog Org Coat 2003;48:92–100.

[97] Ong IW, Julia M, Wilson CB, Robert S. Antimicrobial radiation curable coating. US patent 7098256, 2006.

[98] Price NL. Free radical and cationic photoinitiators in ultraviolet light curable coatings. J Coat Technol 1995; 67(849):27–34.

[99] Zhenglong Yang , Douglas A. Wicks , Charles E. Hoyle , Hongting Pu , Junjie Yuan, Decheng Wan , Yongsheng Liu , Polymer 50 (2009) 1717–1722.

[100] A. Srivastava, D. Agarwal, S. Mistry, J. Singh, 2008 Volume37 ,4 P, 217 – 223.

[101] Krajnik JM, Olesen KR, Vandezande GA. Waterborne coating having improved chemical resistance. US patent 6869996, 2005.

[102] Hart RE. Water-based, solvent-free or low VOC, twocomponent polyurethane coatings. US patent 5693703, 1997.

[103] Dieterich D. Aqueous emulsions, dispersions and solutions of polyurethanes; synthesis and properties. Prog Org Coat 1981; 9:281–340.

[104] Barni A, Levi M. Aqueous polyurethane dispersions: A comparative study of polymerization processes. J Appl Polym Sci 2003; 88:716–23.

[105] Rosthauser JW, Nachtkamp K. Waterborne polyurethanes. In: Frisch KC, Klempner D, editors. Advances in urethane Science and technology, vol. 10. Lancaster, PA: Technomic Publishing; 1987. p. 121–62.

[106] Yang CH, Lin SM, Wen TC. Application of statistical experimental strategies to the process optimization of waterborne polyurethane. Polym Eng Sci 1995; 35:722–30.

[107] Chinwanitcharoen C, Kanoh S, Yamada T, Hayashi S, Sugano S. Preparation of

a. aqueous dispersible polyurethane: effect of acetone on the particle size and storage stability of polyurethane emulsion. J Appl Polym Sci 2004; 91:3455–61.

[108] Anderle GA, Lenhard SL, Lubnin AV, Snow GE, Tamareselvy K. Plasticized waterborne polyurethane dispersions and manufacturing process. US patent 2002028875, 2002.

[109] R. Golden, *J*. Coat. Technol. (1997), 69(871), 83.

[110] J. K. Braddok, *RadTech 96 proc.*, vol. 1 p. 478.

[111] Ph.D. thesis UV-curable acrylate metal oxide nanocomposite coatings / by Willem Posthumus. –Eindhoven Technische Universiteit Eindhoven, 2004. Proefschrift. – ISBN 90-386-2985-0.

[112] C. Decker, Handbook of Polymer Science and Technology, (1989) vol. 3, p. 541

[113] R.S. Davidson, The role of amines in UV-curing, in: J.P. Fouassier, J.F. Rabek (Eds.), Radiation Curing in Polymer Science and Technology: Polymerisation Mechanisms, vol. III, Elsevier Applied Science, London (1993), p. 153.

[114] C. Decker, J. Faure, M. Fizet, L. Rychla, Photogr. Sci. Eng. (1979), 23 (3) 137.

[115] C. Decker, Makromol. Chem. (1979) 180 , 2027

[116] M. Awokola, W. Lenhard, H. Löffler, C. Flosbach, P. Frese, Prog. Org. Coat. (2002) 44, 211.

[117] D.A. Bolon, K.K. Webb, J. Appl. Polym. Sci. (1978) 22 (9) 2543.

[118] E. Selli, I.R. Bellobono, Photopolymerization of multifunctional monomers: kinetic aspects, in: J.P. Fouassier, J.F. Rabek (Eds.), Radiation Curing in Polymer Science and Technology: Polymerisation Mechanisms, vol. III, Elsevier Applied Science, London (1993) p. 1

[119] F.R. Wight, J. Polym. Sci.: Polym. Lett. Ed. (1978) 16, 121.

[120] R. Müller, in: Proceedings of the RadTech Europe Conference (2001) p. 149.

[121] T. Henke, Proceedings of the RadTech Europe Conference (2001) p. 145.

[122] E. Beck, Proceedings of the RadTech Europe Conference (2001) p. 643.

[123] E. Beck O. Deis, P. Enenkel, W. Schrof, German Patent (1999) 19 957 900.

[124] Jonsson, P.-E. Sundell, J.Hultgren, D. Sheng and C. E. Hoyle, *prog. Org*. coat. (1996) 27,107.

[125] C. Decker and K. Moussa, *J. coat. Technol*., (1993) 65 (819), 49.

[126] Bexandale, J.H. Polymer Processes; Interscience: New York, (1956).

[127] Odian, G. Principles of Polymerization: Fourth Edition; John Wiley and Sons: NewJersey, (2004).

[128] Tobolsky, A.V.; Mesrobian, R.B. Organic Peroxides; Interscience: New York, (1954).

[129] Lenz, R.W. Organic Chemistry of Synthetic High Polymers; John Wiley and Sons: New York, (1967).

[130] Schmid U. RadTech Europe Conf Proc (2001):53.

[131] Mills P. RadTech Europe Conf Proc (2001):65.

[132] Peeters S. In: Fouassier JP, Rabek JF, editors. Radiation curing in polymer science and technology, vol. 3. London: Elsevier (1993) p. 177.

[133] Königer R. Farbe und Lack (1999)105(4):233.

[134] Maag K., Lenhard W, Lo¨ffles H. Prog Org Coat (2000) 40:93.

[135] Fisher W., Weikard J. Farbe und Lack (2001)107(3):120.

[136] Decker, C:, Masson F, Schwalm R. Macromol Mater Eng ,(2003)17:288.

[137] Beck E. RadTech. Europe Conf., Berlin (2003).

[138] K. Studer, C. Decker,*, E. Beck and R. Schwalm European Polymer Journal (2005) 41, 157–167.

[139] U. Schmidt, RadTech Eur. 01 Conf. Proc. (2001) 53.

[140] P. Svedja, RadTech Eur. 99 Conf. Proc. (1999) 215.

[141] P. Mills, RadTech Eur. 01 Conf. Proc. (2001) 65.

[142] S. Peeters, in: ‘‘Radiation Curing in Polymer Science and Technology’’ (1993) Vol. 3, J. P. Fouassier, J. F. Rabek, Eds., Elsevier, and London p.177.

[143] R. Ko¨niger, Farbe Lacke (1999) 105, 233.

[144] K. Maag,W. Lenhard, H. Lo¨ ffles, Progr.Org. Coat. (2000) 40, 93.

[145] W. Fischer, J. Weikard, Farbe Lacke (2001) 107, 120.

[146] Eur 1138710 (2001), invs.: J. Weikard, M. Sonntag, H. Mundstock; Chem. Abstr. (2001) 23, 2743253.

[147] Dahotre BD, Kadolkar P, Shah S. Refractory ceramic coatings: processes, systems and wettability/adhesion. Surf Interface Anal 2001; 31:659–72.

[148] Giannelis EP. Polymer layered silicate nanocomposites. Adv Mater 1996; 8:29–35.

[149] Osman MA, Mittal V, Morbidelli M, Suter UW. Polyurethane adhesive nanocomposites as gas permeation barrier. Macromolecules 2003; 36:9851–8.

[150] Osman MA, Ploetze M, Suter UW. Surface treatment of clay minerals—thermal stability, basal-plane spacing and surface coverage. J Mater Chem 2003;13:2359–66

[151] Tien YI, Wei KH. Hydrogen bonding and mechanical properties in segmented montmorillonite/polyurethane nanocomposites of different hard segment ratios. Polymer 2001; 42:3213–21.

[152] Theng BKG. The chemistry of clay–organic reactions. London: Adam Hilger; New York:Wiley; 1974.

[153] Luyer C, Lou L, Bovier C, Plenet J, Mugnier DG. J Opt Mater (2001); 18:211.

[154] Rockwood Additives, www.laponite.com.

[155] The mechanism of hydrohphilic and hydrophobic colloidal silicon dioxide types as glidants , dissertation,der Fakultät für Chemie und Pharmazie,der Eberhard-Karls-Universität Tübingen,zur Erlangung des Grades eines,Doktors,der Naturwissenschaften, (2005),vorgelegt von STÉPHANE JONAT .

[156] Schemiewerk Bad Köstritz GmbH. Heinrichshal 2,07586 Bad Köstritz..

[157] Silane coupling agent version 2, www.gelset.com.

[158] Wen J, Wilkes GL. Organic/inorganic hybrid network materials by the sol–gel approach. Chem Mater 1996; 8:1667–81.

[159] Ribot F, Toledano P, Sanchez C. Hydrolysis-condensation process of beta. diketonates-modified cerium (IV) isopropoxide. Chem Mater 1991; 3:759–64.

[160] Zhu Y, Sun DX. Preparation of silicon dioxide/polyurethane nanocomposites by a sol–gel process. J Appl Polym Sci 2004; 92:2013–6.

[161] Parashar G, Srivastava D, Kumar P. Ethyl silicate binders for high performance coatings. Prog Org Coat 2001; 42:1–14.

[162] Cushing BL, Kolesnichenko VL, O'Connor CJ. Recent advances in the liquid-phase syntheses of inorganic nanoparticles. Chem Rev 2004; 104:3893–946.

[163] Tjong SC, Chen H. Nanocrystalline materials and coatings. Mater Sci Eng: R: Reports 2004; 45:1–88.

[164] Goda H, Frank CW. Fluorescence studies of the hybrid composite of segmented-polyurethane and silica. Chem Mater 2001; 13:2783–7.

[165] Lichtenhan JD, Vu HQ, Carter JA, Gilman JW, Ferer FJ. Silsesquioxane–siloxane copolymers from polyhedral silsesquioxanes. Macromolecules 1993;26:2141–2.

[166] Matejka L, Dukh O, Brus J, Simonsick WJ, Meissner B. Cage-like structure formation during sol–gel polymerization of glycidyloxypropyltrimethoxysilane. J Non-Cryst Solids 2000; 270:34–47.

[167] Daniels MW, Francis LF. Silane adsorption behavior, microstructure, and properties of glycidoxypropyltrimethoxysilane-modified colloidal silica coatings. J Colloid Interf Sci 1998; 205:191–200.

[168] Daniels MW, Francis LF. Effect of curing strategies on porosity in silane-modified silica colloidal coatings. Mater Res Soc Symp—Proc 1999; 576:313–7.

[169] Atanacio AJ, Latella BA, Barbe CJ, Swain MV. Mechanical properties and adhesion characteristics of hybrid sol–gel thin films. Surf Coat Technol 2005; 192:354–64.

[170] Schottner G. Hybrid sol–gel-derived polymers: applications of multifunctional materials. Chem Mater 2001; 13:3422–35.

[171] Zhang T, Xi K, Chen H, Yu X. Synthesis and properties of self-crosslinkable polyurethane-urea with silsesquioxane formation. J Appl Polym Sci 2004; 91:190–5

[172] Zilg C, Thomann R, Mulhaupt R, Finter J. Polyurethane nanocomposites containing laminated anisotropic nanoparticles derived from organophilic layered silicates. Adv Mater 1999; 11(1):49–52.

[173] Ma J, Zhang S, Qi Z. Synthesis and characterization of elastomeric polyurethane/clay nanocomposites. J Appl Polym Sci 2001; 82:1444–8.

[174] Giannelis EP. Polymer layered silicate nanocomposites. Adv Mater1996; 8:29–35.

[175] Alexandre M, Dubois P. Polymer-layered silicate nanocomposites: preparation, properties and uses of a new class of materials. Mater Sci Eng R: Rep 2000;28:1–63

[176] Chen TK, Tien YI, Wie KH. Synthesis and characterization of novel segmented polyurethane/clay nanocomposites. Polymer 2000; 41:1345–53.

[177] Yao KJ, Song M, Hourston DJ, Luo DZ. Polymer/layered clay nanocomposites: 2 polyurethane nanocomposites. Polymer 2002; 43:1017–20.

[178] Yeh JM, Liou SJ, Lai MC, Chang YW, Huang CY, Chen CP, et al. Comparative studies of the properties of poly(methyl methacrylate)-clay nanocomposite materials prepared by in situ emulsion polymerization and solution dispersion. J Appl Polym Sci 2004; 94:1936–46.

[179] Takeichi T, Guo Y. Synthesis and characterization of poly(urethane-benzoxazine)/clay hybrid nanocomposites. J Appl Polym Sci 2003; 90:4075–83.

[180] www.Special4Polymers.com/tc/Antifog-Agents/Index-aspx?id=2504.

[181] Liu, Y. Y.; Chen, X. Q.; Super-hydrophobic surfaces from a simple coating method: a bionic nanoengineering approach. Nanotechenology (2006)17,(13), 3259-3263 .

[182] Birr, E. J., mechanism of Action of anti-fog Agents and emulsion stabilizers, Chimia (1970) 24,(4).

[183] Sanchez-Valdes S., Picazo-Rada, C. J., Lopez-quinranilla, M. L. polyethylene grafted maleic anhydride to improve wettability of liquid on polyethylene films. Journal of applied polymer science, (2001), 79(10), 1802-1808.

[184] U. S. Patent 2005004255.

[185] Industrial science & Technology Network, Inc., 2101 Pennsylvania Ave,. York, PA 17404, USA.

[186] Katia S., Christian D., Celine B.,Erich, B., Reinhold S., N., Progress in Organic Coatings, (2005) 53,134-146.

[187] Jianwen X., Wenmin P., Wenfang S., Thin Sold Films (2006) 514,69-75.

[188] Kim B. K., Ahn B. U., Lee M. H. and Lee S. K. , Progress in Organic Coatings (2006) 55,194.

[189] Chanc-Sik Ha, Soon-Joonj Unc., Eunc-Seobk Im, Won-Soo Kim, Sang-Jin L Ee and Won-Jei Cho, Journal of Applied Polymer Science (1996) 62,1011.

[190] U. S. Patents 20070077399, 20050084581, and 2005004255.

[191] Wang Z. M., Gao D. B., and Yang J. W., Journal of Applied Polymer Science (1999) 73, 2869.

[192] Bai C. Y., Zhan,X. Y., Dai J. B., Li W. H., Anew UV curable waterborne polyurethane: Effect on C=C content of the film properties. Progress in Organic Coatings (2006) 55(3), 291.

[193] http://www.byk.com/instruments

[194] http://en.wikipedia.org/

[195] http://www.pencilpages.com/articles/simmons.htm

[196] Texture analysis, rheology of food, FST 4109.

[197] Emel Yildiz, Atilla Gungor, Huseyin Yildirim, Bahattin M. Baysal, Die Angewandte Makromolekulare Chemie 233 (1995) 33 - 45 (Nr. 3991)

[198] Odian, G. principle of polymerization: fourth eddition; John wiely and Sons:New Jersly,2004

[199] http://www.beltron.de/

[200] W. Stöber, A. Fink, E. Bohn, J. Colloid Interf. Sci. 26(1968) 62.

[201] Youngchan Shin, DEokkyu Lee, Kangtaek Lee ,Kyung Hyun Ahn,Bumsang Kim, Journal of Industrial and Engineering Chem 14(2008) 515-519

[202] M. Sh. Zoromba, A. A. M. Belal, A. E. M. Ali, A. S. Badran and A. A. Abd El-Hakim, Egyptian Journal of Applied Science V21, N6 (2006).

[203] Lev, O. et al. Analytical Chemistry. 1995, 67(1), 22A-30A.

[204] Kelts, L.W.; Effinger, N.J.; Melpolder, S.M. J. Non-Crystalline Solids. 1986, 83, 353-374.

[205] K.D. Keefer, in: Silicon Based Polymer Science: A Comprehensive Resource; eds. J.M. Zeigler and F.W.G. Fearon, ACS Advances in Chemistry Ser. No. 224, (American Chemical Society: Washington, DC, 1990) pp. 227-240.

[206] R.K. Iler, The Chemistry of Silica (Wiley: New York, 1979).

[207] http://www.psrc.usm.edu/mauritz/solgel.html

[208] J. Gonzalez-Irun Rodriguez, P Carreira, A. Garcia-Diez, D. Hui,R. Artiaga, Journal of thermal and carlorimetry, Vol. 87(2007) 1, 45-47

[209] Eliane Ayres, Wande Luiz Vaconcelos, Rodrigo Lambert Orefice, Materials Research, Vol. 10, No. 2, 119-125 (2007).